Title
Characterization of the host macrophage response to intracellular protozoan pathogens

Author
Zhang, Shuyi

Publication Date
2011

Peer reviewed|Thesis/dissertation

Characterization of the host macrophage response to intracellular protozoan pathogens

by

Shuyi Zhang

DISSERTATION

Submitted in partial satisfaction of the requirements for the degree of

DOCTOR OF PHILOSOPHY

in

Biomedical Sciences

in the

GRADUATE DIVISION

of the

UNIVERSITY OF CALIFORNIA, SAN FRANCISCO

Dedications

I owe whatever scientific achievements I have made over the course of my graduate career to a series of mentors who have encouraged and supported me both inside and outside the laboratory. My graduate thesis could not have been accomplished without the mentorship of P'ng Loke, who took me under his wing as a rotation student and taught me everything I know about macrophages and microarrays. I have greatly valued his vast knowledge, tremendous enthusiasm, and generous spirit as both a scientific advisor and as a friend.

The mentorship that led to the completion of my PhD began long before I entered graduate schools. I would be remiss not to also acknowledge Mark Zhang, my first scientific mentor, and Dan Rivera, the mentor of my undergraduate research thesis. It is their guidance, patience, and encouragement that led me down the path towards a PhD in Biomedical Sciences. I am fortunate to call both of them good friends to this day.

Finally, I would like to thank my principal investigator, Jim McKerrow for his support and guidance over the last five years. In addition to being a respected scientist/physician, Jim's fun-loving, easy-going nature created an environment of camaraderie in the lab that has been a pleasure to work in. I would like to specifically thank Jim for allowing me the freedom and flexibility to complete a PhD while starting a new family. It is an endeavor not many attempt, and I'm sure I could not have done it without such a generous and supportive advisor.

My very first mentors and role models were my parents, who came to the U.S. against great odds to provide me with the opportunity to be whatever I wanted to be.

Growing up I have always greatly admired their work ethic, ambition, and dedication to everything they do. I fully appreciate that above everything else, they have dedicated their lives to supporting and providing for me, and I hope that the completion of this work is also in part a fulfillment of the dream they had in coming to this country.

Ironically, no one in my life has taught me more than my two-year-old daughter Ruby. She has given me more perspective, purpose, and joy in the last two years than I have achieved in the entire rest of my life. Not a day has gone by since she was born that I have not laughed or felt happy.

Last but not least, I would like to thank and dedicate this work to my husband Steve, who has stood by my side and taken care of me every single day since the day we met. As our family's first PhD, no one could relate better to the trials and tribulations of graduate school. Over the years, Steve often bore the full brunt of my science-related stress and frustrations. He has been my source of unwavering support and unconditional love. During my time in graduate school, our marriage and the start of our family have been by far my proudest achievements.

Declarations and Acknowledgements

The text of this dissertation is in part (Chapter Two) based on material from a manuscript published in *PLoS Neglected Tropical Diseases* under the title "Delineation of diverse macrophage activation programs in response to intracellular parasites and cytokines."

The following individuals contributed to the data and research presented in this dissertation:

P'ng Loke: contributed experimental ideas throughout this dissertation.

James McKerrow: contributed experimental ideas throughout this dissertation.

Charlie Kim: contributed data for Figures 2.10.2, 2.10.3, and 2.14.10; contributed data for Tables 2.11.2 and 2.11.3.

Sajeev Batra: contributed data for Figures 2.10.2, 2.10.3, and 2.14.10; contributed data for Tables 2.11.2 and 2.11.3.

Anthony DeFranco: contributed experimental ideas throughout this dissertation.

Anita Sil: contributed experimental ideas throughout this dissertation.

Characterization of the host macrophage response to intracellular protozoan pathogens

Shuyi Zhang

Abstract

The ability to reside and proliferate in macrophages is characteristic of several infectious agents that are of major importance to public health. In order for these pathogens to survive in the hostile macrophage environment, they must develop mechanisms to evade the microbicidal activities of the macrophage and to subvert the host immune response. Using broad transcriptional profiling as well as more targeted approaches, we have further elucidated the ways intracellular protozoan pathogens interact with the host macrophage, providing a better understanding of parasite immune evasion.

In order to determine how the macrophage response to intracellular parasites fits into the diverse range of possible macrophage activation programs, we utilized genome-wide microarray analysis to compare the responses of mouse macrophages following infection by the intracellular parasites *Trypanosoma cruzi* and *Leishmania mexicana*, the bacterial product lipopolysaccharide (LPS), and various cytokines. We found that infection by *L. mexicana* produced so few transcriptional changes that the infected macrophages were almost indistinguishable from uninfected cells. Furthermore, the transcriptional response of macrophages infected by the protozoan pathogens more closely resembled the transcriptional response of macrophages stimulated by the

cytokines IL-4, IL-10, and IL-17 than macrophages stimulated by Th1 cytokines IFNG, TNF, and IFNB. These observation suggested that infection by *L. mexicana* may have a suppressive effect on host macrophage activation.

In order to determine if *L. mexicana* actively suppresses macrophage activation, we compared the response to live vs. heat-killed *L. mexicana*. Macrophages treated with heat-killed parasites were activated, producing a transcriptional signature that included upregulation of many interferon-stimulated genes, indicating that live *L. mexicana* actively suppresses this activation. In order to determine the mechanism of suppression, we analyzed the macrophage response to cysteine protease B (CPB)- and cysteine protease A (CPA)-deficient *L. mexicana*. CPB and CPA are related cathepsin L-like proteases that have been shown to play an important role in the inhibition of Th1 immunity in several mouse models of leishmaniasis. We found that infection with CPB-/- and CPB/CPA-/- *L. mexicana* also resulted in upregulation of interferon-stimulated genes, suggesting that suppression of host transcriptional responses by *L. mexicana* is at least partially dependent on CPB and CPA.

Table of Contents

List of Tables

List of Figures

Chapter One:

Introduction

1.1. The Role of Macrophages in Innate Immunity

Macrophages are phagocytic cells that serve as the first line of defense against invading pathogens. They are found in large numbers in areas of the body that represent entry points for microorganisms, such as the submucosa of the gut, the interstitium and aveoli of the lungs, and connective tissues. When macrophages encounter pathogens, they are able to recognize specific motifs on the surface of the pathogen known as pathogen-associated molecular patterns (PAMPs). Ligation of PAMPs by surface receptors on the macrophage leads to phagotycosis and killing of the invading microorganism.

The macrophage employs several mechanisms to neutralize microbial pathogens. The first is acidification of the phagosome to a pH that is toxic to most microorganisms. The second is fusion of the phagosome with lysosomes that contain enzymes capable of degrading the engulfed microorganisms. Finally, macrophages produce toxic products such as nitric oxide, superoxide anion, and hydrogen peroxide via nitric oxide synthase, NADPH oxidase, and superoxide dismutase, respectively, that directly kill the pathogen.

In addition to the mechanisms employed to kill pathogens within the first hours of infection, macrophages also play an essential role in the recruitment of other immune cells to the site of infection and in the mounting of an inflammatory response. These actions are mediated by the secretion of pro-inflammatory cytokines and chemokines and the expression of co-stimulatory molecules by macrophages. Signals that lead to the induction of these immune effectors originate from cell surface and intracellular receptors that interact with PAMPs from foreign microorganisms. The most well-studied of these receptors are Toll-like receptors (TLRs), which recognize a wide array of PAMPs from a

wide variety of bacterial, viral, and eukaryotic pathogens. Activation of macrophages via Toll-like receptor ligation initiates a signaling pathway that results in the secretion of cytokines and chemokines that act upon other immune cells, enhancing the local immune response to infection. These include IL-1 and IL-6, which activate lymphocytes and increase antibody production; IL-8, which is a chemoattractant for neutrophils; TNF, which promotes local inflammation; and IL-12, which activates NK cells and diverts the adaptive immune response to a Th1-type response. In addition to stimulating cytokine and chemokine secretion, activation of macrophages via TLRs also induces surface expression of co-stimulatory molecules that are essential for the activation of naive CD4+ T cells in the adaptive phase of the immune response (1). Therefore, macrophages play a crucial role in both the initial killing of invading microorganisms and also, in the case of pathogens that evade macrophage-mediated killing, in the mounting of a successful adaptive immune response.

1.2. Classical versus Alternative Macrophage Activation

Two decades ago, macrophage activation was defined exclusively by the secretion of pro-inflammatory cytokines and the ability to kill intracellular pathogens (2, 3). Since then, we have come to understand that macrophages display a high level of plasticity and can respond to a vast array of stimuli in very different ways. Macrophage activation as it was originally understood has come to be known as "classical macrophage activation" and results from ligation of toll-like receptors during infection as well as stimulation by the Th1 cytokine IFN•. Defining characteristics of classically activated macrophages include the production of NO, the up-regulation of the antigen presentation molecule

MHCII and the costimulatory molecule CD86, and enhanced pathogen killing (2). Classically activated macrophages secrete the cytokines TNF, IL-12, IL-1, and IL-6, which in turn promote the Th1 response and classical activation of macrophages. Prolonged or uncontrolled activation of macrophages in this manner may lead to tissue damage and immunopathology, so classical activation is held in check by immunoregulatory cytokines such as TGF• and IL-10.

In the early '90s Stein et al described another class of activated macrophages that responded to stimulation by the Th2-type cytokine IL-4 (4). These "alternatively activated macrophages" did not produce NO and failed to kill intracellular pathogens. They were characterized by the induction of arginase and the upregulation of mannose receptor and scavenger receptors (2, 3, 5). Instead of secreting cytokines that promoted T-cell activation, these macrophages secreted IL-10 and IL-1r• which suppressed T-cell activity and proliferation. It is believed that alternatively activated macrophages keep in check the effects of classically activated macrophages and also play a role in tissue repair (2, 5). However, certain pathogens have devised methods to take advantage of alternatively activated macrophages in order to promote their own survival.

1.3. *Leishmania*: An Overview

Leishmania spp. are protozoan parasites belonging to the family, Trypanosomatidae. This family also includes *Trypanosoma cruzi* (etiological agent of Chagas' Disease) and *Trypanosoma brucei* (etiological agent of Human African Sleeping Sickness). The various species in the genus *Leishmania* are etiological agents of visceral, mucocutaneous, and cutaneous leishmaniasis, diseases that affect 12 million people in 88

countries (6). Cutaneous leishmaniasis, the most common form of the disease, is caused by the Old World species *L. tropica* and *L. major*, as well as the New World species *L. mexicana*. These parasites can produce ulcers on the skin that range in severity from self-healing to permanently disfiguring lesions. Mucocutaneous leishmaniasis is a more uncommon version of the disease that affects the mucous membranes. It is most often caused by the species *L. braziliensis* and *L. guyanensis*. Visceral leishmaniasis, the most serious form of the disease, is caused by *L. donovani* and affects the liver and spleen of the host, resulting in death if not properly treated.

Leishmaniasis is a vector-borne disease transmitted by the phlebotamine sandfly. The *Leishmania* parasite exists in two morphological forms, as an intracellular amastigote in the mammalian host and as a promastigote found in the insect vector. The sandfly infects the host by taking a blood meal and regurgitating the infective metacyclic promastigote into the wound site. The promastigotes are phagocytized by macrophages and transform into the amastigote form inside the cell. They divide within the cell and can eventually disrupt the cell and infect other phagocytic cells. The life cycle is completed when the sandfly takes a blood meal and ingests an infected macrophage. Amastigotes transform back into promastigotes in the fly midgut before migrating to the proboscis (7).

1.4. Interaction between *Leishmania* and the Host Macrophage

Leishmania promastigotes preferentially infect mononuclear phagocytes, so the interaction between these cells and the parasite has been an area of particular research interest. The uptake of *Leishmania* by macrophages occurs through receptor mediated

phagocytosis. *Leishmania* promastigotes take advantage of the host complement system to gain access into host cells. CR3, the receptor for C3bi, has been identified as the primary complement receptor responsible for adhesion of parasites to macrophages during phagocytosis (8). The promastigotes are able to withstand the acidic environment of the phagolysosome and transform into amastigotes. In *L. mexicana* infection, these phagolysosomes grow into larger parasitophorous vacuoles that are rich in hydrolases and late-endosomal in nature (9).

During the process of initial invasion, the macrophage employs a number of strategies to defend itself against the parasite. The most well-described are the production of reactive oxygen and nitrogen species formed by NAPDH oxidase and iNOS, respectively (10). However, the ability of the host to mount an effective immune response against *Leishmania* is dependent on the successful initiation of Th1-type immunity (9). In fact, seminal studies on *L. major* revealed the importance of Th1 versus Th2 immunity in the context of intracellular infection (11) and serve as the basis for our current knowledge of the Th1/Th2 paradigm (9). *L. major* produces non-healing cutaneous lesions in infected BALB/c mice. Protective immunity to *L. major* is dependent upon the mounting of a Th1-type response characterized by the production of IFN• by CD4+ T cells and the production of NO by classically activated macrophages. BALB/c mice fail to mount a Th1-type response to *L. major* due to the presence of a Th2-type response, which is detrimental to disease outcome (9). Mice lacking IL-4R• , a common component of the IL-4 and IL-13 receptor complex, control infection to *L. major* despite developing a Th2 response (12), suggesting IL-4R• -expressing cells other than Th2-type CD4+ T cells were responsible for the non-healing phenotype in BALB/c

mice. Macrophage/neutrophil-specific IL-4R• -deficient mice also showed delayed lesion growth in BALB/c mice despite a normal Th2-type response (13). This suggests that it is alternatively activated macrophages that are important in the susceptibility of BALB/c mice to *L. major* infection. The interplay between alternatively activated macrophages and *Leishmania* will be more closely examined in Chapters II and III.

It is now generally accepted that immunity to *Leishmania* infection is dependent on IL-12 production by dendritic cells and macrophages, which induces IFN• production by T-cells and NK cells. IFN• then cooperates with TNF, secreted by infected macrophages, to induce activated macrophages to kill the parasites. However, the mechanisms that contribute to the non-healing phenotype of some animals infected with certain strains of *Leishmania* are still unclear. Studies have implicated the presence of a Th2 response that interferes with Th1 immunity, the presence of a Th2 response along with a Th1 response, the lack of a Th1 response not resulting from the presence of Th2 cytokines, and the failure to induce or respond to IL-12 (9). All of these scenarios can be traced to an inadequate or inappropriate innate immune response to the parasite.

One of the reasons *Leishmania* species have been of such interest to immunologists is its apparent ability to manipulate the host immune response. Some studies have suggested that *Leishmania* modulates host expression of inhibitory cytokines such as IL-10 and TGF• . The production of IL-10 by patients suffering from either visceral or cutaneous leishmaniasis has been correlated to disease progression (14-17). Genetically susceptible mice that were IL-10 deficient were able to control lesion growth compared to their wild-type counterparts (18, 19). The induction of IL-10 during *Leishmania* infection has been shown to be the result of ligation of Fc• receptors by

opsonized *Leishmania* amastigotes (18-20). This is evidenced by the fact that opsonized and lesion-derived but not axenic amastigotes induced IL-10 in infected macrophages. Furthermore, mice deficient in Fc• receptor controlled lesion growth in a manner similar to IL-10-deficient mice (19). IL-10 induced during infection downregulates the production of IL-12 and TNF by macrophages, thus preventing the successful mounting of a Th1 response (18, 20).

TGF• has also been shown to be induced during *Leishmania* infection, and inhibition of TGF• resulted in rapid lesion healing associated with increased nitric oxide production (21, 22). It has been suggested through study of peripheral blood mononuclear cells from humans infected with *L. guyanensis* that TGF• is produced by a subpopulation of CD4+ CD25+ regulatory T cells (Tregs) (23). Further evidence that regulatory T cells play a role in *Leishmania* infection was presented in a study that identified functional Tregs in the skin lesions of patients with cutaneous leishmaniasis. These Tregs were able to produce large quantities of IL-10 and TGF• and were also able to inhibit PHA-induced T cell responses in vitro (24). Furthermore, it has been suggested that live promastigotes of several *Leishmania* spp. as well as promastigote culture supernatants were able to activate latent TGF• in the local environment via the cysteine protease, cathepsin B (25). Induction of TGF• via these mechanisms all serve to enhance parasite survival in the host.

Much attention has been given to the ability of certain species of *Leishmania* to downregulate macrophage production of IL-12. *L. major* promastigotes (26), *L. mexicana* amastigotes (27), and the *Leishmania* surface marker, phosphoglycan (28), have all been implicated in the suppression of IL-12 production. One possible

mechanism of this suppression is the ligation of phagocytic receptors on macrophages. Ligation of both complement receptors, important for promastigote phagocytosis, and Fc• receptors, implicated in amastigote phagocytosis, have been associated with downregulation of IL-12 (29, 30). Another mechanism of IL-12 down-regulation involves the *Leishmania mexicana* virulence factor, cysteine protease B (CPB). *L. mexicana* CPB has been shown to inhibit IL-12 production and the development of Th1-type immunity in several murine models of leishmaniasis (31-33). The role of CPB in *L. mexicana* infection and immune evasion will be described in detail in Chapter III.

1.5. References

1. Janeway C. Immunobiology : the immune system in health and disease. 6th ed. New York: Garland Science; 2005.
2. Mosser DM. The many faces of macrophage activation. J Leukoc Biol. 2003;73(2):209-12.
3. Gordon S. Alternative activation of macrophages. Nat Rev Immunol. 2003;3(1):23-35.
4. Stein M, Keshav S, Harris N, Gordon S. Interleukin 4 potently enhances murine macrophage mannose receptor activity: a marker of alternative immunologic macrophage activation. J Exp Med. 1992;176(1):287-92. PMCID: 2119288.
5. Gordon S, Taylor PR. Monocyte and macrophage heterogeneity. Nat Rev Immunol. 2005;5(12):953-64.
6. ; [cited]; Available from: http://www.who.int/leishmaniasis/burden/magnitude/burden_magnitude/en/index.html.
7. Peters W, Killick-Kendrick R. The Leishmaniases in biology and medicine. London ; Orlando: Academic Press; 1987.
8. Mosser DM, Edelson PJ. The mouse macrophage receptor for C3bi (CR3) is a major mechanism in the phagocytosis of Leishmania promastigotes. J Immunol. 1985;135(4):2785-9.
9. Alexander J, Satoskar AR, Russell DG. Leishmania species: models of intracellular parasitism. J Cell Sci. 1999;112 Pt 18:2993-3002.
10. Kane MM, Mosser DM. Leishmania parasites and their ploys to disrupt macrophage activation. Curr Opin Hematol. 2000;7(1):26-31.
11. Heinzel FP, Sadick MD, Holaday BJ, Coffman RL, Locksley RM. Reciprocal expression of interferon gamma or interleukin 4 during the resolution or progression of murine leishmaniasis. Evidence for expansion of distinct helper T cell subsets. J Exp Med. 1989;169(1):59-72. PMCID: 2189187.
12. Mohrs M, Holscher C, Brombacher F. Interleukin-4 receptor alpha-deficient BALB/c mice show an unimpaired T helper 2 polarization in response to Leishmania major infection. Infect Immun. 2000;68(4):1773-80. PMCID: 97347.
13. Holscher C, Arendse B, Schwegmann A, Myburgh E, Brombacher F. Impairment of alternative macrophage activation delays cutaneous leishmaniasis in nonhealing BALB/c mice. J Immunol. 2006;176(2):1115-21.
14. Karp CL, el-Safi SH, Wynn TA, Satti MM, Kordofani AM, Hashim FA, et al. In vivo cytokine profiles in patients with kala-azar. Marked elevation of both interleukin-10 and interferon-gamma. J Clin Invest. 1993;91(4):1644-8. PMCID: 288142.
15. Kaye PM, Curry AJ, Blackwell JM. Differential production of Th1- and Th2-derived cytokines does not determine the genetically controlled or vaccine-induced rate of cure in murine visceral leishmaniasis. J Immunol. 1991;146(8):2763-70.
16. Ghalib HW, Piuvezam MR, Skeiky YA, Siddig M, Hashim FA, el-Hassan AM, et al. Interleukin 10 production correlates with pathology in human Leishmania donovani infections. J Clin Invest. 1993;92(1):324-9. PMCID: 293600.
17. Louzir H, Melby PC, Ben Salah A, Marrakchi H, Aoun K, Ben Ismail R, et al. Immunologic determinants of disease evolution in localized cutaneous leishmaniasis due to Leishmania major. J Infect Dis. 1998;177(6):1687-95.

18. Kane MM, Mosser DM. The role of IL-10 in promoting disease progression in leishmaniasis. J Immunol. 2001;166(2):1141-7.
19. Buxbaum LU, Scott P. Interleukin 10- and Fcgamma receptor-deficient mice resolve Leishmania mexicana lesions. Infect Immun. 2005;73(4):2101-8.
20. Thomas BN, Buxbaum LU. FcgammaRIII mediates immunoglobulin G-induced interleukin-10 and is required for chronic Leishmania mexicana lesions. Infect Immun. 2008;76(2):623-31. PMCID: 2223473.
21. Barral-Netto M, Barral A, Brownell CE, Skeiky YA, Ellingsworth LR, Twardzik DR, et al. Transforming growth factor-beta in leishmanial infection: a parasite escape mechanism. Science. 1992;257(5069):545-8.
22. Li J, Hunter CA, Farrell JP. Anti-TGF-beta treatment promotes rapid healing of Leishmania major infection in mice by enhancing in vivo nitric oxide production. J Immunol. 1999;162(2):974-9.
23. Kariminia A, Bourreau E, Pascalis H, Couppie P, Sainte-Marie D, Tacchini-Cottier F, et al. Transforming growth factor beta 1 production by CD4+ CD25+ regulatory T cells in peripheral blood mononuclear cells from healthy subjects stimulated with Leishmania guyanensis. Infect Immun. 2005;73(9):5908-14. PMCID: 1231133.
24. Campanelli AP, Roselino AM, Cavassani KA, Pereira MS, Mortara RA, Brodskyn CI, et al. CD4+CD25+ T cells in skin lesions of patients with cutaneous leishmaniasis exhibit phenotypic and functional characteristics of natural regulatory T cells. J Infect Dis. 2006;193(9):1313-22.
25. Gantt KR, Schultz-Cherry S, Rodriguez N, Jeronimo SM, Nascimento ET, Goldman TL, et al. Activation of TGF-beta by Leishmania chagasi: importance for parasite survival in macrophages. J Immunol. 2003;170(5):2613-20.
26. Carrera L, Gazzinelli RT, Badolato R, Hieny S, Muller W, Kuhn R, et al. Leishmania promastigotes selectively inhibit interleukin 12 induction in bone marrow-derived macrophages from susceptible and resistant mice. J Exp Med. 1996;183(2):515-26. PMCID: 2192469.
27. Weinheber N, Wolfram M, Harbecke D, Aebischer T. Phagocytosis of Leishmania mexicana amastigotes by macrophages leads to a sustained suppression of IL-12 production. Eur J Immunol. 1998;28(8):2467-77.
28. Piedrafita D, Proudfoot L, Nikolaev AV, Xu D, Sands W, Feng GJ, et al. Regulation of macrophage IL-12 synthesis by Leishmania phosphoglycans. Eur J Immunol. 1999;29(1):235-44.
29. Sutterwala FS, Noel GJ, Clynes R, Mosser DM. Selective suppression of interleukin-12 induction after macrophage receptor ligation. J Exp Med. 1997;185(11):1977-85. PMCID: 2196339.
30. Marth T, Kelsall BL. Regulation of interleukin-12 by complement receptor 3 signaling. J Exp Med. 1997;185(11):1987-95. PMCID: 2196332.
31. Cameron P, McGachy A, Anderson M, Paul A, Coombs GH, Mottram JC, et al. Inhibition of lipopolysaccharide-induced macrophage IL-12 production by Leishmania mexicana amastigotes: the role of cysteine peptidases and the NF-kappaB signaling pathway. J Immunol. 2004;173(5):3297-304.
32. Buxbaum LU, Denise H, Coombs GH, Alexander J, Mottram JC, Scott P. Cysteine protease B of Leishmania mexicana inhibits host Th1 responses and protective immunity. J Immunol. 2003;171(7):3711-7.

33. Frame MJ, Mottram JC, Coombs GH. Analysis of the roles of cysteine proteinases of Leishmania mexicana in the host-parasite interaction. Parasitology. 2000;121 (Pt 4):367-77.

Chapter Two:

Delineation of diverse macrophage activation programs in response to intracellular parasites and cytokines

2.1. Abstract

Background:

The ability to reside and proliferate in macrophages is characteristic of several infectious agents that are of major importance to public health, including the intracellular parasites, *Trypanosoma cruzi* (the etiological agent of Chagas disease) and *Leishmania* species (etiological agents of Kala-azar and cutaneous Leishmaniasis). Although recent studies have elucidated some of the ways macrophages respond to these pathogens, the relationships between activation programs elicited by these pathogens and the macrophage activation programs elicited by bacterial pathogens and cytokines have not been delineated.

Methodology/Principal findings:

To provide a global perspective on the relationships between macrophage activation programs and to understand how certain pathogens circumvent them, we used transcriptional profiling by genome wide microarray analysis to compare the responses of mouse macrophages following exposure to the intracellular parasites *Trypanosoma cruzi* and *Leishmania mexicana*, the bacterial product lipopolysaccharide (LPS), and the cytokines IFNG, TNF, IFNB, IL-4, IL-10, and IL-17.

We found that LPS induced a classical activation state that resembled macrophage stimulation by the Th1 cytokines IFNG and TNF. However, infection by the protozoan pathogen *Leishmania mexicana* produced so few transcriptional changes that the infected macrophages were almost indistinguishable from uninfected cells. *Trypanosoma cruzi* activated macrophages produced a transcriptional signature

characterized by the induction of interferon-stimulated genes by 24 h post-infection. Despite this delayed IFN response by *T. cruzi*, the transcriptional response of macrophages infected by the kinetoplastid pathogens more closely resembled the transcriptional response of macrophages stimulated by the cytokines IL-4, IL-10, and IL-17 than macrophages stimulated by Th1 cytokines.

Conclusions/Significance:

This study provides global gene expression data for a diverse set of biologically significant pathogens and cytokines and identifies the relationships between macrophage activation states induced by these stimuli. By comparing macrophage activation programs to pathogens and cytokines under identical experimental conditions, we provide new insights into how macrophage responses to kinetoplastids correlate with the overall range of macrophage activation states.

2.2. Author Summary

Macrophages are a type of immune cell that engulf and digest microorganisms. Despite their role in protecting the host from infection, many pathogens have developed ways to hijack the macrophage and use the cell for their own survival and proliferation. This includes the parasites *Trypanosoma cruzi* and *Leishmania mexicana*. In order to gain further understanding of how these pathogens interact with the host macrophage, we compared macrophages that have been infected with these parasites to macrophages that have been stimulated in a number of different ways. Macrophages can be activated by a wide variety of stimuli, including common motifs found on pathogens (known as pathogen associated molecular patterns or PAMPs) and cytokines secreted by other immune cells. In this study, we have delineated the relationships between the macrophage activation programs elicited by a number of cytokines and PAMPs. Furthermore, we have placed the macrophage responses to *Trypanosoma cruzi* and *Leishmania mexicana* into the context of these activation programs, providing a better understanding of the interaction between these pathogens and macrophage.

2.3. Introduction

Macrophages are innate immune cells that respond to a variety of stimuli (1), (2). In the early, acute phase of an infection, they are activated by pathogen-associated molecular patterns (PAMPs), allowing them to recognize, engulf, and kill invading pathogens (3). During the chronic phase of infection, macrophages are further activated by cytokines secreted by T cells (4). Interaction with different PAMPs and cytokines leads to different states of macrophage activation (5). These include innate macrophage activation by microbial products such as LPS through engagement of pattern recognition receptors (PRRs), classical macrophage activation by T helper 1 (Th1) cytokines such as interferon gamma (IFNG) and tumor necrosis factor (TNF), alternative macrophage activation by T helper 2 (Th2) cytokines such as interleukin-4 (IL-4) and interleukin-13 (IL-13), and macrophage "deactivation" by interleukin-10 (IL-10) (6), tumor growth factor beta (TGF-B) or phagocytosis of apoptotic cells (7) and Fc-receptor (FcR) crosslinking (1, 5, 8).

Although many different states of macrophage activation (or deactivation) have been identified, the phenotypic relationships between these states remain unclear at a molecular level. Previous studies have used transcriptional profiling to determine gene expression in macrophages after they are activated with bacteria (9, 10), type I/II interferons (11), and various intracellular parasites (12-22). However, because all of these experiments were performed separately, they cannot be easily compared and do not directly address the phenotypic relationship between the different states of macrophage activation. To clearly determine how the different states of macrophage activation relate to one another under otherwise identical culture conditions, we compared the transcriptional response of bone marrow-derived macrophages to infection by the kinetoplastid intracellular parasites *Leishmania mexicana* and

Trypanosoma cruzi, stimulation by the bacterial PAMP lipopolysaccharide (LPS), and stimulation by the cytokines IFNG, TNF, IFNB, IL-4, IL-10, and IL-17.

Additionally, in order to determine whether different types of macrophages respond differently to activation stimuli, we compared the transcriptional responses of thioglycollate-elicited peritoneal macrophages with transcriptional responses of identically treated bone-marrow derived macrophages following stimulation with IFNG, IL-4, and TNF.

2.4. Methods

Macrophage preparation

Bone marrow-derived macrophages (BMMs) were differentiated from marrow isolated from femurs and tibias of five 6-8 week-old C57BL/6 mice (Charles River). The cells were pooled and cultured in BMM media composed of DMEM + 20% FBS + 10% 3T3 supernatant containing MCSF + 110ug/mL Na Pyruvate + 2mM L-glutamine + 1% Penicillin-streptomycin (BMM media). The cells were differentiated for 6 days, harvested and frozen down in 90% FBS + 10% DMSO. Cryopreserved macrophages were used so that all experiments could be conducted using the same batch of cells. The transcriptional signature of cryopreserved macrophages was compared to that of fresh macrophages to ensure the quality of the frozen and thawed BMMs used in these experiments (**Figure S1**). The purity of BMMs was confirmed by flow cytometry analysis using lymphocyte, granulocyte, monocyte, and dendritic cell surface markers (**Figure S2**). Replicate experiments were performed using a separate batch of BMMs derived from a different set of five C57BL/6 mice. One day before infection, macrophages were thawed and plated on T25 flasks at a density of $5x10^6$ cells per flask in BMM media.

Thioglycollate-elicited macrophages were derived by intraperitoneal injection of five C57BL/6 mice with 2.5 mL sterile thioglycollate. Mice were sacrificed 72 h post-injection. Peritoneal lavage was performed by washing the cavity twice with 5 mL of PBS. Cells were washed and plated in DMEM + 10% FBS. Experiments using thioglycollate-elicited macrophages were performed the following day after removal of non-adherent cells by repeated washing with PBS.

Macrophage infections and stimulations

Leishmania mexicana (strain MNYC/BZ/62/M379) were grown in M199 media and were washed and resuspended in DMEM + 0.5% FBS for infection. *Trypanosoma cruzi* (strain CAI-72) were seeded on a monolayer of BESM (Bovine Embryo Skeletal Muscle) cells (grown in RPMI + 20% FBS). On day 5 after seeding, the media on the cells was replaced, and metacyclic trypomastigotes were collected the following day. *T. cruzi* parasites were then washed and resuspended in DMEM + 0.5% FBS for infection. For *L. mexicana* and *T. cruzi* infections, BMMs were washed once with D-PBS, and their media was replaced with DMEM + 0.5% FBS containing parasites at a MOI of 10 (an MOI of 1 resulted in only 10% of BMMs infected, and an MOI of 50 resulted in extensive lysis by 24 h post-infection). Control, uninfected cells received media without parasites. The flasks were centrifuged at 168xG for 5 m to synchronize the infection. All infections took place over a 24 h time course with RNA collection at 2 h, 6 h, 12 h, and 24 h time points post-infection. Our data represents three biological replicates of *L. mexicana* infection and two biological replicates of *T. cruzi* infection. Each biological replicate was performed independently using macrophages derived from a different group of mice. Macrophages were stimulated with 100 ng/mL LPS (Sigma), 100 ng/mL IFNG (R&D Systems), 20 ng/mL IL-4 (Peprotech), 10 ng/mL of IL-10 (Peprotech), 10 ng/mL TNF (R&D Systems), 100 units/mL IFNB (Fischer Scientific), or 100 ng/mL IL-17 (Peprotech). RNA was collected at 2 h, 6 h, 12 h, and 24 h time points.

Microarray analysis

BMMs were lysed using the TRIzol Reagent (Invitrogen), and RNA was isolated using the RNeasy Mini Kit (Qiagen). RNA was then amplified using the Amino Allyl MessageAmp II aRNA Amplification Kit (Ambion).

All microarray analysis was performed on custom printed Mouse Exonic Evidence-based Oligonucleotide (MEEBO) Arrays. Amplified RNA from each sample was hybridized against a pooled reference consisting of an equal quantity of RNA from all of the time points within a particular infection time course. The arrays were scanned using a GenePix 4000B scanner and GenePix PRO version 4.1 (Axon Instruments/Molecular Devices). The Spotreader program (Niles Scientific) was used for array gridding and image analysis. The resulting data files were uploaded to Acuity version 4.0 (Molecular Devices), where the raw data was log transformed, filtered for "good quality spots" ((('RgnR^2(635/532)'>0.6) AND ('Flags'>=0))AND(('F532Mean-b532'>200) OR ('F635Median-b635'>200))), normalized to the 0 h control, and filtered for data present in at least 70% of samples. The resulting dataset (Dataset S1) was then analyzed for statistically significant genes using the Statistical Analysis of Microarray (SAM) software version 3.0 (available at http://www-stat.stanford.edu/~tibs/SAM/).

Microarrays that were of poor quality (high background, low foreground) were repeated.

Statistical analysis of microarray data

Pairwise comparisons were performed between infected/stimulated cells and uninfected cells in order to determine the number of genes significantly affected by the infection/stimulation and the relative fold changes of these genes. To do this, the two-class unpaired analysis in SAM was employed with a false discovery rate (FDR) cutoff of 1% and the condition that genes must have at least a two-fold change. This stringent FDR cutoff was chosen in order to focus on genes most highly induced or repressed by each condition. We treated each time point as an independent replicate to identify genes that were consistently up or down-regulated over the 24 h time

course. Data for *L. mexicana*-infected, *T. cruzi*-infected, and uninfected BMMs included 3, 2, and 5 replicate time courses, respectively. Biological replicates of *L. mexicana*-infected, *T. cruzi*-infected, or uninfected cells were treated as replicates for the purposes of this analysis.

Multiclass comparisons were also performed between infected/stimulated cells to determine the number of genes significantly different between these groups by multiclass analysis in SAM with a false discovery cutoff of 0.1%. Biological replicates of *L. mexicana* and *T. cruzi* were treated as replicates for the purposes of this analysis. Once a list of significant genes was obtained, data was extracted from the total dataset for this list of significant genes using the Samster tool (23). Data from each of the biological replicates were averaged for each individual time point, filtered for 90% present data, and hierarchically clustered in Cluster version 3.0 (http://bonsai.ims.u-tokyo.ac.jp/~mdehoon/software/cluster/software.htm#ctv). The resulting heat map and trees were visualized using Java Treeview (available at http://sourceforge.net/projects/jtreeview/files/).

Gene ontology analysis was performed using the PANTHER (Protein Analysis Through Evolutionary Relationships) classification system (available at http://www.pantherdb.org/). Genes upregulated by one or multiple stimuli were input into PANTHER along with a background gene list representing all of the genes used in the SAM analysis. The biological processes that were over-represented in the genes of interest were identified and sorted based on classification type and *p*-value.

***Leishmania* and *Trypanosoma* meta-analysis**

For studies that have original array files available in a public database, those files were obtained and used for processing. For studies that did not have original array files available, we relied on the authors' preprocessed data.

Data were $\log_2$ transformed if necessary and arrays were median centered. Biological and technical replicates, if available, were averaged for each time point for infected samples. All infected samples for each probe expression value were then subtracted by either their paired uninfected sample or the time zero expression value. For data generated by this study, each array was median centered and biological replicates for each time point for both infected and uninfected were averaged. The corresponding uninfected expression values were subtracted from infected.

All the columns in the integrated data sets were Z-score transformed and 90% present filtered. SAM one class analysis was performed with a 1% FDR cutoff. HUGO identifiers were converted to Entrez identifiers for functional analysis in PANTHER.

Methods for supplemental materials have been provided as Methods S1.

2.5. Results

2.5.1. Muted macrophage activation signature by kinetoplastids relative to LPS

Macrophages respond to pathogens through engagement of pattern recognition receptors (PRRs), the most well characterized being the Toll-like receptors (TLRs) (3, 24). Innate activation through engagement of TLR4 by LPS (25) is well characterized as being responsible for the majority of the activation program induced by gram-negative bacteria (9). However, intracellular protozoan pathogens induce macrophage responses that are distinct from their bacterial counterparts (19). In order to compare innate macrophage activation programs, bone marrow-derived macrophages (BMM) were infected with the intracellular protozoan pathogens, *Leishmania mexicana* and *Trypanosoma cruzi*, or stimulated with LPS, and host expression responses were analyzed using microarrays.

In comparison to uninfected control cells, *L. mexicana* infection of BMMs resulted in few changes in gene expression (Figure 1B), which is consistent with other reports describing the subtle nature of *Leishmania* infection (13, 16, 18-20, 26). . This lack of response by the infected macrophages was not due to the absence of infectivity by the parasites, as both flow cytometry and microscopy revealed that BMMs were effectively infected by *L. mexicana* (**Figure S3 A-E**).

T. cruzi differed from *L. mexicana* in that it induced a number of genes by 24 h post-infection, many of which are known interferon-stimulated genes (**Figure 1A**). These results were confirmed by quantitative real-time PCR (qPCR) analysis for two interferon-stimulated genes including interferon-induced protein with tetratricopeptide repeats 3 (*Ifit3*) (**Figure S4 A**) and interferon activated gene 205 (*Ifi205*) (**Figure S4 B**). This late activation of an IFN response may correlate with *T. cruzi* escape from

sequestration in a parasitophorous vacuole into the host cell cytosol and is consistent with previous microarray studies on *T. cruzi* infection (17, 21, 22).

In order to ensure that the transcriptional response to *T. cruzi* infection was not being affected by the parasites having been cultured in BESM cells, we compared the transcriptional signature of BMMs treated with supernatant from uninfected BESM cells (mock-infected BMMs) to the uninfected BMMs used in our experiments. The transcriptional signature of mock-infected BMMs was highly correlated with the transcriptional signature of uninfected BMMs (**Figure S5**).

The transcriptional response to LPS stimulation was distinct from the responses to either of the intracellular parasites (**Figure 1A and 1B**). Out of the 247 genes significantly induced by LPS, only 19 were also induced by *T. cruzi*, and 1 was also induced by *L. mexicana*. Genes induced by both LPS and *T. cruzi* include *Ifit1, Ifit2, Ifit3,Ifi204, Ifi44, Isg15, Isg20, Gbp3,* and *Gbp6* (Table 1). The induction of these interferon response genes is consistent with studies showing that *T. cruzi* infection can lead to the induction of IFNB via signalling through host PRRs (27, 28). However, this IFN response is quite restricted relative to the response to LPS. As expected, gene ontology analysis showed that LPS induced genes enriched for a number of biological processes related to the immune response such as immunity and defense, interferon-mediated immunity, cytokine and chemokine mediated signalling pathway, macrophage-mediated immunity, T-cell mediated immunity, JAK-STAT cascade, and granulocyte-mediated immunity (Table 2). However, genes upregulated by the protozoan pathogens alone were not significantly enriched for any known biological processes.

These results indicate that activation by LPS is far more robust than activation by these intracellular kinetoplastids. *L. mexicana* infection of macrophages in

particular appears to be transcriptionally "silent," suggesting either that the parasite lacks PAMPs, or that the parasite can inhibit either cellular signalling or host transcription. Although *T. cruzi* induced several immune-related IFN response genes, many of the genes significantly induced by *T. cruzi* infection are unnamed (having only a RIKEN designation) and have unknown functions (Table 1). These results illustrate our poor understanding of kinetoplastid macrophage interactions relative to TLR signalling in response to LPS.

2.5.2. Meta-analysis of transcriptional responses to *L. mexicana* and *T. cruzi.*

Previous studies have characterized the transcriptional response to several *Leishmania* (13, 14, 16, 19, 20) and *Trypanosoma* (12, 15, 17, 21, 22) species using a variety of *in vitro* and *in vivo* infection models. In order to compare our macrophage derived transcriptional profiling data to previous studies, we performed a "meta-analysis" of all publicly available expression profiling studies of the host response to *Leishmania* and *Trypanosoma* species (**Figure 2 and Figure 3**). This analysis showed that the transcriptional responses of macrophages to *L. mexicana* and *T. cruzi* observed in this study showed commonality with the transcriptional responses to *Leishmania* and *Trypanosoma* species observed in other studies, despite the important differences in the species of parasites and the types of mammalian cells characterized.

Specifically, we found that all *Leishmania* species produced a transcriptional signature in host cells characterized by very small numbers of upregulated genes (n=28) and a much larger number of downregulated genes (n=440) (**Figure 2** and Dataset S2). This observation suggests that infection by *Leishmania* species may have a suppressive effect on host transcription. Furthermore, the ability to infect the host cell in a very "silent" manner, causing minimal induction of host genes and enabling *Leishmania* to establish infection in the host macrophage and remain

protected from the host immune response, may be a phenomenon common to multiple *Leishmania* species.

Our meta-analysis indicated that the transcriptional response to *Trypanosoma* species was far more robust than the response to *Leishmania* species with 781 genes upregulated and 1810 genes downregulated (**Figure 3** and Dataset S3). This was the result of analyzing *in vivo* as well as *in vitro* experiments. The transcriptional responses to *in vivo* infection by *Trypanosoma congolense* (causative agent of bovine African Trypanosomiasis) (15) showed many commonalities with the transcriptional response to *in vitro* infection by *Trypanosoma cruzi* (12, 17, 21, 22). This was surprising since *T. cruzi* is an intracellular pathogen that replicates within the host cell cytoplasm, while *T. congolense* is an extracellular pathogen that replicates in the blood stream. It has previously been reported that *T. brucei*, an etiological agent of human African Trypanosomiasis that is related to *T. congolense*, can activate macrophages via direct stimulation through its Variable Surface Glycoprotein (VSG) as well as via induction of host IFNG (29-31). This may partially explain the similarity in host transcriptional response to *T. congolense* and *T. cruzi*.

In order to determine the biological function of genes induced or suppressed by the kinetoplastid pathogens, gene ontology analysis was performed. Very few biological processes were over-represented at a statistically significant level by the genes induced or suppressed by *Leishmania* species. The only over-represented biological process among genes upregulated by *Leishmania* was intracellular signalling cascade (Table 3). The two processes over-represented in genes downregulated by *Leishmania* were electron transport and oxidative phosphorylation (Table 4).

Genes upregulated by *Trypanosoma* species were involved in a number of immune-related biological processes, including immunity and defense, interferon-mediated immunity, and macrophage-mediated immunity (Table 3). This is consistent with the immune-related nature of *T. cruzi*-induced genes identified in this study (Table 2). Genes downregulated by *Trypanosoma* species were involved with several metabolic processes including lipid, fatty acid and steroid metabolism (Table 4).

2.5.3. Distinct signatures of classical, alternative and deactivation of macrophages

In addition to activation through engagement of PRRs, macrophages can also be activated by various cytokines. We therefore compared pathogen recognition programs to cytokine mediated activation programs in macrophages in order to assess the relationships between the infections and activation states. To first compare the relationship between classical activation, alternative activation, and deactivation of macrophages, we activated BMM with IFNG, IL-4, or IL-10, respectively, and compared the transcriptional profiles of these cells to that of untreated macrophages over a 24 h time course. Genes displaying significant changes in response to the three cytokine treatments were identified by performing multiclass analysis using SAM, and similarities in activation patterns were emphasized by hierarchical clustering. We found that IFNG, IL-4, and IL-10 produced distinct activation profiles in macrophages (**Figure 4A**). An analysis of genes significantly upregulated by IFNG, IL-4, or IL-10 in pairwise SAM analyses compared to untreated macrophages showed that the three cytokines induced mostly non-overlapping sets of genes (Table 5). Out of the 431 genes significantly induced by IFNG, only 38 were also induced by IL-10, and only 27 were also induced by IL-4 (**Figure 4B**). IL-10 and IL-4 only induced 10

of the same genes out of the 138 genes induced by IL-10 and the 108 genes induced by IL-4. The three sets shared only 2 genes in common.

As expected, IFNG induced a large cluster of interferon-stimulated genes that were not induced by IL-4 or IL-10 (e.g. *Ccl2, Ccl7,Gbp3, Gbp5, Gbp6, Ifi44, Ifit2, Ifi204, Ifih1, Ifit1, Ifit3, Ifi203, Ifi205, Ifi35, Isg20, Stat1, and Stat2*). IL-4 induced a number of novel or unclassified genes (*Atp6v0d2, 1810011H11RIK, 2410042D21RIK, Rnf181, Tmem144*) and genes not previously associated with alternative activation (*Erg2, Casp6, Chst7, Daglb, Il1rl2, Rab15, Raly*). For example, the PPAR binding protein (*Pparbp/Med1*) was induced by IL-4 and likely interacts with PPARG to act as a co-activator for this nuclear receptor. Diacylglycerol lipase beta (*Daglb*) could be involved in metabolic regulation by alternatively activated macrophages (32).

IL-10 induced its own distinct transcriptional signature in macrophages. Notable genes induced only by IL-10 include *IL-4ra, Ccl6, Il21r, Mmp8, Mmp19, Timp1, and Tlr1* (Table 5). Surprisingly, there were more genes (n = 38) induced in common by both IL-10 and IFNG (eg. *Casp4, Ccl12, Ccl4, Irf7, Ly6a, Socs3, Ifi47, Stat3*) than genes (n = 10) induced by both IL-10 and IL-4 (eg. *Dhrs9, Fcgr2b, Ptgs1, Tcfec*) (**Figure 4B**). However, one of the genes induced by IL-10 is *IL-4ra*, which is consistent with a previous study that suggested exposure to IL-10 enhanced responsiveness to IL-4 (33). Also of note is the induction of *Il21r*. IL-21 receptor shows significant sequence and structural homology to IL-4 receptor alpha and has been shown to augment alternative macrophage activation (34), further suggesting that IL-10 may indirectly promote alternative activation by increasing sensitivity to IL-4, IL-13 and IL-21.

In order to determine what biological processes and pathways are induced by each of the cytokines, we performed gene ontology analysis on genes upregulated by only one cytokine as well as on genes upregulated by more than one cytokine (Table 6). Gene ontology analysis of the genes induced by IL-4 alone did not reach statistical significance for any biological process classification. This is likely due to the smaller number of genes in this category as well as the fact that many of these genes are novel and have unknown functions, highlighting the need for additional work on IL-4 signaling in macrophages and its associated gene expression patterns. In contrast to IL-4 treatment, IL-10 and IFNG treatment produced unique gene lists that were enriched in the biological processes of immunity and defense and cytokine and chemokine mediated signaling pathways (Table 6). IL-10 activated genes were also enriched in lipid and fatty acid transport, while IFNG activated genes were enriched in interferon mediated immunity, T cell-mediated immunity, ligand-mediated signaling, signal transduction, macrophage-mediated immunity, and apoptosis (Table 6). As noted above, IFNG and IL-10 induced genes that fall into similar categories and were quite distinct from IL-4 induced genes.

2.5.4. IFNG activation signature in macrophages is more similar to TNF than IFNB.

TNF and IFNB contribute to the early inflammatory cytokine milieu and have both been shown to induce classical macrophage activation (1). In contrast to IFNG, which is produced mainly by lymphocytes, TNF and IFNB are cytokines that are often produced at the very early acute stages of an immune response by many other cell types (35, 36). While the IFNs initiate a signalling cascade that involves the JAK family of tyrosine kinases and STAT family of transcription factors (37, 38), TNF signals through TRAFs to activate the transcription factors NF-kB and AP-1 (39, 40).

Signalling via the IL-17 receptor has also been shown to occur through the adaptor molecule TRAF6 leading to the activation of NF-kB and AP-1, suggesting it may activate macrophages in a manner similar to TNF (41-43).

To determine the macrophage activation signatures following stimulation with TNF, IFNB, and IL-17 and their relationship with IFNG, macrophages were activated by IFNB, TNF and IL-17. To identify genes upregulated and downregulated by activation through these cytokines, the resulting data was analyzed by SAM via two-class unpaired statistical comparisons against untreated control macrophages. To compare gene expression changes between all of the different cytokines, multiclass SAM analysis followed by hierarchical clustering analysis was performed on the expression profiles of macrophages activated by IFNG, IFNB, TNF, and IL-17.

We found that the response to IFNG was most related to the response to TNF, whereas IFNB and IL-17 produced more distinct expression profiles (**Figure 5A**). This was surprising given that the interferons signal through overlapping JAK-STAT pathways, while TNF signals through a distinct NF-kB pathway. An analysis of the genes induced by TNF revealed a number of interferon-stimulated genes, suggesting that TNF may be inducing expression of an interferon by macrophages. This is consistent with a previous study which showed that TNF induces IFNB production in macrophages (44). To determine whether TNF induced IFNB, we measured the amount of IFNB mRNA in TNF-stimulated cells by qPCR. TNF-stimulated macrophages upregulated IFNB transcript starting at 2 h after stimulation and peaking at 6 h after stimulation (**Figure S7 A**). Although this explained why TNF induced the expression of interferon-stimulated genes, it did not explain why the macrophage response to TNF is more similar to the response to IFNG than to IFNB. Further analysis of the array data revealed that IFNG stimulation induced expression of TNF

(Table 5 and Table 7), while IFNB stimulation did not. To confirm this finding, we measured the expression of TNF in cells stimulated by IFNG or IFNB by qPCR. We found that IFNG induced significant levels of TNF transcript by 2 h after stimulation, while IFNB failed to induce TNF expression (**Figure S7 B**). In addition, we found through cytometric bead analysis (CBA) of culture supernatants that IFNG-stimulated macrophages secreted high levels of TNF protein by 6 h after stimulation (**Figure S7 C**). The level of TNF peaked at 12 h post-stimulation at approximately 400 pg/mL. These selective interactions between cytokine signalling pathways explain the similarity in gene expression observed for cytokines with disparate signalling pathways.

There was a significant overlap between the genes up-regulated by IFNG, IFNB, and TNF (**Figure 5B**). Of the 219 genes induced by TNF, 164 were also induced by IFNG, consistent with the observation that IFNG induced TNF production by macrophages (**Figure S7 B-C**) as described above. Genes induced by both TNF and IFNG included *Cxcl1, Ifi47, Mmp14, Nod2, Socs3, and Tnf* (Table 7). IFNG and IFNB also up-regulated many of the same genes (n=177) including *Ccl12, Ifi205, Irf7, Nod1, and Stat2* (Table 7). A subset of these genes (n=82) were induced by all three of the cytokines, including *Ccl4, Ccl5,Gbp3, Gbp5, Gbp6, Ifi203, Ifi204, Ifi35, Ifi44, Ifih1, Ifit1, Ifit2, Ifit3, Irf1, Isg20, Mmp13, Socs1, and Stat1* (Table 7). A number of genes were induced by only one cytokine; for example, the pattern recognition receptors *Tlr3, Tlr7,* and *Tlr8* are only induced by IFNB and not by TNF or IFNG.

Gene ontology analysis was performed on genes up-regulated by only one cytokine as well as on genes up-regulated by more than one cytokine. IFNG, TNF, and IFNB function in many of the same biological processes, including immunity and defense, interferon-mediated immunity, and macrophage-mediated immunity (Table

8). Although most of the enriched biological processes are shared between the three cytokines, a few are specific to individual cytokines. For example, only IFNG induced genes enriched for MHCII-mediated immunity (Table 8). TNF induced genes enriched for several unique processes such as neurogenesis and ectoderm development. IFNG and IFNB both induced genes in the biological processes of proteolysis and protein metabolism and modification, but TNF did not (Table 8).

Unexpectedly, IL-17 produced minimal transcriptional changes in comparison to the other cytokines. Only 7 genes were positively regulated based on pairwise SAM analysis against unstimulated controls (Table 9). Although several of the upregulated genes were genes also induced by IFNG, IFNB, and TNF (e.g.*Cxcl1, Oasl2, Phf11*), the magnitude of the upregulation was much lower. In order to determine whether the paucity of transcriptional responses to IL-17 was due to the lack of IL-17 receptor expression on BMMs, we stained BMMs with an anti-IL-17 receptor antibody for analysis by flow cytometry (**Figure S8**). We found that BMMs do express the IL-17 receptor, suggesting that transcriptional responses to IL-17 may require additional co-stimulation or pre-stimulation by another cytokine or antigen.

2.5.5. Relationship between pathogen and cytokine mediated macrophage activation

The PAMPS expressed by intracellular protozoans such as *T. cruzi* and *L. mexicana* are much less well characterized than those of bacterial pathogens. Comparing the transcriptional responses of macrophages infected with kinetoplastids to those of macrophages stimulated by various cytokines may provide insights as to the types of receptors these pathogens engage and the signalling pathways they initiate. In order to compare the transcriptional changes associated with cytokine signalling and intracellular pathogen infection, cluster analysis was performed on all

cytokine and pathogen arrays. This showed that innate activation by LPS was most closely related to classical activation by the cytokines IFNG and TNF (**Figure 6**). Activation by the cytokine IFNB was similar but not as closely related. This is consistent with a previous study showing that macrophage responses to LPS and immune complexes are more similar to classical activation than to alternative activation (45). The similarity between LPS and TNF can also be attributed to the induction of *Tnf* in macrophages stimulated with LPS (Table 1). Furthermore, flow cytometry analysis showed that TNF was produced by approximately 15% of BMMs 4 h post-stimulation by LPS (**Figure S9**).

Innate macrophage activation by the protozoan pathogens branched separately from classical activation. Instead, macrophages infected by *T. cruzi* and *L. mexicana* clustered with macrophages stimulated by IL-17, IL-10, and IL-4. This suggests that infection by kinetoplastids results in a macrophage activation state that is more similar to alternative macrophage activation and macrophage deactivation than to classical macrophage activation. Although there are signs of an IFN response at later time points of *T. cruzi* infection, this signature is not strong enough to affect the overall clustering results.

2.5.6. The transcriptional response of bone marrow-derived macrophages differs from that of identically treated thioglycollate-elicited macrophages

Historically, intra-peritoneal injection with Brewer's thioglycollate medium has been a convenient method to procure large numbers of macrophages for use in functional and biochemical studies (46). More recently, bone marrow-derived macrophages have become widely used for such experiments. The transcriptional profile of these two types of macrophages may be divergent. Since all transcriptional profiling studies to date have been performed using a single type of macrophage, it is

unknown how transcriptional responses may vary depending on the type of macrophage used.

To address this question, we treated BMMs and thioglycollate-elicited macrophages (TM) with the cytokines IFNG, TNF, and IL-4 and compared their transcriptional responses. We used hierarchical clustering analysis to identify the conditions in which the transcriptional responses were most similar. We found that arrays clustered based on the type of macrophage instead of the type of cytokine stimulation (**Figure 7A**). In order to determine whether this was due to differential expression of background transcripts or differential response to cytokine stimulation, we performed multiclass SAM analysis on only the bone marrow macrophage arrays. The genes identified from this analysis (n = 168) were then extracted from the thioglycollate macrophage dataset, and a hierarchical clustering analysis was performed (**Figure 7B**). We found that the arrays clustered based on the cytokine instead of the macrophage type, with the IFNG and TNF arrays clustering together and away from the IL-4 arrays irrespective of macrophage type. A similar result was obtained when the cluster analysis was performed on genes identified by a multiclass SAM analysis of only the thioglycollate arrays (n = 124) (**Figure 7C**). This shows that although the baseline transcriptional signatures of bone marrow-derived and thioglycollate-elicited macrophages are very different, the two types of macrophages respond to cytokines in a relatively similar fashion.

In order to determine more specific differences in gene induction in the two different types of macrophages, we analyzed genes upregulated by IFNG, TNF and IL-4 by pairwise SAM analysis to untreated controls for both thioglycollate and bone marrow-derived macrophages and compared the genes induced in the two types of macrophages (**Figures 7D-F**). Interestingly, a large number of genes induced by

these cytokines were specific for the type of macrophage used. IFNG induced 209 genes in both TMs and BMMs, 320 genes only in TMs, and 223 genes only in BMMs (**Figure 7D**). Only five genes were induced in both TMs and BMMs by IL-4, while seven genes were induced only in TMs and 104 genes were induced only in BMMs (**Figure 7E**). TNF induced 85 genes in both TMs and BMMs, 122 genes only in TMs, and 135 genes only in BMMs (**Figure 7F**). Table 10 shows specific genes induced by these cytokines in one or both types of macrophages. These results suggest that TMs are somewhat more predisposed to classical activation whereas BMMs are more predisposed to alternative activation. Future work will define the basal differences between these two types of macrophages and determine why they respond differently to different forms of activation.

2.6. Discussion

In this study, we have comprehensively evaluated the relationship between macrophage activation states induced by two intracellular protozoan parasites (*L. mexicana* and *T. cruzi*), a bacterial endotoxin (LPS), and various cytokines (IL-4, IL-10, IFNG, IFNB, TNF). We found that innate activation of mouse bone marrow-derived macrophages by LPS was most similar to classical macrophage activation by the cytokines IFNG and TNF. However, infection by the protozoan pathogens *T. cruzi* and *L. mexicana* elicited responses most similar to alternative activation by the Th2 cytokine IL-4 and to macrophage deactivation by the cytokine IL-10. Collectively, these results suggest that the macrophage activation state induced by kinetoplastid parasites is disparate from the activation state induced by bacterial PAMPs and Th1 cytokines.

The distinct signature of macrophage transcriptional responses to kinetoplastids is in contrast to a meta-analysis by Jenner and Young suggesting that immune cells respond to pathogens with a generalized common transcriptional program (47). Jenner and Young compiled data from 32 published microarray studies, representing 77 different host-pathogen interactions. A cluster of 511 genes were identified that appeared to be co-regulated across the entire dataset, and these genes were termed the "common host response." These transcripts were enriched for genes involved in the immune response against invading pathogens. In this study, we observed that the transcriptional response to the cytokines IFNG and TNF is highly related to the response to LPS. A meta-analysis of the microarrays from this study and the Jenner and Young "common host response" genes indicated that the cluster of genes shared by classical activation cytokines and LPS is highly related to the human common host response genes (**Figure S10**). This cluster includes many genes

involved in the immune response, such as *Nfkb*, *Irf1*, *Irf7*, *Ifit1*, *Ifit2*, and *Myd88*. However, the transcriptional signature of early time points during kinetoplastid infection is clearly distinct from this common host response, highlighting again the difference between these protozoan parasites and bacterial pathogens.

The variability we found between pathogens/pathogen products likely reflect the differences in pattern recognition receptors utilized by each pathogen. Both protozoan pathogens induced fewer transcriptional responses than LPS, consistent with previous microarray studies comparing infection of macrophages by protozoan and non-protozoan pathogens (19). However, *T. cruzi* induced a number of interferon stimulated genes by 24 h post-infection, consistent with a recent study by Chessler et al showing upregulation of interferon-stimulated genes in mice 24 h following intradermal infection with *T. cruzi* (22). The upregulation of interferon-stimulated genes has been shown to be dependent on the induction of IFNB via signalling through a novel toll-like receptor-independent pathway (27, 28, 48).

The timing of the IFNB-induced gene upregulation in *T. cruzi*-infected macrophages is consistent with a previous study performed by de Avalos et al that implicated *T. cruzi* escape from a parasitophorous vacuole into the cytoplasm (21). A possible explanation for the differences in responses to the two protozoan pathogens is that they reside in different intracellular compartments. *Leishmania* persists in a membrane-bound vacuole within the cell, while *T. cruzi* leaves this compartment within hours to freely replicate in the macrophage cytoplasm. Strikingly, infection by *L. mexicana* was so transcriptionally "silent" that the resulting activation profile was almost indistinguishable from uninfected cells. This is consistent with several other studies showing limited responses in various host tissues to various species of *Leishmania* (13, 14, 16, 19, 20). One explanation for this silent infection could be

that *Leishmania* shields itself from host detection by residing within the parasitophorous vacuole. Another explanation is that *L. mexicana* does not express any potent pattern recognition ligands and therefore cannot activate the host cell. A third explanation is that the parasite is actively suppressing host responses via binding of a host receptor or secretion of a virulence factor that interferes with the inflammatory response. Evidence for this explanation can be found in previous studies which have shown that *Leishmania* species can down-modulate macrophage responses using a variety of mechanisms (49, 50). *L. mexicana* amastigotes have been shown to inhibit IL-12 production by disrupting the NF-kB signalling pathway (51, 52). This has been shown to downregulate the Th1 response in infected mice, leading to increased pathology (53). Any one or a combination of these factors may play a role in the transcriptional silence of macrophages infected by *L. mexicana*.

The protozoan pathogens *T. cruzi* and *L.mexicana* produced transcriptional signatures in infected macrophages that were more closely related to alternative macrophage activation and macrophage deactivation than to classical macrophage activation. This lends support to studies showing that immunization with the immunodominant *T. cruzi* antigen, cruzipain, results in increased Th2 cytokine secretion (54) and increased arginase activity (55). The induction of alternatively activated macrophages in *T. cruzi* infection results in persistent parasite growth within the cells (56), suggesting that *T. cruzi* may evade the host immune response by promoting alternative macrophage activation. The similarity in the transcriptional signatures resulting from *L. mexicana* infection and IL-10 stimulation is consistent with studies showing that *Leishmania* induces IL-10 during infection and that IL-10 plays an essential role in *Leishmania* pathogenesis (57-59). These studies have demonstrated that IL-10 is induced via FcGR ligation by opsonized parasites (57, 59).

Hence, IL-10 may play a role in dampening the transcriptional response of macrophages to *Leishmania* infection.

Our analysis of macrophage responses to cytokine stimulation revealed stark differences in the activation profile of macrophages treated with IL-4 relative to macrophages treated with IFNG or IL-10 (**Figure 2** and Table 5). A number of genes have been previously classified as markers of alternative macrophage activation (60), but were not identified in our analysis of genes induced by IL-4 (Table 5). These include *Ym1*/*Ym2* (*Chi3l3*/*Chi3l4*), *Fizz1/Relm-alpha* (*Retnla*), and *Arg1*. Because these genes are so specifically regulated by IL-4 and are not expressed under other conditions included in this study, they did not pass our pre-analysis filter of being 'present in at least 70% of arrays' and were not included in the final dataset used for statistical analysis by SAM (Dataset S1). This problem highlights a limitation of our analysis, in that genes that are expressed at very low levels and induced very specifically by individual cytokines may be filtered out of the overall analysis. When the data for these specific markers of alternative activation were extracted from the unfiltered dataset, they are clearly upregulated in IL-4 stimulated BMMs, as shown in **Figure S6**.

By conducting the experiments as time courses over 24 hours and grouping the time points for analysis, our statistical comparisons identify genes that are consistently up or down-regulated. Although important kinetic information is still preserved upon more detailed analysis (e.g. the identification of a late 24 h interferon response in *T. cruzi* infection), such detailed kinetic data cannot be extracted statistically due to the absence of sufficient replicates for each time point. Although we have added additional biological replicates to our kinetoplastid infections,

resources have limited our ability to replicate the time courses for all of the different cytokines.

Despite the limitations described above, we have for the first time directly compared global gene expression profiles from macrophages activated by a diverse group of biologically important cytokines and pathogens. This dataset will be valuable to both the parasitology and macrophage biology communities as a resource for future experiments. Our data identified unique properties of classically activated, alternatively activated and deactivated macrophages as well as identified unexpected relationships between macrophage responses to pathogens and cytokines.

The functional phenotypes of macrophages in peripheral tissues depend on both their origin and the cytokine microenvironment to which they are exposed. In addition to the relationships between pathogen infection and cytokine stimulation, we have also evaluated the importance of macrophage origin on these transcriptional studies. The activation profiles of bone marrow derived macrophages were distinct from those of identically treated thioglycollate-elicited macrophages. Discrepancies between studies investigating macrophage activation can be at least partly attributed to the use of different types of macrophages. However, we observed that the two types of macrophage produced a similar transcriptional response to activation stimuli, indicating that although baseline gene expression in these macrophages is different, signalling and transcriptional responses are largely shared. Further understanding of the underlying mechanism for the differences between various types of macrophages will be important to the study of both macrophage biology and host-pathogen interactions.

2.7. Acknowledgements

We thank Juan Engel and Patricia Doyle-Engel for help with *L. mexicana* and *T. cruzi* experiments. We thank A. Carroll, P. Nittler, and K. Hermens (UCSF Center for Advanced Technology) for help with printing MEEBO arrays. We thank the P01 group, Intracellular Pathogens and Innate Immunity for helpful discussions. We thank Steve Zhang for writing Perl scripts that greatly facilitated the data analysis.

2.8. References

1. Mosser DM. The many faces of macrophage activation. J Leukoc Biol. 2003;73(2):209-12.

2. Adams DO, Hamilton TA. The cell biology of macrophage activation. Annu Rev Immunol. 1984;2:283-318.

3. Janeway CA, Jr., Medzhitov R. Innate immune recognition. Annu Rev Immunol. 2002;20:197-216.

4. Harty JT, Tvinnereim AR, White DW. CD8+ T cell effector mechanisms in resistance to infection. Annu Rev Immunol. 2000;18:275-308.

5. Gordon S. Alternative activation of macrophages. Nat Rev Immunol. 2003;3(1):23-35.

6. Fiorentino DF, Zlotnik A, Mosmann TR, Howard M, O'Garra A. IL-10 inhibits cytokine production by activated macrophages. J Immunol. 1991;147(11):3815-22.

7. Fadok VA, Bratton DL, Konowal A, Freed PW, Westcott JY, Henson PM. Macrophages that have ingested apoptotic cells in vitro inhibit proinflammatory cytokine production through autocrine/paracrine mechanisms involving TGF-beta, PGE2, and PAF. J Clin Invest. 1998;101(4):890-8.

8. Mantovani A, Sica A, Locati M. Macrophage polarization comes of age. Immunity. 2005;23(4):344-6.

9. Nau GJ, Richmond JF, Schlesinger A, Jennings EG, Lander ES, Young RA. Human macrophage activation programs induced by bacterial pathogens. Proc Natl Acad Sci U S A. 2002;99(3):1503-8.

10. McCaffrey RL, Fawcett P, O'Riordan M, Lee KD, Havell EA, Brown PO, et al. A specific gene expression program triggered by Gram-positive bacteria in the cytosol. Proc Natl Acad Sci U S A. 2004;101(31):11386-91.

11. Der SD, Zhou A, Williams BR, Silverman RH. Identification of genes differentially regulated by interferon alpha, beta, or gamma using oligonucleotide arrays. Proc Natl Acad Sci U S A. 1998;95(26):15623-8.

12. Shigihara T, Hashimoto M, Shindo N, Aoki T. Transcriptome profile of Trypanosoma cruzi-infected cells: simultaneous up- and down-regulation of proliferation inhibitors and promoters. Parasitol Res. 2008;102(4):715-22.

13. Osorio y Fortea J, de La Llave E, Regnault B, Coppee JY, Milon G, Lang T, et al. Transcriptional signatures of BALB/c mouse macrophages housing multiplying Leishmania amazonensis amastigotes. BMC Genomics. 2009;10:119. PMCID: 2666765.

14. Gregory DJ, Sladek R, Olivier M, Matlashewski G. Comparison of the effects of Leishmania major or Leishmania donovani infection on macrophage gene expression. Infect Immun. 2008;76(3):1186-92. PMCID: 2258831.

15. Fisher P, Hedeler C, Wolstencroft K, Hulme H, Noyes H, Kemp S, et al. A systematic strategy for large-scale analysis of genotype phenotype correlations: identification of candidate genes involved in African trypanosomiasis. Nucleic Acids Res. 2007;35(16):5625-33. PMCID: 2018629.

16. Ettinger NA, Wilson ME. Macrophage and T-Cell Gene Expression in a Model of Early Infection with the Protozoan Leishmania chagasi. PLoS Negl Trop Dis. 2008;2(6):e252. PMCID: 2427198.

17. Costales JA, Daily JP, Burleigh BA. Cytokine-dependent and-independent gene expression changes and cell cycle block revealed in Trypanosoma cruzi-infected host cells by comparative mRNA profiling. BMC Genomics. 2009;10:252. PMCID: 2709661.

18. Buates S, Matlashewski G. General suppression of macrophage gene expression during Leishmania donovani infection. J Immunol. 2001;166(5):3416-22.

19. Chaussabel D, Semnani RT, McDowell MA, Sacks D, Sher A, Nutman TB. Unique gene expression profiles of human macrophages and dendritic cells to phylogenetically distinct parasites. Blood. 2003;102(2):672-81.

20. Rodriguez NE, Chang HK, Wilson ME. Novel program of macrophage gene expression induced by phagocytosis of Leishmania chagasi. Infect Immun. 2004;72(4):2111-22.

21. Vaena de Avalos S, Blader IJ, Fisher M, Boothroyd JC, Burleigh BA. Immediate/early response to Trypanosoma cruzi infection involves minimal modulation of host cell transcription. J Biol Chem. 2002;277(1):639-44.

22. Chessler AD, Unnikrishnan M, Bei AK, Daily JP, Burleigh BA. Trypanosoma cruzi triggers an early type I IFN response in vivo at the site of intradermal infection. J Immunol. 2009;182(4):2288-96.

23. Mueller A, O'Rourke J, Chu P, Kim CC, Sutton P, Lee A, et al. Protective immunity against Helicobacter is characterized by a unique transcriptional signature. Proc Natl Acad Sci U S A. 2003;100(21):12289-94. PMCID: 218751.

24. Medzhitov R, Preston-Hurlburt P, Janeway CA, Jr. A human homologue of the Drosophila Toll protein signals activation of adaptive immunity. Nature. 1997;388(6640):394-7.

25. Beutler B, Rietschel ET. Innate immune sensing and its roots: the story of endotoxin. Nat Rev Immunol. 2003;3(2):169-76.

26. Bennett CL, Misslitz A, Colledge L, Aebischer T, Blackburn CC. Silent infection of bone marrow-derived dendritic cells by Leishmania mexicana amastigotes. Eur J Immunol. 2001;31(3):876-83.

27. Koga R, Hamano S, Kuwata H, Atarashi K, Ogawa M, Hisaeda H, et al. TLR-dependent induction of IFN-beta mediates host defense against Trypanosoma cruzi. J Immunol. 2006;177(10):7059-66.

28. Tarleton RL. Immune system recognition of Trypanosoma cruzi. Curr Opin Immunol. 2007;19(4):430-4.

29. Mansfield JM. Immunology of African trypanosomiasis. Wyler DJ, editor. New York: W. H. Freeman and Co.; 1990.

30. Schleifer KW, Filutowicz H, Schopf LR, Mansfield JM. Characterization of T helper cell responses to the trypanosome variant surface glycoprotein. J Immunol. 1993;150(7):2910-9.

31. Paulnock DM, Coller SP. Analysis of macrophage activation in African trypanosomiasis. J Leukoc Biol. 2001;69(5):685-90.

32. Odegaard JI, Ricardo-Gonzalez RR, Goforth MH, Morel CR, Subramanian V, Mukundan L, et al. Macrophage-specific PPARgamma controls alternative activation and improves insulin resistance. Nature. 2007;447(7148):1116-20.

33. Lang R, Patel D, Morris JJ, Rutschman RL, Murray PJ. Shaping gene expression in activated and resting primary macrophages by IL-10. J Immunol. 2002;169(5):2253-63.

34. Pesce J, Kaviratne M, Ramalingam TR, Thompson RW, Urban JF, Jr., Cheever AW, et al. The IL-21 receptor augments Th2 effector function and alternative macrophage activation. J Clin Invest. 2006;116(7):2044-55. PMCID: 1479424.

35. Pfeffer K. Biological functions of tumor necrosis factor cytokines and their receptors. Cytokine Growth Factor Rev. 2003;14(3-4):185-91.

36. Durbin JE, Fernandez-Sesma A, Lee CK, Rao TD, Frey AB, Moran TM, et al. Type I IFN modulates innate and specific antiviral immunity. J Immunol. 2000;164(8):4220-8.

37. Schindler C, Shuai K, Prezioso VR, Darnell JE, Jr. Interferon-dependent tyrosine phosphorylation of a latent cytoplasmic transcription factor. Science. 1992;257(5071):809-13.

38. Silvennoinen O, Ihle JN, Schlessinger J, Levy DE. Interferon-induced nuclear signalling by Jak protein tyrosine kinases. Nature. 1993;366(6455):583-5.

39. Dempsey PW, Doyle SE, He JQ, Cheng G. The signaling adaptors and pathways activated by TNF superfamily. Cytokine Growth Factor Rev. 2003;14(3-4):193-209.

40. Hsu H, Shu HB, Pan MG, Goeddel DV. TRADD-TRAF2 and TRADD-FADD interactions define two distinct TNF receptor 1 signal transduction pathways. Cell. 1996;84(2):299-308.

41. Schwandner R, Yamaguchi K, Cao Z. Requirement of tumor necrosis factor receptor-associated factor (TRAF)6 in interleukin 17 signal transduction. J Exp Med. 2000;191(7):1233-40. PMCID: 2193168.

42. Hunter CA. Act1-ivating IL-17 inflammation. Nat Immunol. 2007;8(3):232-4.

43. Shen F, Hu Z, Goswami J, Gaffen SL. Identification of common transcriptional regulatory elements in interleukin-17 target genes. J Biol Chem. 2006;281(34):24138-48.

44. Yarilina A, Park-Min KH, Antoniv T, Hu X, Ivashkiv LB. TNF activates an IRF1-dependent autocrine loop leading to sustained expression of chemokines and STAT1-dependent type I interferon-response genes. Nat Immunol. 2008;9(4):378-87.

45. Edwards JP, Zhang X, Frauwirth KA, Mosser DM. Biochemical and functional characterization of three activated macrophage populations. J Leukoc Biol. 2006;80(6):1298-307.

46. Cohn ZA. Activation of mononuclear phagocytes: fact, fancy, and future. J Immunol. 1978;121(3):813-6.

47. Jenner RG, Young RA. Insights into host responses against pathogens from transcriptional profiling. Nat Rev Microbiol. 2005;3(4):281-94.

48. Chessler AD, Ferreira LR, Chang TH, Fitzgerald KA, Burleigh BA. A novel IFN regulatory factor 3-dependent pathway activated by trypanosomes triggers IFN-beta in macrophages and fibroblasts. J Immunol. 2008;181(11):7917-24. PMCID: 2597000.

49. Alexander J, Satoskar AR, Russell DG. Leishmania species: models of intracellular parasitism. J Cell Sci. 1999;112 Pt 18:2993-3002.

50. Kane MM, Mosser DM. Leishmania parasites and their ploys to disrupt macrophage activation. Curr Opin Hematol. 2000;7(1):26-31.

51. Cameron P, McGachy A, Anderson M, Paul A, Coombs GH, Mottram JC, et al. Inhibition of lipopolysaccharide-induced macrophage IL-12 production by Leishmania mexicana amastigotes: the role of cysteine peptidases and the NF-kappaB signaling pathway. J Immunol. 2004;173(5):3297-304.

52. Weinheber N, Wolfram M, Harbecke D, Aebischer T. Phagocytosis of Leishmania mexicana amastigotes by macrophages leads to a sustained suppression of IL-12 production. Eur J Immunol. 1998;28(8):2467-77.

53. Buxbaum LU, Denise H, Coombs GH, Alexander J, Mottram JC, Scott P. Cysteine protease B of Leishmania mexicana inhibits host Th1 responses and protective immunity. J Immunol. 2003;171(7):3711-7.

54. Giordanengo L, Guinazu N, Stempin C, Fretes R, Cerban F, Gea S. Cruzipain, a major Trypanosoma cruzi antigen, conditions the host immune response in favor of parasite. Eur J Immunol. 2002;32(4):1003-11.

55. Stempin C, Giordanengo L, Gea S, Cerban F. Alternative activation and increase of Trypanosoma cruzi survival in murine macrophages stimulated by cruzipain, a parasite antigen. J Leukoc Biol. 2002;72(4):727-34.

56. Stempin CC, Tanos TB, Coso OA, Cerban FM. Arginase induction promotes Trypanosoma cruzi intracellular replication in Cruzipain-treated J774 cells through the activation of multiple signaling pathways. Eur J Immunol. 2004;34(1):200-9.

57. Buxbaum LU, Scott P. Interleukin 10- and Fcgamma receptor-deficient mice resolve Leishmania mexicana lesions. Infect Immun. 2005;73(4):2101-8.

58. Jones DE, Ackermann MR, Wille U, Hunter CA, Scott P. Early enhanced Th1 response after Leishmania amazonensis infection of C57BL/6 interleukin-10-deficient mice does not lead to resolution of infection. Infect Immun. 2002;70(4):2151-8.

59. Kane MM, Mosser DM. The role of IL-10 in promoting disease progression in leishmaniasis. J Immunol. 2001;166(2):1141-7.

60. Loke P, Nair MG, Parkinson J, Guiliano D, Blaxter M, Allen JE. IL-4 dependent alternatively-activated macrophages have a distinctive in vivo gene expression phenotype. BMC Immunol. 2002;3:7.

2.9. Figure legends

Figure 1 - Comparison of transcriptional responses following infection by the intracellular pathogens *Leishmania mexicana* and *Trypanosoma cruzi* and following stimulation by LPS

A. Unsupervised two-dimensional cluster analysis was performed on genes exhibiting statistically significant variability between the three conditions, as determined by multiclass SAM (n=636). Replicate experiments of *L. mexicana* (n=3) and *T. cruzi* (n=2) infection were averaged prior to cluster analysis. B. Close-up of gene cluster upregulated by LPS and the 24 h timepoint of *T. cruzi*. This cluster includes many interferon-stimulated genes which are not induced by *L. mexicana*. C. The Venn diagram depicts the overlap of genes significantly upregulated, as determined by pairwise SAM analysis to uninfected controls, by *L. mexicana*, *T. cruzi*, LPS, both *T. cruzi* and LPS, both *T. cruzi* and *L. mexicana*, and both *L. mexicana* and LPS. There were no genes significantly upregulated by all three conditions.

Figure 2 – Comparison of transcriptional response to *Leishmania* infection compiled from this study and previous microarray studies

Meta-analysis was performed on the transcriptional response to *Leishmania* infection using data from this study and 5 additional studies. The heatmap shows genes upregulated (n=28) and downregulated (n=440) by *Leishmania* species. List of genes are shown in Dataset S2.

hMDC - human monocyte-derived dendritic cells

hMDM - human monocyte-derived macrophages

mBMM - mouse bone marrow-derived macrophages

hMDMT - human monocyte-derived macrophages and T cells

mTEM - mouse thioglycollate-elicited macrophages

Figure 3 – Comparison of transcriptional response to *Trypanosoma* infection compiled from this study and previous microarray studies

Meta-analysis was performed on the transcriptional response to *Trypanosoma* infection using data from this study and 5 additional studies. The heatmap shows genes upregulated (n=781) and downregulated (n=1810) by *Trypanosoma* species. List of genes are shown in Dataset S3.

hFF - human foreskin fibroblasts

mKID - mouse whole kidney

mLIV - mouse whole liver

mSPL - mouse whole spleen

HeLa - HeLa cells

mSKN - mouse whole skin

hSMC - human vascular smooth muscle cells

hCEC - human cardiac microvascular endothelial cells

mBMM - mouse bone marrow-derived macrophages

Figure 4 - Comparison of transcriptional responses to classical activation, alternative activation, and macrophage deactivation

A. Unsupervised two-dimensional cluster analysis was performed on genes exhibiting statistically significant variability between the three conditions, as determined by multiclass SAM (n=1489). B. The Venn diagram depicts the overlap of genes significantly upregulated, as determined by pairwise SAM analysis to unstimulated

controls, by IFNG, IL-4, IL-10, both IFNG and IL-4, both IFNG and IL-10, both IL-4 and IL-10, and all three cytokines.

Figure 5 - Comparison of transcriptional responses to cytokines implicated in classical macrophage activation

A. Unsupervised two-dimensional cluster analysis was performed on genes exhibiting statistically significant variability between stimulation with IFNG, IFNB, TNF, and IL-17, as determined by multiclass SAM (n=773). B. The Venn diagram depicts the overlap of genes significantly upregulated, as determined by pairwise SAM analysis to unstimulated controls, by IFNG, IFNB, TNF, both IFNG and IFNB, both IFNG and TNF, both IFNB and TNF, and all three cytokines.

Figure 6 - Comparison of transcriptional responses to cytokines and intracellular parasites

Unsupervised two-dimensional cluster analysis was performed on all pathogen and cytokine arrays, using genes exhibiting statistically significant variability between these conditions, as determined by SAM (n=5414). Arrays in red text highlight the relationship between cytokines involved in classical macrophage activation and the bacterial antigen LPS. Arrays in blue text highlight the relationship between the protozoan pathogens *L. mexicana* and *T. cruzi* and the cytokines IL-4, IL-10, and IL-17.

Figure 7 - Differences in the transcriptional response in differentially derived macrophages

A. Unsupervised two-dimensional cluster analysis was performed on genes exhibiting statistically significant variability between the 6 groups (n=3671): IFNG stimulation of bone marrow macrophages, TNF stimulation of bone marrow macrophages, IL-4

stimulation of bone marrow macrophages, IFNG stimulation of thioglycollate macrophages, TNF stimulation of thioglycollate macrophages, and IL-4 stimulation of thioglycollate macrophages. Arrays clustered based on the type of macrophage, not the type of cytokine. B. Multiclass SAM analysis was performed on arrays representing IFNG, TNF, and IL-4 stimulation of bone marrow macrophages. Cluster analysis was performed on genes exhibiting statistically significant differences amongst bone marrow derived macrophages only (n=168). Arrays clustered based on the type of cytokine, not the type of macrophage. C. Multiclass SAM analysis was performed on arrays representing IFNG, TNF, and IL-4 stimulation of thioglycollate macrophages. Cluster analysis was performed on genes exhibiting statistically significant differences amongst thioglycollate macrophages only (n=124). Arrays clustered based on the type of cytokine, not the type of macrophage. D. Genes induced by IFNG in thioglycollate-elicited macrophages (TM) were compared to genes induced by IFNG in bone marrow-derived macrophages (BMM). E. Genes induced by IL-4 in TMs were compared to genes induced by IL-4 in BMMs. F. Genes induced by TNF in TMs were compared to genes induced by TNF in BMMs.

2.10. Figures

Figure 1 - Comparison of transcriptional responses following infection by the intracellular pathogens *Leishmania mexicana* and *Trypanosoma cruzi* and following stimulation by LPS

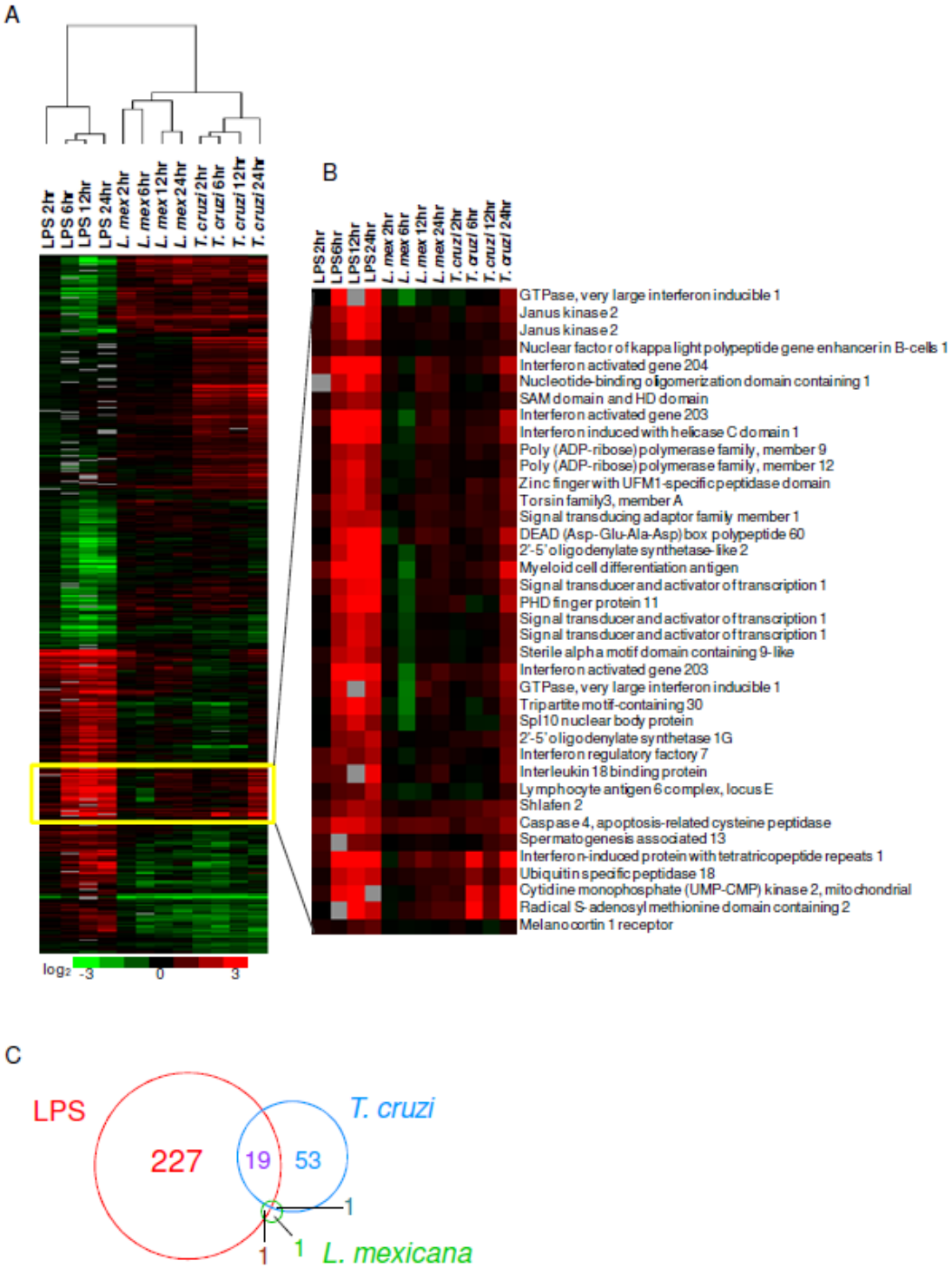

Figure 2 – Comparison of transcriptional response to *Leishmania* infection compiled from this study and previous microarray studies

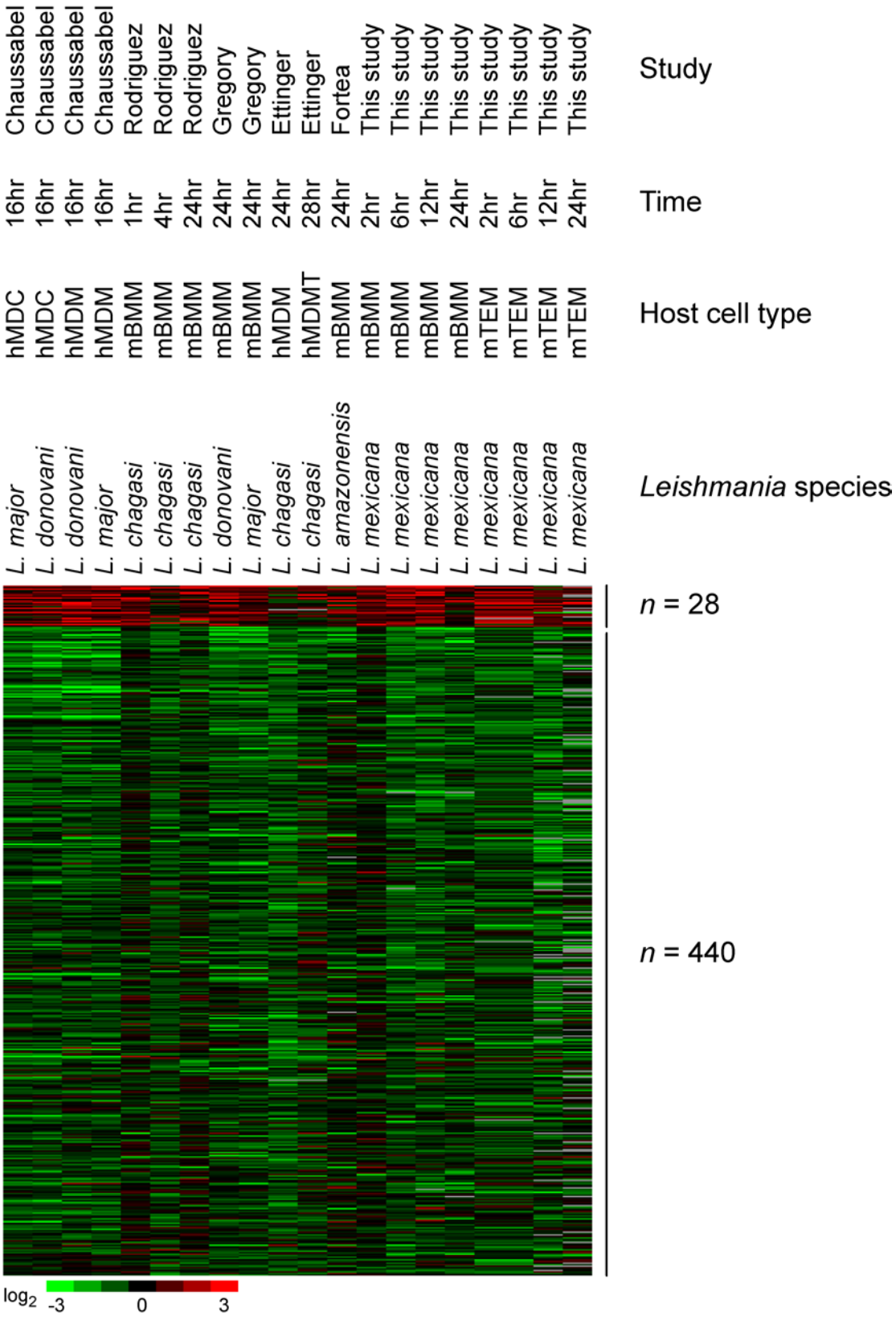

Figure 3 – Comparison of transcriptional response to *Trypanosoma* infection compiled from this study and previous microarray studies

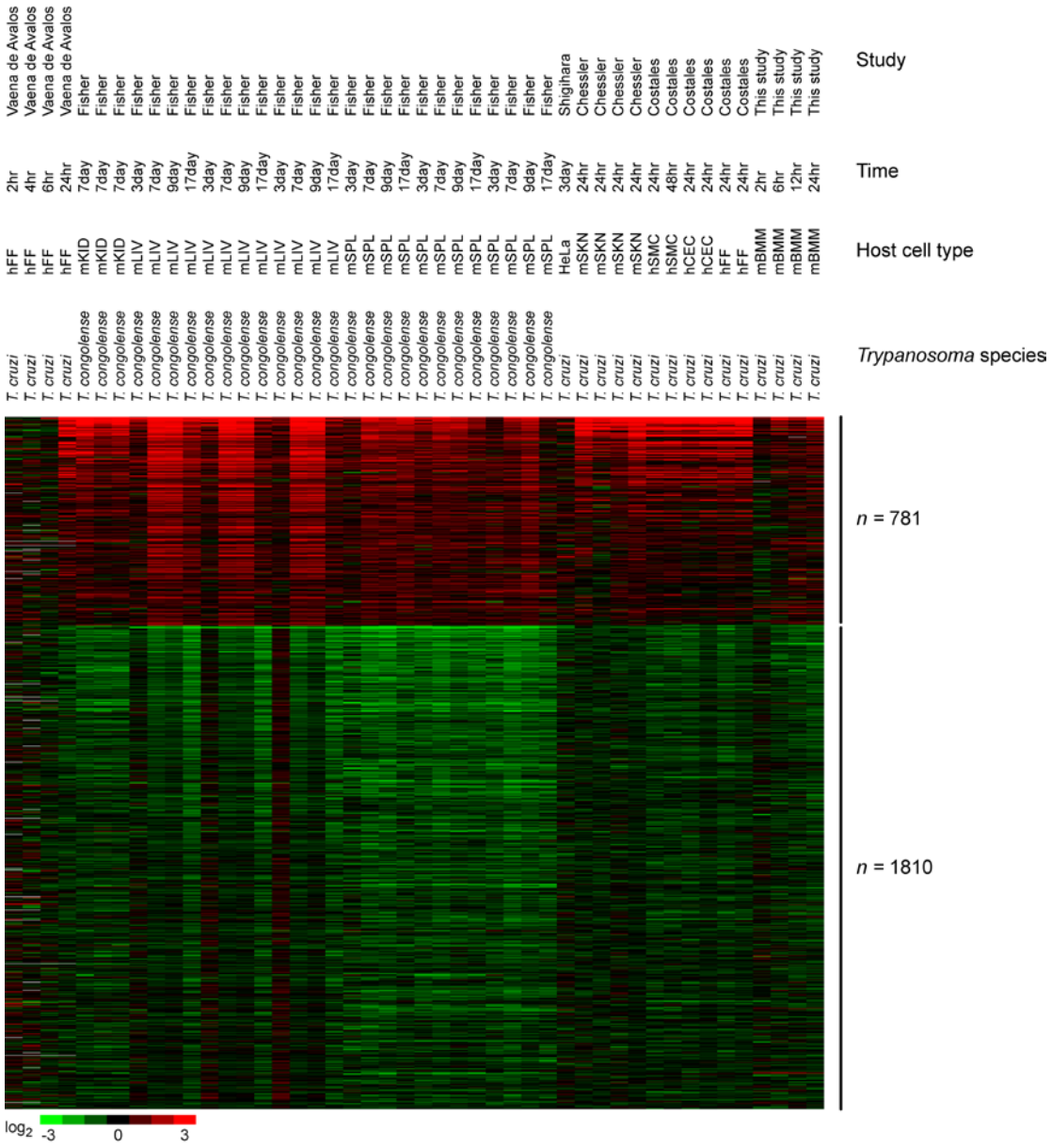

Figure 4 - Comparison of transcriptional responses to classical activation, alternative activation, and macrophage deactivation

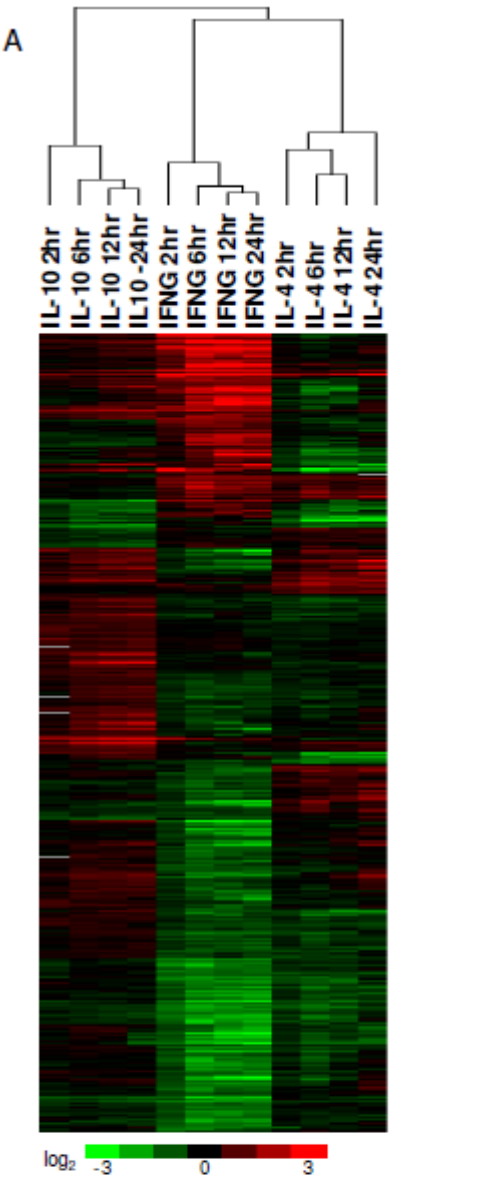

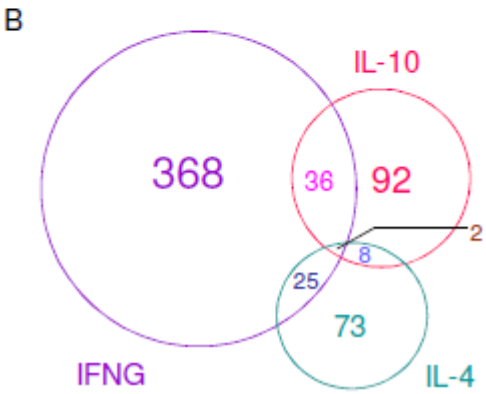

Figure 5 - Comparison of transcriptional responses to cytokines implicated in classical macrophage activation

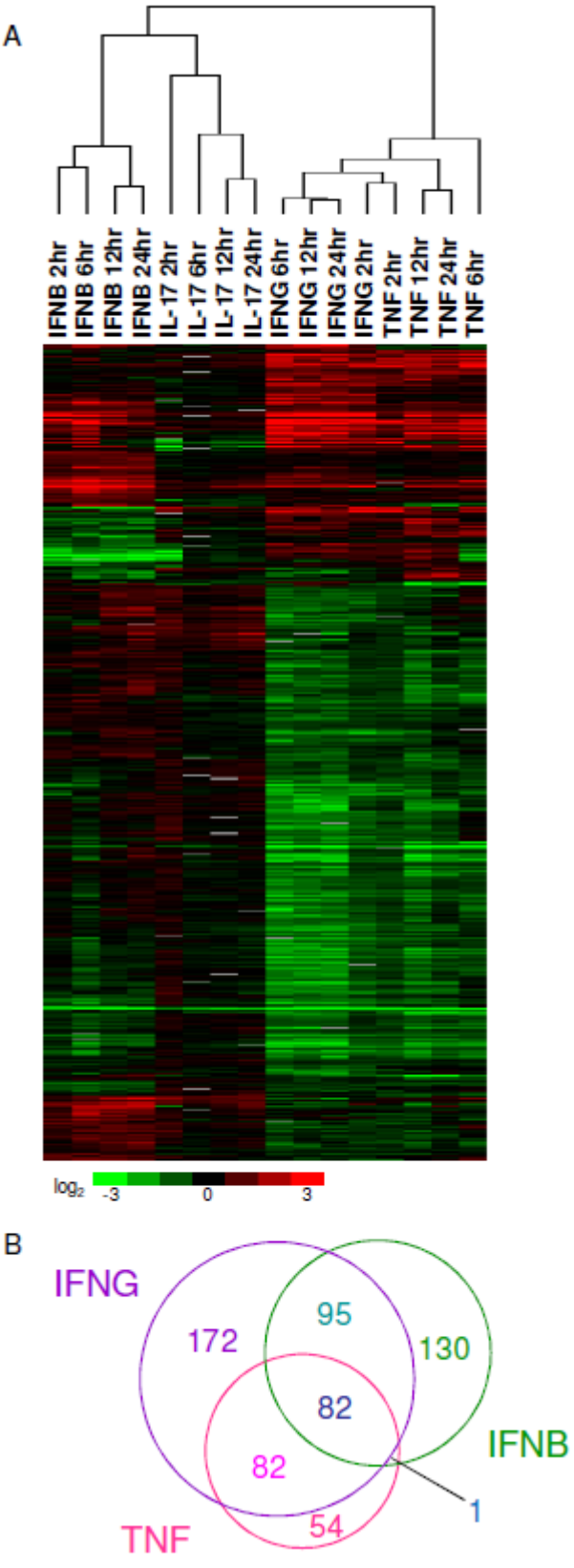

Figure 6 - Comparison of transcriptional responses to cytokines and intracellular parasites

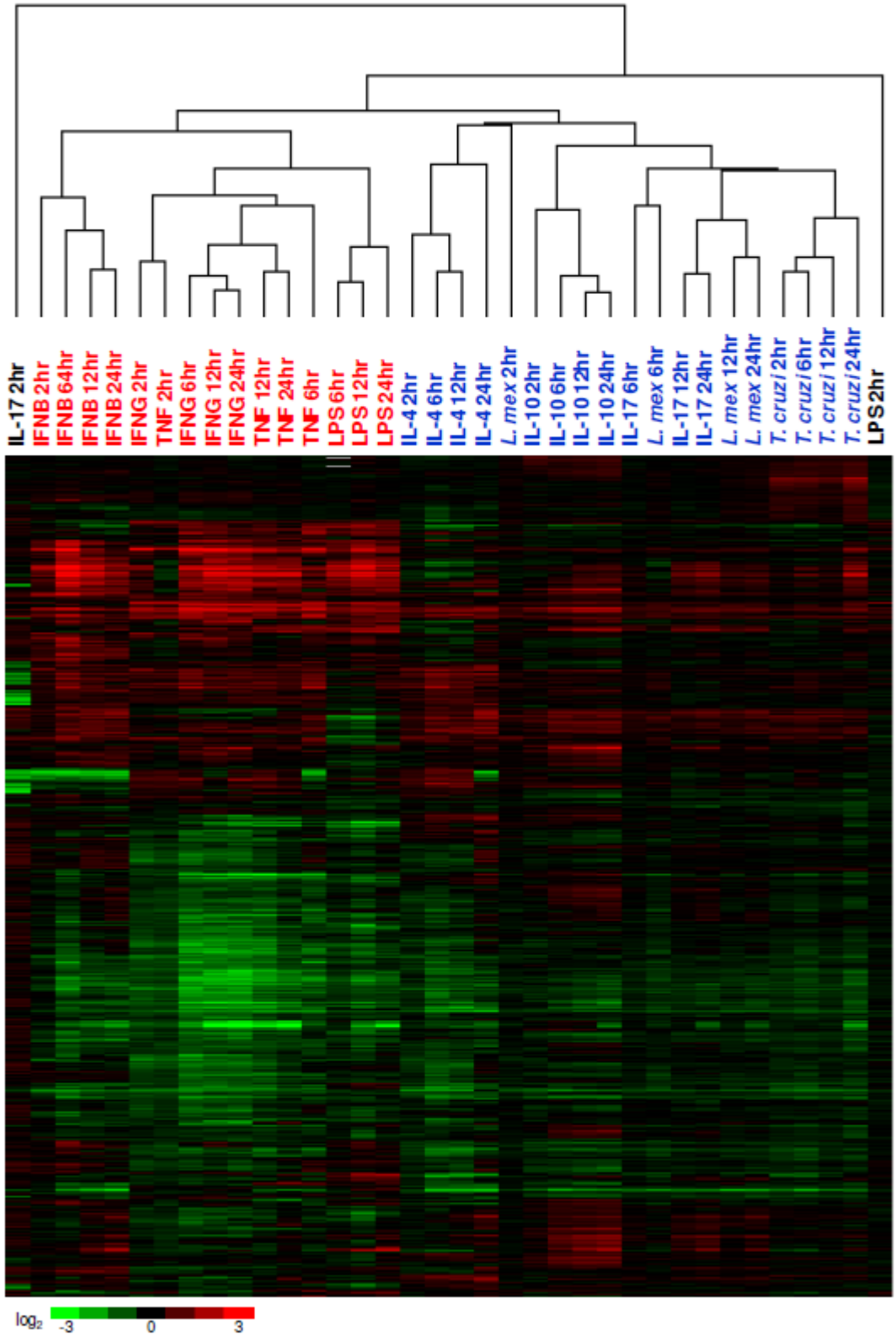

Figure 7 - Differences in the transcriptional response in differentially derived macrophages

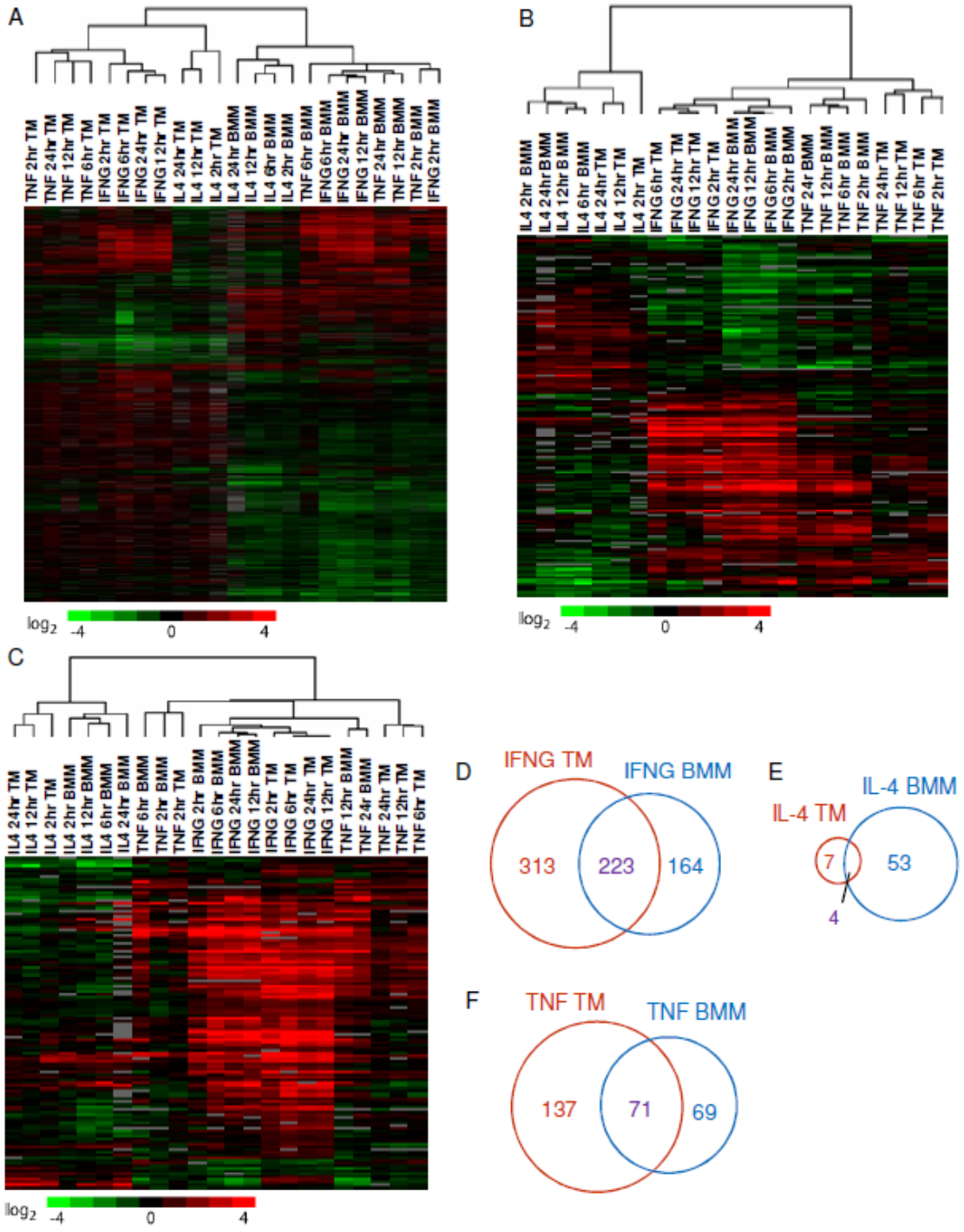

2.11. Tables

Table 1 - Comparison of genes induced by *L. mexicana*, *T. cruzi*, and LPS

Expression ratio (log2) of genes induced by one pathogen/pathogen product only			
Pathogen/ pathogen product	**>3**	**2-3**	**1-2**
L. mexicana			*Mt2*
T. cruzi	*Ccdc54, Derl1, Lce1i*	*Col16a1, Sycn, Wipi1*	*0610010O12Rik, 1700029M20Rik, 1700049J03Rik, 1700113H21Rik, 2300005B03Rik, 2610007O09Rik, 2610034N15Rik, 2810030D12Rik, 9430076C15Rik, A130038J17Rik, Angptl4, Apba2, Atp1b1, BC023814, Bcl6b, Bhlhe41, Cbfa2t3, Chrna4, Dio2, EG330070, Ebag9, Fibcd1, Hspb8, Ifrd1, Igdcc3, Inpp4a, Mcts2, Naca, Nat15, Nat6, Olfr380, Osm, Ppm2c, Ppp1r1c, Prss33, Rgs1, Rnf216, Slc25a19, Slc25a22, Snx5, Sphk1, Tbl3, Tnfrsf9, Tspan17, Ugt1a10, Usp42, Zbtb48*
LPS	*Ccl12, Ch25h, Cxcl1, Nfkbiz*	*Adora2b, Bcl2a1c, Cav1, Ccl4, Ctsc, Cxcl2, Ddx60, Dusp1, Ell2, Ets2, Fcgr1, Fos, Glrx, Gpr85, Gvin1, Hspa1b, Ifi205, Ifih1, Jag1, Lcp2, Lpar1, Marcksl1, Ms4a6b, Oasl2, Plek, Slco3a1, Slfn4, Slfn5, Socs3, Stat1, Trim30*	*1200003I10Rik, 1200016E24Rik, 9230105E10Rik, AI451617, Abca1, Adar, Agrn, Aif1, Ak3l1, Alas1, Arhgef3, Ass1, Axud1, Azi2, Bcl2a1b, Bst1, C330023M02Rik, Casp4, Ccdc50, Ccr5, Cd302, Cd40, Cd52, Cd69, Cdkn1a, Chst7, Clec4e, Clec5a, Clic4, Cpd, Creb5, Ctla2b, Cx3cr1, Cxcl16, Cybb, Cysltr1, D14Ertd668e, Dck, Dcp2, Ddx58, Dtx3l, Dusp16, Ehd1, Eif2ak2, Epsti1, Errfi1, Fas, Fbxw17, Fgr, Filip1l, Flrt3, Fmnl2, Fndc3a, Gbp2, Gbp5, Gch1, Gda, Ggct, Glipr2, Gpd2, Gpr84, H2-T9, Herc5, Hivep3, Hmgn3, Hspa5, Ier3, Ifi203, Ifi35, Ifi47, Ift57, Igtp, Ikbke, Il15, Il15ra, Il18, Il18bp, Il1rn, Irak3, Irf1, Irf7, Irf9, Irgm1, Itga5, Jak2, Jdp2, Kctd12, Klf7, Lgals9, Lmo4, Lpcat2, Lrrc8c, Ly6a, Ly6e, Magohb, Marco, Mfsd7a, Mitd1, Mlkl, Mmp13, Mmp14, Msr1, Mx1, Mx2, N4bp1, Nfkbia, Nfkbie, Nmi, Nod1, Nod2, Oas1g, Oas2, Oasl1, Parp12, Parp14, Parp9, Pcdh7, Pde4b, Phf11, Phlda1, Pid1, Pilra, Pilrb1, Pion, Pla2g16, Pla2g4a, Plaur, Pml, Pnpt1, Pnrc1, Pols, Ppap2a, Psmb9, Psme1, Psme2, Pstpip2, Rap2c, Rapgef2, Rasgef1b, Rbpj, Rel, Ripk2, Rnf114, Rnf213, Samd9l, Samhd1, Samsn1, Sdc3, Sdc4, Sgk3, Skil, Sla, Slamf9, Slc15a3, Slc28a2, Slc2a1, Slc2a6, Slc31a2, Slpi, Smpdl3b, Sp100, Sp110, Spred1, St7, Stap1, Stat2, Stx11, Tank, Tgfbi, Tlr1, Tmem2, Tmem49, Tnf, Tnfaip3, Tnfsf9, Tor3a, Tpm4, Traf1, Trex1, Trim13, Trim21, Trim34, Ttc39c, Ube2l6, Usp25, Vasp, Zc3h11a, Zc3h12c, Zfp263, Zfp36, Zfp800, Zufsp*
Specific genes induced by more than one pathogen/pathogen product (expression ratio varies)			
L. mexicana and *T. cruzi*	*4930578M01Rik*		
L. mexicana and LPS	*Ccl7*		
T. cruzi and LPS	*Ccl2, Cmpk2, Csf1, Cxcl10, Dhx58, Gbp3, Gbp6, I830012O16Rik, Ifi204, Ifi44, Ifit1, Ifit2, Ifit3, Irgm2, Isg15, Isg20, Mnda, Rsad2, Usp18*		

Table 2 - Comparison of biological processes induced by *L. mexicana, T. cruzi*, and LPS

Biological processes induced by one or more pathogen/pathogen product			
	P value	**Biological process**	**Genes**
LPS only	1.65E-19	Immunity and defense	*Adora2b, Aif1, Ccl12, Ccl4, Ccr5, Cd40, Cd69, Clec4e, Clec5a, Cx3cr1, Cxcl1, Cysltr1, Dusp16, Fcgr1, Fgr, Gbp2, Gbp5, H2-T9, Hspa5, Ier3, Ifi203, Ifi205, Ifi35, Ikbke, Il15, Il15ra, Il18, Il1rn, Irak3, Irf1, Irf7, Isgf3g, Jag1, Lgals9, Lrrc8c, Marco, Msr1, Nfkbia, Nmi, Nod1, Nod2, Oas1g, Oas2, Oasl1, Oasl2, Pla2g4a, Plaur, Rel, Samhd1, Sdc4, Sla, Slamf9, Slfn5, Stat2, Tnf*
	4.41E-13	Interferon-mediated immunity	*Gbp2, Gbp5, Ifi203, Ifi205, Ifi35, Irf1, Isgf3g, Nmi, Oas1g, Oas2, Oasl1, Oasl2, Stat2*
	4.63E-06	Cytokine and chemokine mediated signaling pathway	*Ccl12, Ccl4, Ccr5, Cd40, Cx3cr1, Cxcl1, Cxcl2, Fas, Il15, Il5ra, Il18, Il1rn, Tlr1, Tnf, Traf1*
	2.82E-05	Macrophage-mediated immunity	*Adora2b, Clec42, Cxcl1, Cxcl16, Cxcl2, Fcgr1, Gbp2, Gbp5, Msr1, Sdc4, Stat2*
	3.45E-05	Apoptosis	*Adora2b, Arhgef3, Axud1, Bcl2a1c, Casp4, Ddx58, Fas, Ifih1, Ift57, Il15, Jak2, Lgals9, Nfkbia, Nod1, Nod2, Rel, Ripk2, Sgk3, Socs3, Tnf, Traf1*
	1.03E-04	Signal transduction	*Adora2b, Agrin, AI586015, Arhgef3, Azi2, Cav1, Ccl12, Ccl4, Ccr5, Cd40, Creb5, Cx3cr1, Cxcl1, Cxcl2, Cysltr1, Dusp1, Edg2, Errfi1, Ets2, Fas, Fcgr1, Fgr, Flrt3, Gpr84, Gpr85, Hrasls3, Ifi35, Ikbke, Il15, Il15ra, Il18, Il1rn, Irak3, Jak2, Lcp2, Marcksl1, Marco, Nfkbia, Nmi, Pcdh7, Pde4b, Ppap2a, Pstpip2, Rap2c, Rapgef2, Rasgef1b, Rel, Ripk2, Sgk3, Sla, Socs3, Stat2, Tgfbi,Tlr1, Tnf, Traf1, Zfp36*
	5.73E-04	T-cell mediated immunity	*Adora2b, Dc40, Cd69, Cxcl1, Cxcl2, H2-T9, Ifi35, Il15ra, Nmi, Sla, Slamf9, Slfn5*
	1.54E-03	Intracellular signaling cascade	*AI586015, Izi2, Creb5, Cxcl1, Cxcl2, Dusp1, Dusp16, Edg2, Fgr, Ifi35, Il15, Il15ra, Il18, Jak2, Lcp2, Marcksl1, Nfkbia, Nmi, Pstpip2, Rap2c, Rapgef2, Rel Ripk2, Sgk3, Socs3, Stat2, Zfp36*
	3.11E-03	JAK-STAT cascade	*Ifi35, Il15, Il15ra, Il18, Jak2, Nmi, Socs3, Stat2*
	3.87E-03	NF-kappaB cascade	*Azi2, Cxcl1, Cxcl2, Ikbke, Nfkbia, Real, Ripk2*
	6.57E-03	Ligand-mediated signaling	*Adora2b, Ccl12, Ccl4, Cxcl1, Cxcl2, Edg2, Il15, Il15ra, Il18, Il1rn, Marco, Tnf*
	9.24E-03	Cell proliferation and differentiation	*AI586015, Aif1, Cdkn1a, Cxcl1, Cxcl2, Errfi1, Ets2, Fgr, Ifi203, Ifi205, Jag1, Jak2, Nfkbia, Pcdh7, Pa2g4a, Rel, Sdc3, Slfn5, Tgfbi, Trim13*
	1.61E-02	Granulocyte-mediated immunity	*Ccr5, Cd69, Cx3cr1, Cxcl1, Cxcl2*
	4.37E-02	Cell surface receptor mediated signal transduction	*Adora2b, AI586015, Cav1, Ccl12, Ccl4, Ccr5, Cd40, Cx3cr1, Cxcl1, Cxcl2, Cysltr1, Edg2, Fas, Flrt3, Gpr84, Gpr85, Il15, Il15ra, Il18, Il1rn, Irak3, Jak2, Ppap2a, Rapgef2, Rasgef1b, Sla, Tlr1, Tnf, Traf1*
	4.66E-02	Induction of apoptosis	*Fas, Ift57, Lgals9, Nod1, Nod2, Ripk2, Tnf, Traf1*
***T. cruzi* and LPS**	5.73E-11	Interferon-mediated immunity	*Cxcl10, Gbp3, Gbp6, Ifit1, Ifit2, Ifit3*
	9.38E-06	Immunity and defense	*Ccl2, Csf1, Cxcl10, Gbp3, Gbp6, Ifit1, Ifit2, Ifit3*
	4.84E-04	Macrophage-mediated immunity	*Csf1, Cxcl10, Gbp3, Gbp6*

Table 3 – Biological processes induced by *Leishmania* and *Tryapanosoma* species as determined by multi-study meta-analysis

Biological processes induced by protozoan pathogens			
Pathogen	**p-value**	**Biological process**	**Genes**
T. cruzi	3.58E-19	Immunity and defense	*Abcc4, Angptl4, B2m, C3ar1, Ccl2, Ccl5, Ccl7, Ccr1, Ccr2, Cd47, Cd69, Cd86, Cebpb, Chek1, Chek2, Ctss, Cxcl1, Cxcl16, Cxcl2, Cxcl9, Dph2, F10, Fcer1g, Fos, Gadd45b, Gbp1, Gbp4, Gca, Gsg2, Hla-dma, Hla-e, Hspa1b, Hspa5, Hspb8, Icam1, Ier3, Ifi16, Ifi30, Ifi35, Ifit1, Ifit2, Ifitm1, Ifitm3, Il15, Il18, Il1a, Il1b, Il1rn, IL-4r, Irf1, Irf7, Irf8, Isgf3g, Klf6, Klrg1, Lair1, Lgals1, Lgals3, Lgals3bp, Lgals9, Litaf, Lrrc59, Lrrc8c, Mocos, Myd88, Ncf2, Nfil3, Nmi, Nod1, Oasl, Parp3, Pbef1, Pla2g4a, Pla2g7, Plscr1, Ppid, Ppp2r2a, Ppp3cc, Ptgs2, Ptpn22, Pvr, Pvrl2, Rnpep, Samhd1, Slamf8, Slc11a1, Slfn5, Sod2, Stat2, Stat3, Tap1, Tap2, Tapbp, Tbk1, Tcirg1, Thbs1, Tnf, Tnfaip2, Tnfrsf1b, Was, Xbp1*
	1.56E-08	Cytokine and chemokine mediated signaling pathway	*Ccl2, Ccl5, Ccl7, Ccr1, Ccr2, Cx3cl1, Cxcl1, Cxcl2, Cxcl9, Il15, Il18, Il1a, Il1b, Il1rn, IL-4r, Osm4, Ptpn2, Sirpa, Tlr1, Tlr2, Tlr3, Tlr4, Tnf, Tnfrsf1b, Traip*
	2.65E-08	Interferon-mediated immunity	*Cxcl9, Gbp1, Gbp4, Ifi16, Ifi35, Ifit1, Ifit2, Irf1, Irf7, Irf8, Isgf3g, Nmi, Oasl, Slamf8, Stat2*
	1.19E-03	Macrophage-mediated immunity	*Cxcl1, Cxcl16, Cxcl2, Cxcl9, Gbp1, Gbp4, Il1a, Il1b, Lgals3bp, Litaf, Stat2, Tnfaip2*
	1.68E-03	Cytokine/chemokine mediated immunity	*Ccl2, Ccl5, Ccl7, Ccr1, Ccr2, Cxcl9, Il1a, Il1b, Tbk1, Tnfaip2, Tnfrsf1b*
	5.32E-03	Granulocyte-mediated immunity	*Ccr1, Ccr2, Cd47, Cd69, Cxcl1, Cxcl2, Gca, Ncf2*
	1.18E-02	T-cell mediated immunity	*B2m, Cd69, Cd86, Ctss, Cxcl1, Cxcl2, Hla-dma, Hla-e, Ifi30, Ifi35, Nmi, Slamf8, Slfn5, Tapbp, Tcirg1*
	2.28E-02	JAK-STAT cascade	*Ifi35, Il15, Il18, IL-4r, Jak2, Nmi, Ptpn2, Stambp, Stat2, Stat3*
	2.69E-02	DNA replication	*Cdc6, Fen1, Gins1, Hmgn3, Lig1, Mcm3, Mcm4, Mcm5, Mcm6, Orc6l, Pole, Prim2a, Rfc3, Rfc4, Rfc5, S100a11, Top2a, Wrn*
	3.00E-02	Ligand-mediated signaling	*Ccl2, Ccl5, Ccl7, Cd86, Cxcl1, Cxcl2, Cxcl9, Edg5, Grn, Il15, Il18, Il1a, Il1b, Il1rn, IL-4r, Lair1, Pbef1, Slc1a3, Tnf*
	4.79E-02	Other immune and defense	*Cxcl9, Gsg2, Lgals1, Lgals3, Lgals9, Lrrc59, Lrrc8c, Myd88, Nod1, Pla2g4a, Pla2g7, Ptpn22, Rnpep, Tnfaip2*
L. mexicana	1.30E-02	Intracellular signaling cascade	*Cxcl1, Cxcl2, Dusp1, Gadd45g, Jak3, Pik3c2a, Stam2*

Table 4 – Biological processes suppressed by *Leishmania* and *Tryapanosoma* species as determined by multi-study meta-analysis

Biological processes repressed by protozoan pathogens			
Pathogen	**p-value**	**Biological process**	**Genes**
T. cruzi	2.69E-04	Lipid, fatty acid and steroid metabolism	*Aacs, Abca3, Abcd3, Acad8, Acadm, Acadsb, Acadvl, Acbd4, Acly, Acot11, Acox1, Acp6, Acsl1, Adipor1, Adipor2, Agpat2, Apoe, Ascc1, Atp11c, C2orf43, C7orf10, Cav1, Cav2, Cdipt, Chkb, Cmas, Cpt2, Crat, Crot, Cyb5a, Cyp2e1, Dci, Decr2, Dgat1, Dgka, Ebpl, Echdc3, Elovl5, Ephx1, Fasn, Fdx1, Gba2, Gcdh, Gpam, Gpx1, Gpx4, Habp4, Hadh, Hadha, Hmgcl, Hmgcs2, Hpgd, Hsd17b4, Hsdl1, Impad1, Ivd, Kiaa0274, Lpgat1, Lpin1, Mcat, Mgll, Mmd, Mmd2, Mtmr3, Nudt3, Nudt4, Osbpl2, Osbpl5, Osbpl9, Pccb, Pcyt1a, Pcyt2, Pex19, Phyh, Pik4ca, Pip5k1c, Plscr4, Pmvk, Ppap2b, Ppapdc2, Ppara, Prkab1, Prkab2, Prkag1, Pten, Rnpepl1, Sacm1l, Sc5dl, Scap, Scarb1, Sec14l2, Slc27a4, Slc37a4, Sorl1, Srebf1, Srebf2, St3gal2, Stard10, Stard4, Sult1c1, Tmem23, Tns1, Usf2*
	1.85E-02	Fatty acid metabolism	*Aacs, Acad8, Acadm, Acadsb, Acadvl, Acot11, Acox1, Acsl1, Adipor1, Adipor2, Cpt2, Crat, Crot, Cyp2e1, Dci, Decr2, Echdc3, Elovl5, Fasn, Gcdh, Hadh, Hadha, Hmgcl, Ivd, Mcat, Mmd, Mmd2, Pccb, Phyh, Prkag1, Rnpepl1, Slc27a4*
	1.91E-02	Amino acid metabolism	*Acy1, Adi1, Aga, Akap13, Aldh5a1, Aldh6a1, Arhgef12, Arhgef18, Arhgef3, Asnsd1, Bcat2, Bckdhb, Bckdk, Cbs, Ccbl1, Cpt2, Crat, Crot, Csad, Ctbp1, Dph5, Fah, Fahd1, Fahd2a, Fasn, Fbx08, Glud1, Glul, Grhpr, Hibadh, Ilvbl, Kmo, Kynu, Me1, Nadsyn1, Nfs1, Papss1, Papss2, Qdpr*
L. mexicana	1.25E-03	Electron transport	*Atp5j2, Blvra, Cat, Cox5b, Cox6a1, Cox7a2l, Cyb5r1, Ndufa2, Ndufa5, Ndufa6, Ndufa9, Ndufb5, Ndufb8, Ndufs3, Ndufv1, Sdha, Sdhb, Sdhc, Tbxas1, Txn2, Uqcr, Uqcrb, Uqcrc1, Uqcrc2, Uqcrh*
	3.25E-03	Oxidative phosphorylation	*Atp5j2, Cox5b, Cox6a1, Ndufa2, Ndufa5, Ndufa6, Ndufa9, Ndufb5, Ndufb8, Ndufs3, Ndufv1, Sdha, Sdhb, Uqcr, Uqcrb, Uqcrh*

Table 5 - Comparison of genes induced by IFNG, IL-4, and IL-10

Expression ratio (log2) of specific genes induced by one cytokine only			
Cytokine	**>3**	**2-3**	**1-2**
IFNG	*Ccl2, Ccl7, Cd69, Gbp3, Gbp5, Gbp6, Ifi44, Ifit2, Igtp, Mnda, Rgs1, Serpina3f, Slamf8, Slco3a1*	*Acsl1, B230207M22Rik, Ccl5, Ccnd2, Ccrl2, Cd83, Cd86, Cmpk2, Ctsc, Cxcl1, Cxcl10, D14Ertd668e, Denr, Ets2, Fcgr4, Fzd7, Gch1, Gdap10, Ggct, Herc5, I830012O16Rik, Ifi204, Ifih1, Ifit1, Ifit3, Il1rn, Irgm1, Irgm2, Jdp2, Lmo4, Mx1, Nod1, Oasl2, Parp14, Phf11, Pla2g16, Rnf213, Rsad2, Slamf7, Slc7a11, Slfn4, Slfn5, Stx11, Tnf, Tnfaip3, Usp18, Wars*	*0610038D11Rik, 1110002E22Rik, 1110038F14Rik, 1190002H23Rik, 1200003I10Rik, 1200009I06Rik, 2010106G01Rik, 2210012G02Rik, 2310007H09Rik, 2310016C08Rik, 2310058D17Rik, 2410039M03Rik, 4921509J17Rik, 4930403L05Rik, 4930427A07Rik, 5031414D18Rik, 9030607L20Rik, 9130209A04Rik, 9230105E10Rik, 9930023K05Rik, A930033M14Rik, AA960436, AI451617, Acsl5, Adar, Agfg1, Ak3l1, Ampd3, Ankrd57, Arhgef3, Armc8, Arrdc4, Asns, Ass1, Atf4, Atp8a2, B4galt3, B4galt5, BB123696, BC006779, BC013712, BC046404, Bambi-ps1, Basp1, Bat2d, Bcl2a1b, Bcl2a1c, Bfar, Birc2, Birc3, Bmi1, Bst2, Car13, Ccdc25, Ccl3, Cd1d1, Cdc42ep2, Chac1, Chmp4b, Ciita, Clcn7, Clec2d, Clec4e, Creb1, Creb5, Crem, Csnk1d, Csprs, Cxcl16, Cxcl2, Cybb, Daxx, Dcp2, Ddit3, Ddx58, Ddx60, Dhx58, Dio2, Dlk1, Dock4, Dtx3l, Dusp16, Dusp28, Egr1, Ehd1, Eif2ak2, Emr1, Enc1, Etnk1, Fabp3, Fam102b, Fam46c, Fam82a2, Farp2, Fas, Fndc3a, Foxred1, Glipr2, Glrp1, Gna13, Gnaq, Gpd2, Gpr141, Gtf2h1, Gtpbp2, Gvin1, H2-Q7, H2-T10, H2-T23, H2-T24, Haghl, Herc3, Hk1, Hk2, Hspa2, Icam1, Ifi203, Ifi205, Ifi35, Ifrd1, IL-12rb2, Il15, Il15ra, Il27, Inpp5b, Insig1, Irak2, Irf8, Isg20, Itgav, Jak2, Katna1, Kdr, Kitl, Lass6, Lcp2, Lgals9, Lpar1, Lrrc14, Lrrc8c, Ltbp1, Ly6c1, M6pr, Mafk, Mdk, Mdm2, Mfsd7a, Mitd1, Mlkl, Mmp14, Mobkl1a, Mov10, Mpzl1, Mt2, Mtmr14, Mx2, Myd88, Nampt, Nfkb1, Nfkbie, Nmi, Nod2, Nr3c1, Nrp2, Nsbp1, Nt5c3, Oas1b, Oas1g, Oas2, Oasl1, Obfc2a, Ogfr, Olfr319, Olfr635, Otud1, P4ha1, Parp12, Parp9, Pcgf5, Pcmtd1, Pde4b, Peli1, Pfkfb3, Pfkp, Phlda1, Phlpp, Pla2g4a, Plaur, Plk2, Pml, Pmm2, Poldip3, Ppa1, Ppap2a, Ppap2b, Ppfibp2, Ppm1k, Ppp1r15b, Ppp2r2a, Prkx, Prpf38a, Psat1, Psmb10, Psmb9, Pstpip2, Ptafr, Rab11fip1, Rab12, Rab20, Ralgds, Rasa4, Rasgef1b, Rassf1, Rbm7, Rgl1, Rnf114, Rnf135, Rnf14, Rnf34, Samd9l, Samhd1, Sco1, Sema3c, Serpinb1a, Sestd1, Sgk1, Slc15a3, Slc2a6, Slc30a1, Slc31a1, Slc31a2, Slc3a2, Slc43a3, Slc6a9, Slfn1, Slfn2, Smpdl3b, Snx20, Soat2, Sp100, Sp110, Spata13, Spred1, Spred2, Spty2d1, Srgn, Srxn1, St3gal1, St3gal5, St6galnac4, St7, Stam2, Stat1, Stat2, Stk19, Stoml1, Stradb, Stx2, Tank, Tap1, Tapbp, Tapbpl, Tbc1d9, Tgm2, Tgoln1, Tgs1, Tm9sf4, Tmcc3, Tmem132a, Tmem2, Tnfrsf1a, Tnfrsf1b, Tnfsf9, Tor3a, Tpm4, Traf1, Trafd1, Trex1, Trib3, Trim13, Trim21, Trim30, Trim34, Trps1, Ttc39b, Ttc9c, Tyk2, Ubash3b, Ubd, Ube2l6, Ube2z, Ugcg, Usp12, Wdr20b, Wdr37, Wnt9a, Xkr8, Zbtb5, Zc3h12c, Zc3hav1, Zc3hc1, Zcchc2, Zfp429, Zfp800, Znfx1, Zufsp, Zyx*
IL-4		*Atp6v0d2, Egr2*	*1810011H11Rik, 2410042D21Rik, Acad8, Ak2, Arfgap2, Atic, Atp6v0a1, Baiap2, Batf3, Bcar3, Brd4, Brwd1, C030015D21Rik, Casp6, Chst7, Ctdp1, Cyp20a1, Daglb, Dusp4, ENSMUSG00000055697, Fam63a, Fchsd2, Fem1c, Flcn, Fyn, Herpud1, Herpud2, Hsph1, Il11ra1, Il1rl2, Il6st, Ipmk, Itgax,*

			Itgb1, Lsm14b, Mat2a, Med1, Med15, Mettl9, Mgl1, Mgl2, Mllt3, Mybbp1a, Nat13, Necap1, OTTMUSG00000016703, P2ry1, Pcyt2, Pde12, Peo1, Pnpla8, Pparg, Ppp2r3a, Prosc, Prpf19, Prps1, Psmc4, Ptcd2, Rab15, Raly, Rnf181, Rragd, Sh3kbp1, Slc25a13, Slc30a4, Slc39a8, Tmco3, Tmed9, Tmem144, Ubqln1, Wdr45l
IL-10	*Ednrb, IL-4ra*	*Gda, Tnfsf14*	*4930435H24Rik, 4930471M23Rik, 5430427O19Rik, 6430527G18Rik, AB124611, Abcg1, Acat2, Aldh3b1, Aldoa, Ap1b1, Apoc2, Auh, BB031773, Bcl3, C1qb, C1qc, Ccl6, Ccr5, Cd74, Cdk2ap2, Cdkn2d, Cebpb, Coro1a, Cox7a2l, Ctsa, Cyth4, EG625174, Enpp1, Eps8, Fabp4, Fcgr1, Fcgr3, Fdps, Flot1, Fxc1, Fxyd2, Gbp2, Gcnt2, H2-DMa, H2-gs10, Hist1h3a, Hlx, Hmox1, Hsd17b10, Htra1, Ifitm2, Ifitm6, Il21r, Kif3a, Lilrb4, Lrrc25, Ly6e, Mafb, Malat1, Mefv, Mmp19, Mmp8, Mvd, Naaa, Ndrg1, Nfil3, Olfm1, Pdpn, Pld3, Plek, Pltp, Ppil2, Psme1, Ptpn1, Rac2, Sbno2, Sirpb1a, Smox, Spint1, Tcirg1, Tgfbi, Tha1, Timp1, Tle3, Tlr1, Tm2d2, Tmem49, Tmem8, Tnfaip8l2, Trim46, Tspan13, Tspo, Zic4*
Specific genes induced by more than one cytokine (expression ratio varies)			
IFNG and IL-4		*Arg2, Cd274, Ch25h, Cish, Clic4, Csf1, Flrt2, Flt1, Fmnl2, Gigyf2, Klf4, Maea, Mmp13, Psmd2, Rai12, Rars, Rel, Ripk2, Rnf19b, Snn, Socs1, Stam, Tlr4, Vegfc, Yme1l1*	
IFNG and IL-10		*1200016E24Rik, 4933412E12Rik, Axud1, Btg1, Casp4, Ccl12, Ccl4, Cd40, Cdkn1a, F10, Fam26f, Fgl2, Flrt3, Gadd45b, Gsdmd, H2-Aa, H2-Ab1, H2-Eb1, Ier3, Ifi47, Igf2bp2, Il18bp, Il1b, Irf7, Ly6a, Ly6f, Mcoln2, Mxd1, Nfkbiz, Pgs1, Psmb8, Saa3, Slc28a2, Socs3, Stat3, Zfp36*	
IL-4 and IL-10		*Csf2rb, Dhrs9, Fcgr2b, Mrc1, Ncoa4, Ptgs1, Rab3il1, Tcfec*	
IFNG and IL-4 and IL-10		*Irf1, Pim1*	

Table 6 - Comparison of biological processes induced by IFNG, IL-4, and IL-10

Biological processes induced by one or more cytokine			
	P value	**Biological process**	**Genes**
IFNG only	4.63E-18	Interferon-mediated immunity	*Cxcl10, Gbp3, Gbp5, Gbp6, Ifi203, Ifi205, Ifi35, Ifit1, Ifit2, Ifit3, Irf8, Nmi, Oas1b, Oas1g, Oas2, Oasl1, Oasl2, Slamf7, Slamf8, Stat2*
	5.23E-16	Immunity and defense	*C2ta, Ccl2, Ccl3, Ccl5, Ccl7, Ccrl2, Cd1d1, Cd69, Cd86, Clec2d, Clec4e, Cxcl1, Cxcl10, Cxcl16, Cxcl2, Dusp16, Fcgr3a, Gbp2, Gbl5, Gbl6, H2-D4, H2-Q7, H2-T24, Haghl, Hspa2, Icam1, Ifi203, Ifi205, Ifi35, Ifit1, Ifit2, Ifit3, IL-12rb2, Il15, Il15ra, Il1rn, Irak2, Irf8, Lgals9, Lrrc8c, Myd88, Nfkb1, Nmi, Nod1, Nod2, Oas1b, Oas1g, Oas2, Oasl1, Oasl2, Pbef1, Phlpp, Pla2g4a, Plaur, Ppp2r2a, Ptafr, Rgs1, Samhd1, Slamf7, Slamf8, Slfn5, Stat2, Tap1, Tapbp, Tapbpl, Tnf, Tnfrsf1a, Tfnrsf1b*
	6.48E-06	T-cell mediated immunity	*C2ta, Cd1d1, Cd69, Cd86, Cxcl1, Cxcl2, H2-D4, H2-Q7, H2-T24, Ifi35, Il15ra, Nmi, Slamf7, Slamf8, Slfn5, Tapbp, Tapbpl, Tnfrsf1a*
	4.49E-05	Ligand-mediated signaling	*Ccl2, Ccl3, Ccl5, Ccl7, Cd86, Cxcl1, Cxcl10, Cxcl2, Edg2, IL-12rb2, Il15, Il15ra, Il1rn, Kitl, Mdk, Pbef1, Tnf, Tnfrsf1a, Wnt9a*
	7.97E-05	Cytokine and chemokine mediated signaling pathway	*Ccl2, Ccl3, Ccl5, Ccl7, Ccrl2, Cxcl1, Cxcl10, Cxcl2, Fas, IL-12rb2, Il15, Il15ra, Il1rn, Tnf, Tnfrsf1a, Tnfrsf1b, Traf1*
	2.34E-04	Signal transduction	*0710001B24Rik, 2010206G01Rik, 9130017C17Rik, Arhgef3, Ccl2, Ccl3, Ccl5, Ccl7, Ccrl2, Cd86, Creb1, Creb5, Crem, Csnk1d, Csprs, Cxcl1, Cxcl10, Cxcl2, Dock4, Dusp16, Edg2, Emr1, Ets2, Fabp3, Fas, Fcgr3a, Gna13, Gnag, Gpr141, Hrasls3, Hrb, Icam1, Ifi35, IL-12rb2, Il15, Il15ra, Il1rn, Inpp5b, Irak2, Jak2, Kdr, Kitl, Lcp2, Ltbp2, M6pr, Mdk, Myd88, Nfkb1, Nmi, Nrp2, Ogfr, Olfr319, Pbef1, Pde4b, Plk2, Ppap2a, Ppap2b, Ppm1k, Prkx, Pstpip2, Ptafr, Rab12, Rab20, Ralgds, Rasa4, Rasgef1b, Rassf1, Rgl1, Rgs1, Rnf14, Sema3c, Sgk, Spata13, Stam2, Stat2, Tnf, Tnfrsf1a, Tnfrsf1b, Traf1, Trib3, Tyk2, Wnt9a*
	2.55E-03	Macrophage-mediated immunity	*Clec4e, Cxcl1, Cxcl10, Cxcl16, Cxcl2, Fcgr3a, Gbp3, Gbp5, Gbp6, Stat2, Tnfrsf1a*
	2.74E-02	Cytokine/chemokine mediated immunity	*Ccl2, Ccl3, Ccl5, Ccl7, Ccrl2, Cxcl10, Tnfrsf1a, Tnfrsf1b*
	2.98E-02	Apoptosis	*Arhgef3, Bcl2a1c, Birc2, Birc3, D11Lgp2e, Ddx58, Fas, Ifih1, Il15, Jak2, Lgals9, Mdm2, Nfkb1, Nod1, Nod2, Rassf1, Sgk, Tnf, Tnfrsf1a, Traf1, Ube2z*
IL-10 only	1.20E-05	Immunity and defense	*C1gb, C1gc, Ccl6, Ccr5, Cd74, Cebpb, Fcgr1, Fcgr3, Gbp2, H2-DMa, H2-Q5, Ifitm2, Ifitm6, Il21r, IL-4ra, Nfil3, Ppil2, Tcirg1, Tnfaip8l2, Tnfsf14*
	7.47E-03	Cytokine and chemokine mediated signaling pathway	*Ccl6, Ccr5, IL-4ra, Ptpn1, Sirpb1, Tlr1, Tnfsf14*
	3.40E-02	Lipid and fatty acid transport	*Abcg1, Apoc2, Fabp4, Pltp, Tspo*
IFNG and IL-10	1.04E-06	Immunity and defense	*Ccl12, Ccl4, Cd40, F10, Gadd45b, H2-Aa, H2-Ab1, H2-Eb`, H2-T23, Ier3, Il1b, Irf7, Saa3, Stat3*
	1.67E-03	MHCII-mediated immunity	*H2-Aa, H2-Ab1, H2-Eb1*

	5.47E-03	T-cell mediated immunity	*Cd40, H2-Aa, H2-Ab1, H2-Eb1, H2-T23*
	1.52E-02	Apoptosis	*Axud1, Casp4, Gadd45b, Il1b, Socs3, Stat3*

Table 7 - Comparison of genes induced by IFNG, IFNB, and TNF

Expression ratio (log2) of specific genes induced by one cytokine only			
Cytokine	**>3**	**2-3**	**1-2**
IFNG	*Ccl2, Ccl7*	*Cd83, Ly6a, Wars*	*0610038D11Rik, 1110038F14Rik, 1190002H23Rik, 1200009I06Rik, 2210012G02Rik, 2310007H09Rik, 2310016C08Rik, 4921509J17Rik, 4930403L05Rik, 4930427A07Rik, 5031414D18Rik, 9030607L20Rik, 9130209A04Rik, 9930023K05Rik, A930033M14Rik, Acsl5, Agfg1, Ak3l1, Arhgef3, Armc8, Arrdc4, Atp8a2, B4galt5, BB123696, BC046404, Basp1, Bat2d, Birc2, Bmi1, Bst2, Btg1, Ccdc25, Ccl3, Cdkn1a, Chmp4b, Ciita, Clcn7, Creb1, Creb5, Crem, Csnk1d, Cxcl16, Cxcl2, Cybb, Ddit3, Dlk1, Dock4, Egr1, Emr1, Enc1, Etnk1, Fam102b, Fmnl2, Foxred1, Gadd45b, Gigyf2, Glipr2, Gna13, Gsdmd, Gtf2h1, Gtpbp2, H2-Aa, H2-Ab1, H2-Eb1, H2-T23, H2-T24, Haghl, Hk2, Hspa2, Ier3, Ifrd1, Igf2bp2, IL-12rb2, Il1b, Il27, Inpp5b, Irak2, Irf8, Itgav, Klf4, Lass6, Lcp2, Lrrc14, Lrrc8c, Ly6c1, Maea, Mobkl1a, Mt2, Mtmr14, Myd88, Nfkb1, Nr3c1, Nrp2, Nsbp1, Obfc2a, Olfr319, P4ha1, Pcmtd1, Pde4b, Pfkp, Pgs1, Phlpp, Plaur, Pmm2, Poldip3, Ppp2r2a, Prpf38a, Psat1, Psmd2, Ptafr, Rai12, Ralgds, Rars, Rassf1, Rbm7, Saa3, Sco1, Sema3c, Serpinb1a, Sestd1, Sgk1, Slc31a1, Slc3a2, Slc43a3, Smpdl3b, Snn, Snx20, Spata13, Spred2, Spty2d1, Srgn, St3gal5, St6galnac4, St7, Stam, Stat3, Stk19, Stoml1, Stradb, Stx2, Tapbp, Tapbpl, Tbc1d9, Tgm2, Tgoln1, Tlr4, Tm9sf4, Tmem132a, Tmem2, Tnfrsf1b, Trps1, Ttc9c, Ubash3b, Ubd, Ugcg, Wdr20b, Wdr37, Wnt9a, Xkr8, Yme1l1, Zbtb5, Zc3hav1, Zc3hc1, Zfp36, Zfp429, Zfp800, Zyx*
IFNB		*Fcgr1*	*100040620, 1110018G07Rik, 1700016D18Rik, 1810035L17Rik, 2810474O19Rik, 4932438A13Rik, 5-Mar, 5430427O19Rik, 5730508B09Rik, 6330442E10Rik, 6820401H01Rik, A230046K03Rik, Aadacl1, Aftph, Aipl1, Aldh1l2, Ankle2, Apol9a, Apol9b, Arid4a, Asb13, Ascc3, Asxl3, Atp10a, Atp11b, Axl, B2m, BB031773, Bco2, C330011K17Rik, C330023M02Rik, Ccdc86, Ccdc90a, Cdkal1, Chd6, Cnp, Ctla2b, Cycs, Dhh, Dhrs9, E130102H24Rik, Endod1, Epsti1, Erap1, Fam46a, Fbxw17, Fem1c, Frmd4a, Gcnt2, Glcci1, Gng11, H2-T22, H2-T9, Hfe, Hmgn3, Ier5, Il18, Ilk, Iqwd1, Irf2, Irf9, Itpr1, Kat2b, Kif5c, Klra8, Kpna4, Lamp2, Ly6e, Ly86, Mllt3, Ms4a6b, Ms4a6c, Mtcp1, Nub1, OTTMUSG00000016703, Oas1c, Oas3, Olfr843, P2ry14, P2ry6, Papd4, Pi4kb, Plekhf2, Pltp, Pnpt1, Pols, Rab9, Rabep1, Rin2, Rnf139, Rnf31, Rtp4, S1pr2, Sdc3, Serpinb1c, Serpinb6b, Sgcb, Sgk3, Slamf9, Slc2a8, Slfn10, Smc5, Snw1, Spock2, Stxbp3a, Sumf2, Taok3, Tfb2m, Timeless, Tlr3, Tlr7, Tlr8, Tmem184b, Tmem209, Tor1aip1, Tor1aip2, Tpst1, Tspan13, Uba7, Usf1, Usp25, Usp42, Vcpip1, Zc3hav1l, Zcchc6, Zfp281, Zfp295, Zfp319, Zfp455*
TNF		*Ednrb, Gbp2*	*4833445I07Rik, 9030425E11Rik, 9130221J17Rik, Abcc1, Ahr, C730045O03Rik, Cav1, Chpf, Clec5a, Coq10b, Ddit4, Dnmt3l, Dusp4, Egr2, Ext1, Gbe1, Gss, Gtf2a1, Herpud1, Hmox1, Irak3, Jag1, Lox, M6pr-ps, Mafg, Mfap3l, Nqo1, Olfr1272, Olfr214, Orai2, Osbpl3, Pcdh7, Pim3, Prdx6-rs1, Prkar2b, Psmd10, Psmd11, Reln, Rps6ka2, Slc11a1, Slpi, Src, Syk, Tcfec, Tiparp, Ttc39c, Txnrd1, Ugt1a6a, Unc5b, Vasp, Vcan, Zfp719*
Specific genes induced by more than one cytokine (expression ratio varies)			
IFNG and IFNB	*1110002E22Rik, 2310058D17Rik, 4933412E12Rik, 9230105E10Rik, AA960436, Adar, B4galt3, BC006779, BC013712, Bambi-ps1, Bfar, Ccl12, Ccnd2, Cd86, Cish, Clec2d, Csprs, Ctsc, Daxx, Dcp2, Dhx58, Dusp28, Eif2ak2, Fam26f, Fam82a2, Farp2, Fcgr4, Fgl2, Flt1, Fndc3a, Fzd7, Gch1, Gnaq, H2-Q7, H2-T10, Hk1, Ifi205, Irf7, Katna1, Kdr, Kitl, Ltbp1, Ly6f, Mafk, Mdk, Mitd1, Mlkl, Mov10, Nmi, Nod1, Oas1b, Oas2, Ogfr, Olfr635, Otud1, Parp12, Parp9, Pcgf5, Peli1, Pfkfb3, Pml, Ppa1, Ppm1k, Ppp1r15b, Prkx, Psmb10, Psmb8, Psmb9, Rasa4, Rgl1, Rnf114, Rnf135, Rnf19b, Rnf34, Samd9l, Samhd1, Serpina3f, Slamf8, Slc28a2, Slc30a1, Slfn1, Sp110, Stat2, Tap1, Tgs1, Tmcc3, Tnfrsf1a, Tor3a, Trim21, Trim30, Ttc39b, Tyk2, Usp12, Znfx1, Zufsp*		

IFNG and TNF	*1200003I10Rik, 1200016E24Rik, 2410039M03Rik, Acsl1, Ampd3, Ankrd57, Asns, Ass1, Atf4, Bcl2a1b, Bcl2a1c, Birc3, Car13, Cd1d1, Cdc42ep2, Chac1, Clec4e, Cxcl1, Denr, Dusp16, Ehd1, Ets2, F10, Fas, Flrt3, Gdap10, Ggct, Gpd2, Gpr141, Herc3, Icam1, Ifi47, Insig1, Jdp2, Lmo4, Lpar1, M6pr, Mcoln2, Mdm2, Mfsd7a, Mmp14, Mpzl1, Nampt, Nfkbie, Nfkbiz, Nod2, Phlda1, Pim1, Pla2g4a, Ppap2a, Ppap2b, Ppfibp2, Pstpip2, Rab11fip1, Rab12, Rab20, Rel, Rnf14, Rsad2, Slc2a6, Slc31a2, Slc6a9, Slc7a11, Slfn2, Soat2, Socs3, Spred1, Srxn1, St3gal1, Stam2, Stx11, Tank, Tnf, Tnfaip3, Tnfsf9, Tpm4, Traf1, Trib3, Trim13, Ube2z, Vegfc, Zc3h12c*
IFNB and TNF	*Mthfr*
IFNG and IFNB and TNF	*2010106G01Rik, AI451617, Arg2, Axud1, B230207M22Rik, Casp4, Ccl4, Ccl5, Ccrl2, Cd274, Cd40, Cd69, Ch25h, Clic4, Cmpk2, Csf1, Cxcl10, D14Ertd668e, Ddx58, Ddx60, Dio2, Dtx3l, Fabp3, Fam46c, Flrt2, Gbp3, Gbp5, Gbp6, Glrp1, Gvin1, Herc5, I830012O16Rik, Ifi203, Ifi204, Ifi35, Ifi44, Ifih1, Ifit1, Ifit2, Ifit3, Igtp, Il15, Il15ra, Il18bp, Il1rn, Irf1, Irgm1, Irgm2, Isg20, Jak2, Lgals9, Mmp13, Mnda, Mx1, Mx2, Mxd1, Nt5c3, Oas1g, Oasl1, Oasl2, Parp14, Phf11, Pla2g16, Plk2, Rasgef1b, Rgs1, Ripk2, Rnf213, Slamf7, Slc15a3, Slco3a1, Slfn4, Slfn5, Socs1, Sp100, Stat1, Trafd1, Trex1, Trim34, Ube2l6, Usp18, Zcchc2*

Table 8 - Comparison of biological processes induced by IFNG, IFNB, and TNF

Biological processes induced by one or more cytokine			
	P value	**Biological process**	**Genes**
IFNG only	3.81E-07	Immunity and defense	*C2ta, Ccl2, Ccl3, Ccl7, Cxcl16, Cxcl2, Gadd45b, H2-Aa, H2-Ab1, Hd-D4, H2-Eb1, H2-T24, Haghl, Hspa2, Ier3, IL-12rb2, Il1b, Irak2, Irf8, Lrrc8c, Maea, Myd88, Nfkb1, Phlpp, Plaur, Ppp2r2a, Ptafr, Saa3, Stat3, Tapbp, Tapbpl, Tnfrsf1b*
	1.71E-03	T-cell mediated immunity	*C2ta, Cxcl2, H2-Aa, H2-Ab1, H2-D4, H2-Eb1, H2-T23, H2-T24, Tapbp, Tapbpl*
	3.76E-03	MHCI-mediated immunity	*H2-D4, H2-T23, H2-T24, Tapbp, Tapbpl*
	6.54E-03	MHCII-mediated immunity	*C2ta, H2-Aa, H2-Ab1, H2-Eb1*
IFNB only	3.09E-05	MHCI-mediated immunity	*B2m, H2-Q5, H2-T22, H2-T9, Hfe*
	6.83E-03	T-cell mediated immunity	*B2m, H2-Q5, H2-T22, H2-T9, Hfe, Slamf9*
TNF only	9.11E-04	Neurogenesis	*Ednrb, Egr2, Jag1, Pcdh7, Reln, Rps6ka2, Src, Unc5b*
	1.74E-03	Ectoderm development	*Ednrb, Egr2, Jag1, Pcdh7, Reln, Rps6ha2, Src, Unc5b*
	2.01E-03	Immunity and defense	*9030425E11Rik, Abcc1, Ahr, Clec5a, Cog10b, Gbp2, Irak3, Jag1, Prdx6-rs1, Slc11a1, Src, Syk*
IFNG and IFNB	1.97E-05	Interferon-mediated immunity	*Irf7, Nmi, Oas1b, Oas2, Slamf8, Stat2*
	2.50E-03	Immunity and defense	*Ccl12, Cd86, Cish, Clec2d, Fcgr3a, H2-Q7, Irf7, Nmi, Nod1, Oas1b, Oas2, Samhd1, Slamf8, Stat2, Tap1, Tnfrsf1a*
	2.91E-02	Proteolysis	*9230105E10Rik, Ctsc, Pml, Psmb10, Psmb8, Psmb9, Rnf135, Rnf34, Serpina3f, Trim21, Trim30, Trim34, Usp12*
	3.66E-02	Protein metabolism and modification	*0710001B24Rik, 9230105E10Rik, B4galt3, Ctsc, Eif2ak, Flt1, Ibrdc3, Katna1, Kdr, Mlkl, Mov10, Pml, Ppm1k, Prkx, Psmb10, Psmb8, Psmb9, Rnf135, Rnf34, Serpina3f, Tor3a, Trim21, Trim30, Trim 34, Tyk2, Usp12*
IFNG and TNF	1.60E-03	Apoptosis	*Bcl2a1c, Birc3, Fas, Mdm2, Nod2, Rel, Socs3, Tnf, Traf1, Ube2z*
	3.23E-03	Inhibition of apoptosis	*Bcl2a1c, Birc3, Mdm2, Rel, Socs3, Ube2z*
	1.24E-02	Signal transduction	*Cxcl1, Dusp16, Edg2, Ets2, Fas, Flrt3, Gpr141, Icam1, M6pr, Pbef1, Ppap2a, Ppap2b, Pstpip2, Rab12, Rab20, Rel, Rnf14, Socs3, Stam2, Tnf, Traf1, Trib3, Vegfc*
IFNG and IFNB and TNF	1.49E-20	Interferon-mediated immunity	*Cxcl10, Gbp3, Gbp5, Gbp6, Ifi203, Ifi35, Ifit1, Ifit2, Ifit3, Irf1, Oas1g, Oasl1, Oasl2, Slamf7*
	9.42E-14	Immunity and defense	*Ccl4, Ccl5, Ccrl2, Cdc274, Cd40, Cd69, Csf1, Cxcl10, Gbp3, Gbp6, Ifi203, Ifi35, Ifit1, Ifit2, Ifit3, Il15, Il15ra, Il1rn, Irf1, Lgals9, Oas1g, Oasl1, Oasl2, Rgs1, Slamf7, Slfn5*
	2.48E-06	Cytokine and chemokine mediated signaling pathway	*Ccl4, Ccl5, Ccrl2, Cd40, Csf1, Cxcl10, Il15, Il15ra, Il1rn, Socs1*
	2.43E-03	T-cell mediated immunity	*Cd274, Cd490, Cd69, Ifi35, Il15ra, Slamf7, Slfn5*

	1.95E-02	Macrophage-mediated immunity	*Csf1, Cxcl10, Gbp3, Gbp5, Gbp6*
	4.37E-02	Apoptosis	*Axud1, Casp5, Ddx58, Ifih1, Il15, Jak2, Lgals9, Ripk2*

Table 9 – Genes altered by IL-17 stimulation of bone marrow-derived macrophages

Upregulated by IL-17		
Gene Name	**Gene Symbol**	**Fold change**
Early growth response 1	*Erg1*	3.3
chemokine (C-X-C motif) ligand 1	*Cxcl1*	2.6
2'-5' oligoadenylate synthetase-like 2	*Oasl2*	2.4
PHD finger protein 11	*Phf11*	2.1
Ring finger protein 213	*Rnf213*	2.1
beta-2 microglobulin	*B2m*	2.1
ARP3 actin-related protein 3 homolog (yeast)	*Arp3*	2.0

Table 10 - Comparison of genes induced in bone marrow-derived versus thioglycollate-elicited macrophages

	BMM and TM	**BMM only**	**TM only**
IFNG	*Ccl2, Ccl5, Ccl7, Cd40, Cd69, Cd83, Cd86, Cxcl10, Cxcl16, Fcgr4, Gbp3, Gbp5, Gbp6, Ifi203, Ifi205, Ifi35, Ifi47, Ifih1, Ifit2, Ifit3, Igf2bp2, Igtp, Il15ra, Il18bp, Il1rn, Il27, Irf1, Irgm, Jak2, Myd88, Nfkbie, Nfkbiz, Nmi, Nod1, Nod2, Oas1g, Oas2, Oasl1, Oasl2, Socs1, Socs3, Stat1, Stat2, Tap1, Tapbpl, Tnfaip3, Tnfrsf1a, Traf1 **</*	*Ccl12, Ccl3, Ccl4, Ccrl2, Cxcl1, Cxcl2, H2-Aa, H2-Ab1, H2-Eb1, H2-Q7, H2-T10, H2-T23, H2-T24, Ifi44, Ifit1, IL-12rb2, Il15, Il1b, Irf7, Irf8, Isg20, Mmp13, Mmp14, Nfkb1, Stat3, Tnf, Tnfrsf1b, Tnfsf9 **</*	*Cxcl3, Cxcl9, Ifi27, IL-10ra, IL-12a, IL-12rb1, Il13ra1, IL-4ra, Irf2, Irf9, Isg15, Nfkb2, Nfkbia, Tlr1, Tnfsf13b **</*
IL-4	*C030015D21Rik, Cish, Mmp13, Rab15, Rab3il1*	*Casp6, Cd274, Ch25h, Chst7, Daglb, Dhrs9, Dusp4, Fcgr2b, Il11ra1, Il1rl2, Il6st, Irf1Pparg, Socs1, Tlr4 **</*	*2610030P05Rik, B430119L13Rik, Chi3l3, Hist2h3c2, Mafb, Pdcd1lg2, Zcchc2*
TNF	*Ccl5, Cd69, Cxcl1, Gbp5, Gbp6, Ifi203, Ifih1, Ifit2, Ifit3, Il18bp, Irak3, Isg20, Jak2, Mmp13, Mx1, Mx2, Nfkbie, Nfkbiz, Nod2, Oasl2, Stat1, Tnfaip3, Tnfsf9, Traf1 **</*	*Ccl4, Ccrl2, Cd274, Cd40, Cxcl10, Gbp2, Gbp3, Ifi35, Ifi44, Ifi47, Ifit1, Igtp, Il15, Il15ra, Il1rn, Irf1, Mmp14, Oas1g, Oasl1, Socs1, Socs3, Tnf, Trafd1 **</*	*Ccl7, Cd14, Cd86, Cxcl3, Cxcl5, Ifi205, Il17ra, Il1a, Irf9, Isg15, Oas2, Tlr1, Traf5 **</*
* Selected genes			

2.12. Methods for supplementary materials

Cryopreserved bone marrow macrophages

Newly derived BMMs and previously frozen BMMs were plated overnight in BMM media. RNA was collected from the fresh and previously frozen BMMs and prepped for microarray analysis. RNA from fresh BMMs was labelled with Cy5 and hybridized directly against RNA from previously frozen BMMs (labelled with Cy3). The background subtracted median fluorescence intensities of each color channel was plotted against one another, and linear regression analysis was performed. The correlation coefficient was found to be 0.986 (Supplementary Figure 1), suggesting that cryopreservation does not affect the transcriptional signature of BMMs.

Mock infection of *T. cruzi*

BMMs were treated with supernatant from uninfected BESM cells in parallel with BMMs treated with supernatant from BESM cells infected with *T. cruzi*. RNA was collected from mock-infected BMMs 24 h post-treatment. RNA from mock-infected BMMs were processed for microarray analysis, labeled with Cy5 dye, and hybridized against RNA from uninfected BMMs (labeled with Cy3 dye). The median fluorescence intensities of mock-infected and uninfected cells were plotted against one another, and linear regression analysis was performed. The correlation coefficient was found to be 0.995 (Supplementary Figure 5), suggesting that supernatant from uninfected BESM cells did not affect the transcriptional signature of BMMs.

Leishmania and *Trypanosoma* meta-analysis

Raw Affymetrix CEL files were obtained from the following repositories: studies by Fortea, Chessler, Costales, Shighara from GEO (http://www.ncbi.nlm.nih.gov/geo/), studies by Ettinger and Fisher from ArrayExpress (http://www.ebi.ac.uk/microarray-

as/ae/), and the study by Chaussabel from GPX-MEA (http://gpxmea.gti.ed.ac.uk/). Processed Affymetrix data was obtained for the study by Gregory from ArrayExpress. For the study by Rodriguez, processed data was obtained directly from the author. For the spotted cDNA study by Vaena de Avalos, filtered normalized ratio of means for all spots on all arrays, was obtained from SMD (http://smd.stanford.edu/) using the following filters: (SF >=0) and (regression correlation > .6) and ((% pixels ch1 > BG ch1 + 1SD > 70) or (% pixels ch2 > BG ch2 + 1SD > 70)) .

For the studies with Affymetrix CEL files (Chaussabel, Fortea, Chessler, Costales, Shighara, Ettinger, and Fisher) normalization was done by using the justRMA function in the affy library in R (http://www.bioconductor.org/packages/release/Software.html). For the studies with the processed Affymetrix data (Gregory and Rodriguez), we used the authors' MAS5 normalized data. Expression values < 50, were floored at 50.

For the studes with Affymetrix CEL files, the function detection.p.val from the R library simpleaffy (http://www.bioconductor.org/packages/release/Software.html) was used to obtain probe set present, marginal, or absent calls in each array. Probe sets absent in all arrays were removed. For the studies with the processed Affymetrix data, we used the authors' present, marginal, or absent calls to filter out probe sets that were absent in all arrays.

Human HGNC gene identifiers along with all the corresponding fields were obtained (http://www.genenames.org/data/gdlw_index.html). Probe sets for the Affymetrix arrays were mapped to the HGNC gene identifiers using the human gene symbols provided by the corresponding Affymetrix gene list (http://www.affymetrix.com/). For the Vaena de Avalos study, the human gene symbols provided for the data from SMD were mapped directly to the HGNC gene identifiers.

For the MEEBO arrays, oligos were mapped to mouse gene identifiers from MGI using the mouse to human gene orthology table obtained from the MGI website (http://www.informatics.jax.org/).

Jenner & Young ortholog mapping

Mouse genes were organized by hierarchical clustering using a Pearson correlation distance metric. To assess the degree of similarity between the mouse and human responses to pathogens, mouse orthologs for the human "common host response" expression signature identified by Jenner and Young [33] were mapped to the MEEBO probe set using Mouse Genome Informatics and NCBI ortholog assignments. 474 of the 511 human common host response genes were mapped to MEEBO probes. Of these, 239 human common host response genes mapped to the probes in the mouse dataset (*i.e.* those which passed all filtering criteria). The mapped human genes were organized in the same order in which the mouse genes appear in the cluster, and the frequency of appearance was tallied in blocks of 50 genes. Frequencies were smoothed using a moving window average of 5 and plotted along the gene axis of the cluster heatmap in order to demonstrate the location of the human response genes relative to the responding genes in the mouse dataset.

Quantitative real-time PCR

Two micrograms of RNA from each sample was reverse transcribed in a 20 µL reaction. One microliter of the resulting cDNA was used in quantitative real-time PCR reactions with SYBR green labelling. All values were normalized to GAPDH values. The following primers were used for qRT-PCR: *gapdh*-F – 5'-AACTTTGGCATTGTGGAAGG, *gapdh*-R – 5'- ACACATTGGGGGTAGGAACA, *ifnb*-F – 5'-CTGGAGCAGCTGAATGGAAAG, *ifnb*-R – 5'-CTTGAAGTCCGCCCTGTAGGT, *tnfa*-F – 5'-GCACCACCATCAAGGACTCAA,

tnfa-R – 5'-TCGAGGCTCCAGTGAATTCG, *ifit3*-F – 5'-CTGAACTGCTCAGCCCACAC, *ifit3*-R – 5'- TGGACATACTTCCTTCCCTGA, *ifi205*-F – 5'- TCCACAACCCAGGAAGAGAC, *ifi205*-R – 5'-GAAGCCGAAGATGAGACCTG.

Flow cytometry

Cell surface marker analysis was performed to confirm the purity of bone marrow-derived macrophages. BMMs were thawed and plated overnight in BMM media. The following day the cells were washed twice with PBS, and taken off the plate using a cell scraper. The cells were then treated with Fc Block (BD Biosciences), incubated for 15 m, and then stained with antibodies. Six antibodies were used in the analysis: FITC-CD11c (eBiosciences), PE-CD11b (eBiosciences), PeCy5-F4/80 (eBiosciences), APC-GR1 (BD Biosciences), APC-CD19 (BD Biosciences), and APC-CD3 (BD Biosciences). After a 15 m incubation in the dark, cells were washed and resuspended in 500 uL of PBS + 10% FBS for flow cytometry analysis. The analysis was performed using a BD FACScalibur system with four-color florescence capability.

Cell surface markers were chosen to represent a range of immune cells. CD11c is a marker for dendritic cells [34,35]. CD11b is a marker for macrophages [36,37,38]. F4/80 is considered the best marker for identifying mature macrophages [39,40]. GR1 is a marker for bone marrow granulocytes and peripheral neutrophils [41,42]. CD19 is a marker for B cells [43,44]. CD3 is a marker for T cells [45]. As our population of BMMs were not expected to be positive for GR1, CD19, and CD3, antibodies chosen for these markers were all conjugated to a single florescent marker (APC). We found that 99.4% of the BMMs were CD11b+ (Supplementary Figure

2a), and 93.8% were F4/80+ (Supplementary Figure 2b). The cells stained negative for CD11c, GR1, CD19, and CD3 (data not shown).

Flow cytometry analysis was performed to confirm infectivity of *L. mexicana* in bone marrow-derived macrophages. BMMs were thawed and plated overnight on 6-well plates. *L. mexicana* were labelled with 10uM CFSE (Invitrogen) for 5 m at 37°C, mixing every 2 m. After 5 m, an equal volume of FBS was added to the labelled parasites, and the tube was spun down and washed with 15 mL of DMEM + 10% FBS. Labelled parasites were then resuspended in DMEM + 0.5% FBS for infection. BMMs were infected at a MOI of 10 and harvested 6 h post-infection using a cell scraper. The cells were washed with PBS and fixed in PBS + 0.2% formaldehyde for flow cytometry analysis.

Cell surface antigen staining and flow cytometry analysis were used to determine IL-17 receptor expression on BMMs. BMMs were thawed and stained with PE-conjugated anti-mouse IL-17R (eBiosciences). IL-17R-stained BMMs were compared to BMMs stained with PE rat IgG2a isotype control (eBiosciences) (Supplementary Figure 8).

Flow cytometry was also used to measure TNF and IL-12 production by BMMs stimulated with LPS. BMMs were thawed and plated overnight on 6-well plates. The next day 1 uM Monensin (BD Biosciences) and 100 ng of LPS (Sigma) were added to the cells. Four hours later, intracellular cytokine staining was performed by harvesting the cells using a cell lifter and resuspending the cells in 250 uL Cytofix/Cytoperm (BD Biosciences). The cells were incubated for 10 m at 4°C. They were then washed with Perm/Wash solution (BD Biosciences) and stained with PE-conjugated IL-12 (BD Biosciences) and APC-conjugated TNF (BD Biosciences).

After incubating for 15 m in the dark, the cells were washed again Perm/wash and resuspended in 200 uL PBS + 200 uL 0.4% Formaldehyde.

Cytometric bead analysis

BMMs were plated in 96-well plates at a density of 10^5 cells/well and stimulated with 100 ng/mL IFNG (R&D Systems). Supernatants were collected from wells at 2 h, 6 h, 12 h, and 24 h post-infection. Cytokine stimulation was performed in triplicate (3 wells per time point), and the supernatants from the 3 wells were pooled for the analysis. Cell supernatants were analyzed using the Cytometric bead array mouse inflammation kit (BD Biosciences) by following the manufacturer's instructions. Data was collected using a BD Facscalibur.

Cell staining

BMMs infected with *L. mexicana* along with uninfected BMMs were stained at 24 h post-infection by Diff-Quik and mounted using Prolong with Dapi (Invitrogen).

2.13. Supplementary figures legends

Supplementary Figure 1 – Comparative analysis of RNA isolated from fresh versus frozen bone marrow derived macrophages (BMMs).

RNA from freshly prepared and cryopreserved BMMs were collected and hybridized post amplification against each other (cryopreserved BMM RNA labelled with Cy3 and fresh BMM RNA labelled with Cy5) on a MEEBO oligonucleotide array. The scatter plot shows the resulting median fluorescence intensities (MFI) plotted on the X and Y axis for fresh and frozen macrophages. The correlation coefficient (R) is shown.

Supplementary Figure 2 – Purity of cultured bone marrow-derived macrophages (BMMs).

The purity of bone marrow derived macrophages that were used in microarray experiments was confirmed by flow cytometry analysis using antibodies against CD11b and F4/80. (A) Histogram showing the percentage of BMMs (99.4%) stained with CD11b (filled) against unstained BMMs (unfilled). (B) Histogram showing the percentage of BMMs (93.8%) stained with F4/80 (filled) against unstained BMMs (unfilled).

Supplementary Figure 3 – Infection of BMM with *L. mexicana*.

(A) Uninfected BMMs stained with Diff-Quik. (B) BMMs infected with *L. mexicana* at a MOI of 10 and stained with Diff-Quik 24 h post-infection. (C) BMMs infected with CFSE labelled *L. mexicana* at a MOI of 10, visualized by fluorescent

microscopy. (D) Flow cytometry analysis on uninfected BMMs (D) and BMMs infected with CFSE-labelled *L. mexicana* at a MOI of 10 (E).

Supplementary Figure 4 – Induction of interferon-stimulated genes by *T. cruzi.*

Quantitative real-time PCR analysis on cDNA from cells infected with *T. cruzi* or *L. mexicana* and from uninfected cells using primers directed against the interferon-stimulated genes IFIT3 (A) and IFI205 (B).

Supplementary Figure 5 – Comparative analysis of uninfected versus *T. cruzi* mock-infected BMMs.

RNA from uninfected BMMs and BMMs treated with supernatant from uninfected BESM cells for 24 h (mock-infected BMMs) were collected and hybridized post amplification against each other (uninfected BMM RNA labelled with Cy3 and mock-infected BMM RNA labelled with Cy5) on a MEEBO oligonucleotide array. The scatter plot shows the resulting median fluorescence intensities (MFI) plotted on the X and Y axis for fresh and frozen macrophages. The correlation coefficient (R) is shown.

Supplementary Figure 6 – Induction of alternative macrophage activation markers by IL-4 stimulated BMMs.

Heatmap showing the expression of genes that are known to be induced by IL-4 in alternatively activated macrophages, extracted from our IL-4 time course data. Black indicates unchanged level of expression relative to time 0 h, and red indicates upregulated levels expression.

Supplementary Figure 7 – Cross induction of classical activation cytokines.

(A) Quantitative real-time PCR analysis of *Ifnb* expression in cells stimulated with recombinant TNF and on unstimulated cells. TNF induced production of *Ifnb* transcript by 6 h post-stimulation. (B) Quantitative real-time PCR analysisof *Tnf* expression in cells stimulated with recombinant IFNG and IFNB and on unstimulated cells. TNF induced production of *Ifnb* transcript by 6 h post-stimulation. IFNG induced expression of *Tnf* transcript by 2 h post-stimulation, but IFNB does not. (C) TNF protein secretion into the supernatant of IFNG-stimulated BMMs 6 h post treatment was measured by cytometric bead analysis (BD).

Supplementary Figure 8 – IL-17 receptor expression on bone marrow-derived macrophages

Cell surface antigen staining was performed on BMMs using PE-conjugated IL-17R antibody. The histogram shows cells stained with IL-17R (filled) and cells stained with IgG2a isotype control (unfilled).

Supplementary Figure 9 – Induction of TNF by BMMs activated with LPS.

Intracellular cytokine staining analysis of TNF and IL-12 p40 in unstimulated BMMs (A) and BMMs stimulated with 100 ng/uL of LPS for 4 h (B).

Supplementary Figure 10 - Relating mouse macrophage responses to the human "common host response"

Heat map showing significantly altered genes as determined by multiclass SAM analysis for all cytokine and pathogen arrays (n=5414). The four lanes per each condition represent the kinetic timepoints 2h, 6h, 12h, and 24h. The graph on the

right side represents the frequency that genes in the heat map appear in the human common host response set determined by Jenner and Young (Nat Rev Mircrobiol 2005).

2.14. Supplementary figures

Supplementary figure 1

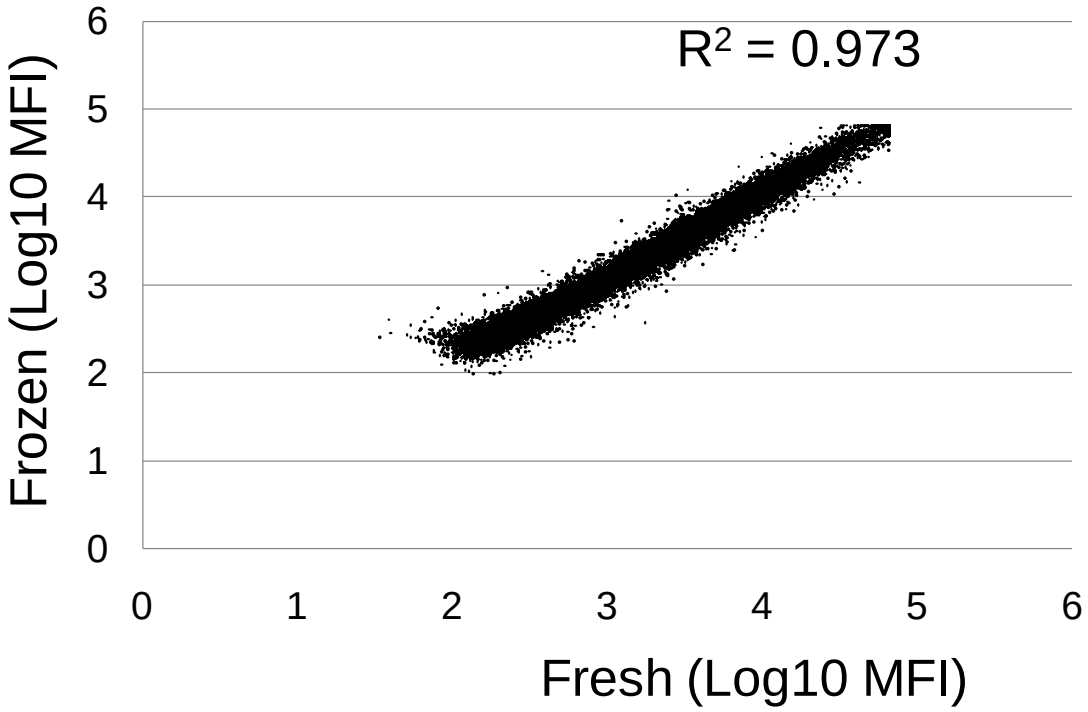

Supplementary figure 2

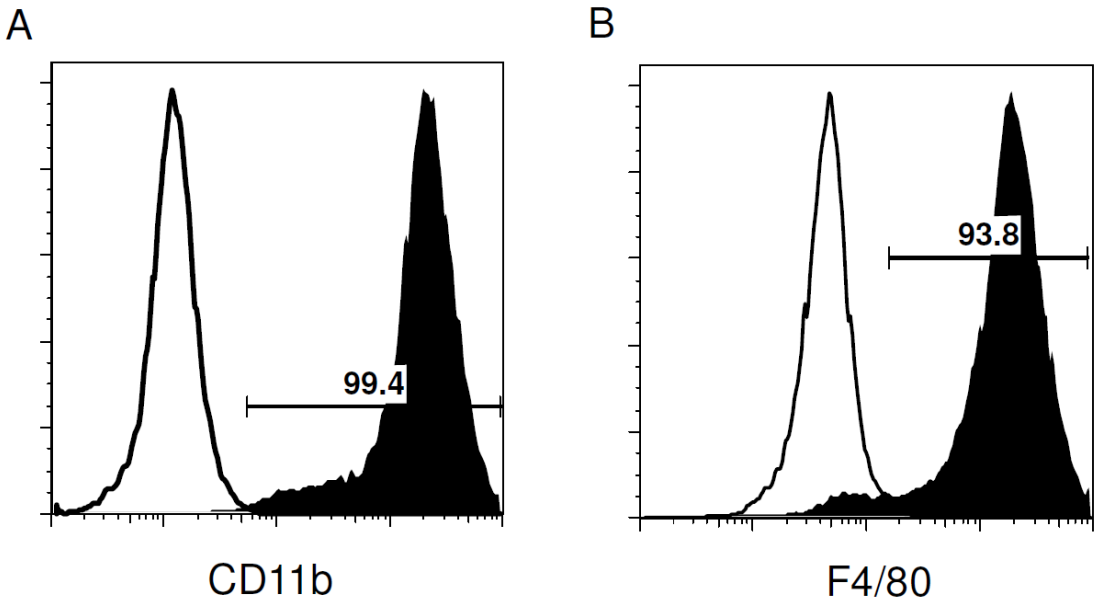

Supplementary figure 3

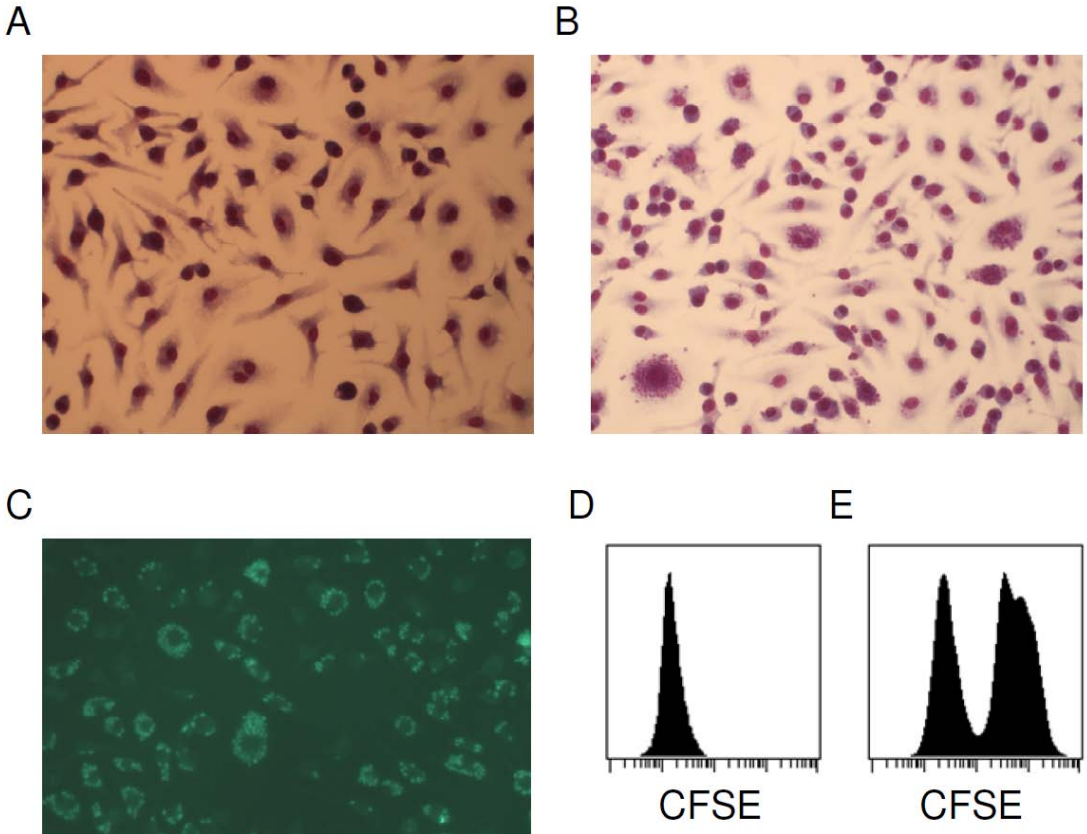

Supplementary figure 4

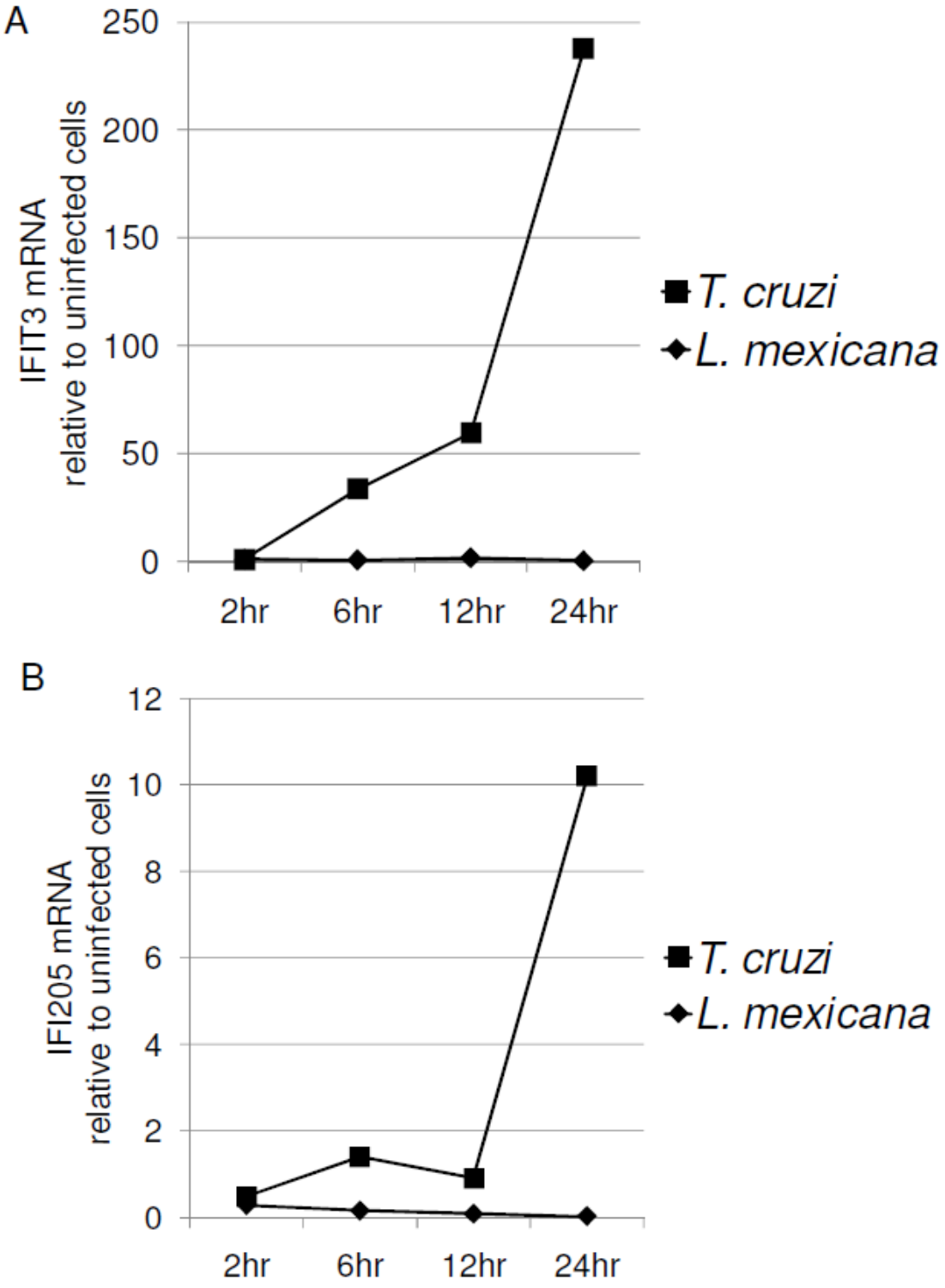

Supplementary figure 5

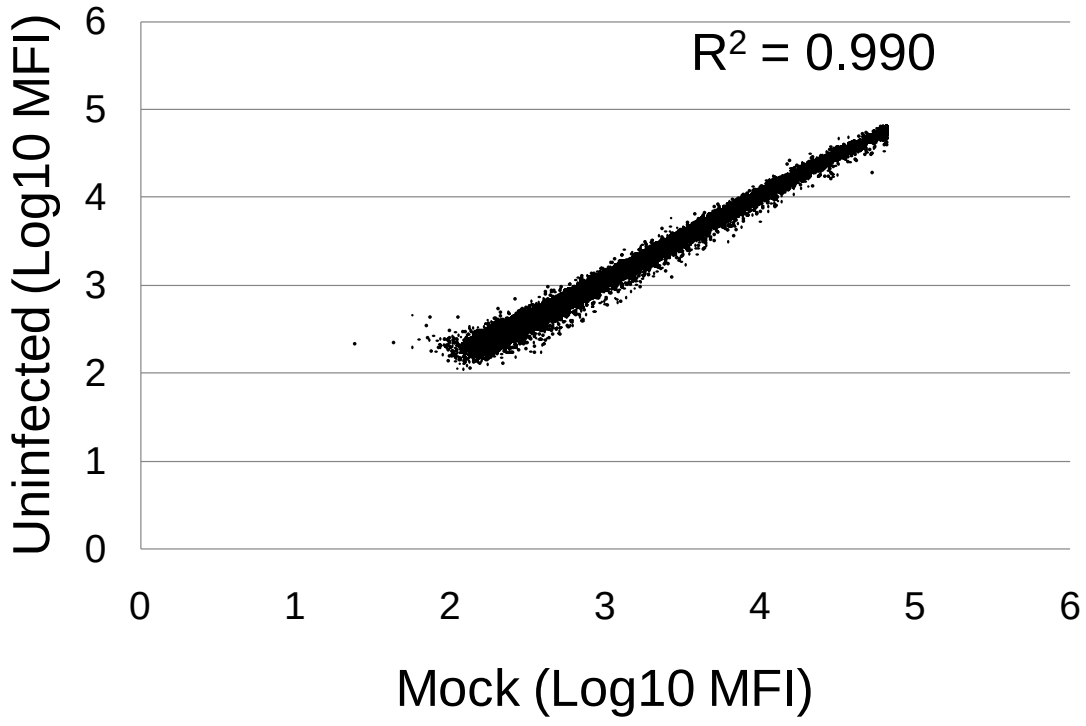

Supplementary figure 6

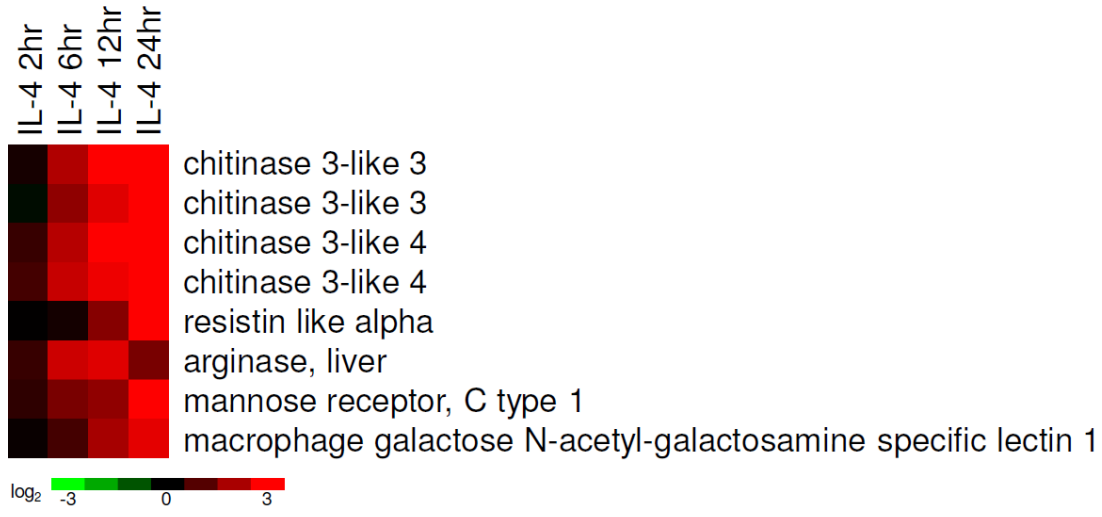

Supplementary figure 7

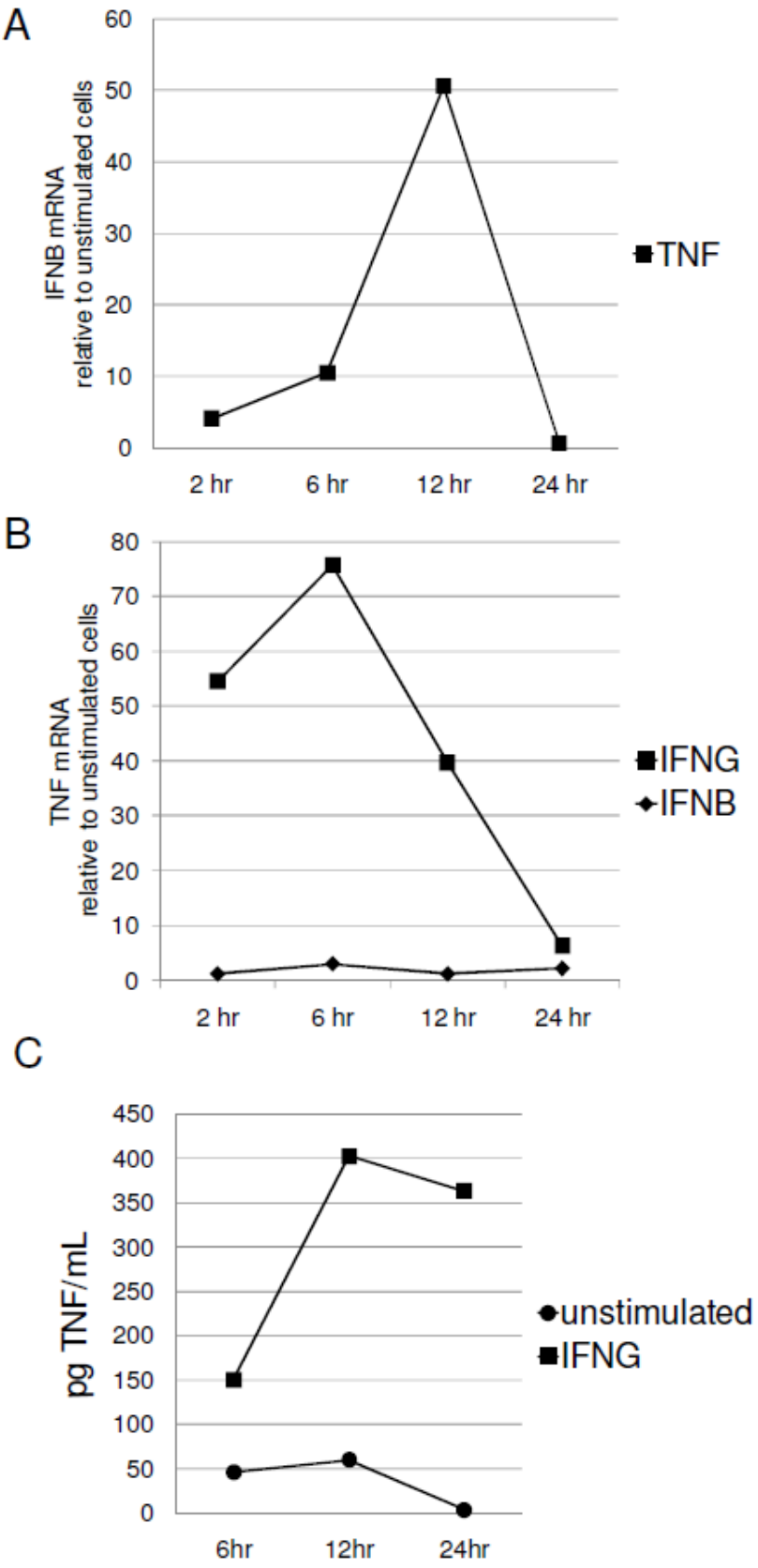

Supplementary figure 8

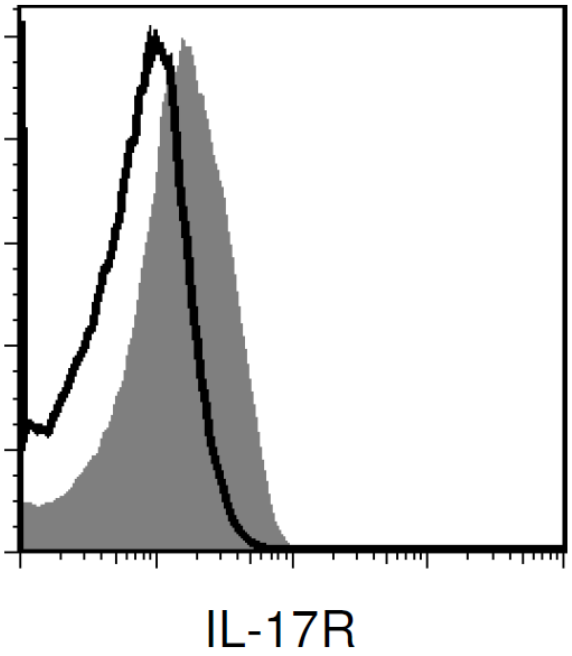

Supplementary figure 9

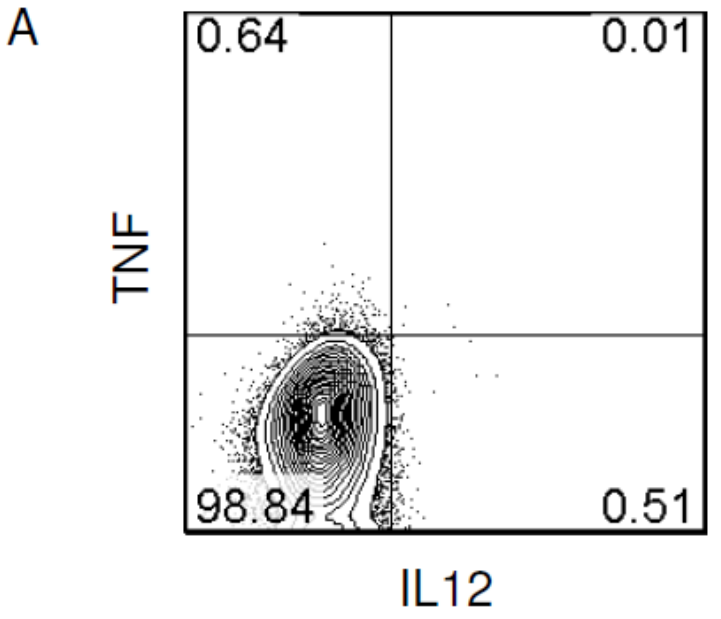

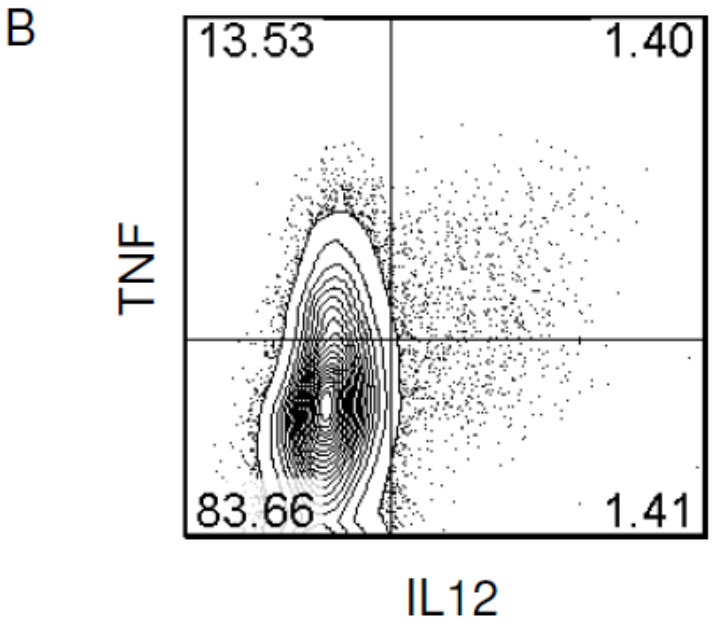

Supplementary figure 10

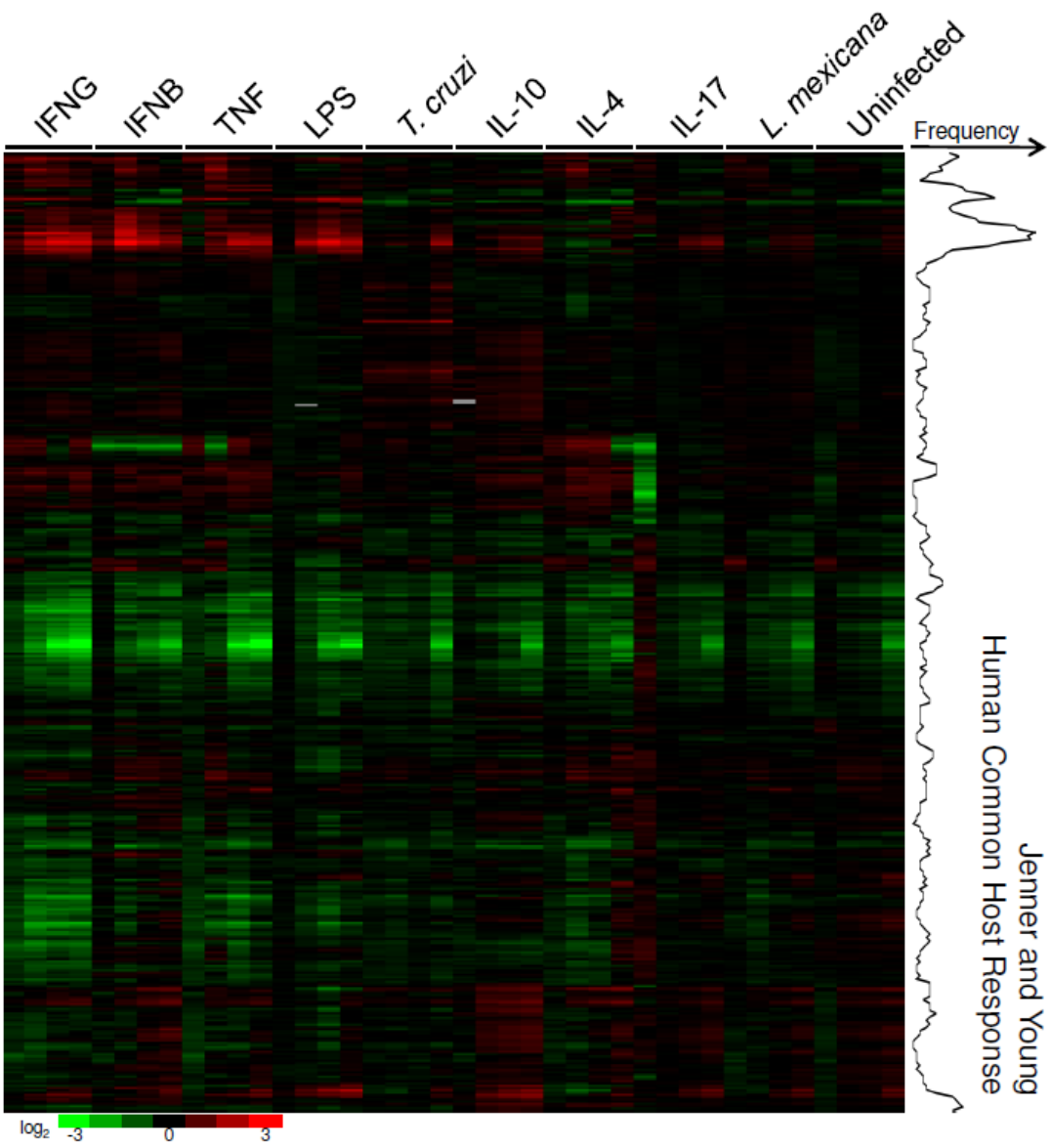

Chapter Three:

Immune Evasion Mechanisms of *Leishmania mexicana*

3.1. Introduction

The etiological agent of Cutaneous Leishmaniasis, *Leishmania mexicana* causes chronic, non-healing lesions in humans and in most mouse strains. This is in contrast to *Leishmania major*, a *Leishmania* species that causes a much milder, self-healing version of the same disease. The non-healing phenotype associated with *L. mexicana* results from the lack of an effective Th1-type immune response characterized by low levels of IFNG (1). Much attention has been given to a particular *L. mexicana* virulence factor, cysteine protease B (CPB), for its role in the suppression of Th1-type immunity in the host.

Cysteine protease B is a cathepsin L-like protease in the C1 family and CA clan. It is encoded by a tandem array of 19 genes located in a single locus. The majority of these genes are expressed in the amastigote stage of the parasite, but 2 out of the 19 genes are expressed in the promastigote stage (2). *L. mexicana* lacking the CPB gene array exhibit reduced virulence in several mouse strains as evidenced by smaller lesion size and parasite burden (3-5). The healing phenotype in mice infected with CPB-/- *L. mexicana* was associated with the presence of a protective Th1-type response as evidenced by higher levels of IFNG (5). Although *L. major* expresses a homologous array of CPB genes, CP activity is significantly lower than in *L. mexicana*. When the CPB gene array of *L. mexicana* was transfected into *L. major*, mice infected with CPB-transfected *L. major* displayed significantly higher parasite burden and corresponding lower levels of IFNG compared to mice infected with untransfected *L. major* (5). This suggested that *L. mexicana* CPB played an essential role in the suppression of Th1-type immunity in the host.

Although much work had been done to elucidate the role of CPB in the suppression of the adaptive immune response to *L. mexicana* infection, whether or not the protease played a role in the suppression of host responses in the initial stage of infection was unknown. Since only 2 out of the 19 genes in the CPB gene array are expressed in the life stage of the parasite that initially infects host cells, the suppressive effect of CPB would presumably be less robust than in the amastigote stage when the majority of the genes are expressed. However, another related protease, cysteine protease A, is expressed in the infective promastigote form of *leishmania*, and CPB/CPA-/- *L. mexicana* were less infective in BALB/c mice than CPB-/- *L. mexicana*, suggesting that CPA also plays a role in parasite virulence perhaps specific to the promastigote stage (2).

Infection of primary mouse macrophages by *L. mexicana* promastigotes results in very few transcriptional changes in the host cell, suggesting that the parasite employs strategies to either evade detection or suppress transcription in the host (6). In order to determine if the lack of transcriptional responses was the result of active suppression on the part of the parasite, we compared the transcriptional response of macrophages treated with killed *L. mexicana* with that of macrophages infected with live *L. mexicana*. In order to determine if *L. mexicana* CPB and CPA contributed to the silent nature of *L. mexicana* infection, we compared the transcriptional response of macrophages infected with CPB-/- and CPB/CPA-/- *L. mexicana* with that of macrophages infected with WT *L. mexicana*.

3.2. Methods

Macrophage preparation

See Chapter Two Section 2.4. Methods.

Macrophage infections and stimulations

Wild-type, CPB-/-, and CPB/CPA-/- *Leishmania mexicana* MNYC/BZ/62/M379 (obtained from J. Mottram), *L. major* LV39 MRHO/SU/59/P, and *L. donovani donovani* MHOMISD/OO/1S-2D (Ldd IS C12) were grown in M199 media. For bone marrow-derived macrophage (BMM) infection, cells were washed once with D-PBS, and their media was replaced with DMEM + 0.5% FBS containing parasites at a MOI of 10. For thioglycollate-elicited macrophage (TM) infection, cells were washed once with DMEM + 10% FBS, and their media was replaced with DMEM + 10% FBS containing parasites at a MOI of 10. Control, uninfected cells received media without parasites. The flasks were centrifuged at 168xG for 5 m to synchronize the infection. All infections took place over a 24 h time course with RNA collection at 2 h, 6 h, 12 h, and 24 h time points post-infection.

Heat-killed parasites were prepared by incubation at 65°C for 10 min. Parasites were then centrifuged and resuspended in appropriate media for infection. Lysed parasites were prepared by 3 rounds of rapid freeze-thaw between dry ice and 37°C water bath. BMMs were stimulated with LPS following *L. mexicana* infection to determine whether infected could inhibit macrophages responses to LPS. *L. mexicana* were labelled with 10uM CFSE (Invitrogen) and resuspended in DMEM + 0.5% FBS for infection. LPS was titrated and added to the media of infected and uninfected cells at 2 h post-infection at the concentrations 100ng/mL, 10ng/mL, 1ng/mL, 100pg/mL, and 10pg/mL. BMMs

were harvested 6 h post-infection using a cell scraper. The cells were washed with PBS and fixed in PBS + 0.2% formaldehyde for flow cytometry analysis.

Microarray analysis

For BMMs, cells were lysed using the TRIzol Reagent (Invitrogen), and RNA was isolated using the RNeasy Mini Kit (Qiagen). RNA was then amplified using the Amino Allyl MessageAmp II aRNA Amplification Kit (Ambion). Amplified RNA from each sample was hybridized against a pooled reference consisting of an equal quantity of RNA from all of the time points within a particular infection time course.

For TMs, cells were lysed and RNA was isolated using the RNeasy Mini Kit (Qiagen). RNA was then amplified using the Amino Allyl MessageAmp II aRNA Amplification Kit (Ambion). Amplified RNA from cells infected with WT *L. mexicana* was hybridized directly against amplified RNA from cells infected with CPB/CPA-/- *L. mexicana* and also against amplified RNA from cells stimulated with heat-killed *L. mexicana*.

All microarray analyses was performed on custom printed Mouse Exonic Evidence-based Oligonucleotide (MEEBO) Arrays. The arrays were scanned using a GenePix 4000B scanner and GenePix PRO version 4.1 (Axon Instruments/Molecular Devices). The Spotreader program (Niles Scientific) was used for array gridding and image analysis. The resulting data files were uploaded to Acuity version 4.0 (Molecular Devices), where the raw data was log transformed, filtered for "good quality spots" ((('RgnR^2(635/532)'>0.6) AND ('Flags'>=0))AND(('F532Mean-b532'>200) OR ('F635Median-b635'>200))), normalized to the 0 h control, and filtered for data present in at least 70% of samples. The resulting dataset was then analyzed for statistically

significant genes using the Statistical Analysis of Microarray (SAM) software version 3.0 (available at http://www-stat.stanford.edu/~tibs/SAM/).

Microarrays that were of poor quality (high background, low foreground) were repeated.

Statistical analysis of microarray data

Pairwise comparisons were performed between infected and uninfected cells in order to determine the number of genes significantly affected by the infection/stimulation and the relative fold changes of these genes. To do this, the two-class unpaired analysis in SAM was employed with a false discovery rate (FDR) cutoff of 1% and the condition that genes must have at least a two-fold change. We treated each time point as an independent replicate to identify genes that were consistently up or down-regulated over the 24 h time course.

Multiclass comparisons were also performed between groups of macrophages infected with different species of *Leishmania* in SAM with a false discovery cutoff of 0.1%. Once a list of significant genes was obtained, data was extracted from the total dataset for this list of significant genes using the Samster tool. The data was then hierarchically clustered in Cluster version 3.0 (http://bonsai.ims.u-tokyo.ac.jp/~mdehoon/software/cluster/software.htm#ctv), and the resulting heat map and trees were visualized using Java Treeview (available at http://sourceforge.net/projects/jtreeview/files/).

Quantitative real-time PCR

Two micrograms of RNA from each sample was reverse transcribed in a 20 µL reaction. One microliter of the resulting cDNA was used in quantitative real-time PCR reactions with SYBR green labelling. All values were normalized to GAPDH values. The

following primers were used for qRT-PCR: *gapdh*-F – 5'- AACTTTGGCATTGTGGAAGG, *gapdh*-R – 5'- ACACATTGGGGGTAGGAACA, *ifit3*-F – 5'- CTGAACTGCTCAGCCCACAC, *ifit3*-R – 5'- TGGACATACTTCCTTCCCTGA, *ifi205*-F – 5'- TCCACAACCCAGGAAGAGAC, *ifi205*-R – 5'- GAAGCCGAAGATGAGACCTG. *arg1*-F – 5'- CAGAAGAATGGAAGAGTCAG, *arg1*-R – 5'- CAGATATGCAGGGAGTCACC. *nos2*-F – 5'- CACTTGGATCAGGAACCTGAAGCCC, *nos2*-R – 5'- CTTTGTGCTGGGAGTCATGGAGCCG.

Flow cytometry

Flow cytometry was used to measure TNF and IL-12 production by BMMs stimulated with LPS. Infected and uninfected BMMs were treated with various concentrations of LPS (Sigma) and 1 uM Monensin (BD Biosciences). Four hours later, intracellular cytokine staining was performed by harvesting the cells using a cell lifter and resuspending the cells in 250 uL Cytofix/Cytoperm (BD Biosciences). The cells were incubated for 10 m at 4°C. They were then washed with Perm/Wash solution (BD Biosciences) and stained with PE-conjugated IL-12 (BD Biosciences) and APC-conjugated TNF (BD Biosciences). Cells were analyzed using a BD Facscalibur (BD Biosciences).

Cytometric bead analysis

BMMs were plated in 96-well plates at a density of 10^5 cells/well and infected with *L. mexicana* or treated with heat-killed *L. mexicana* in triplicate. Supernatants were collected from wells at 2 h, 6 h, 12 h, and 24 h post-infection, and each triplicate was pooled. Cell supernatants were analyzed using the Cytometric bead array mouse

inflammation kit (BD Biosciences) by following the manufacturer's instructions. Data was collected using a BD Facscalibur.

Intracellular amastigote high throughput assay

Sterile, black, 96-well, clear bottom plates (Greiner Bio-One) were seeded with TMs from C57BL/6 or BALB/c mice ($5x10^5$cells/ml). Two days after plating, the cells were infected with WT, CPB-/-, or CPB/CPA-/- *L. mexicana* and an MOI of 10. At 2 h post-infection, cells were washed 2 times with PBS to remove extracellular parasites. Media containing 100ng/mL IL-4 (Peprotech) or various concentrations (10uM, 100uM, or 1mM) of nor-NOHA (Enzo Life Sciences) or media alone were added to the cells. At 2, 4, 8, 24, and 48 h post-infection, cells were washed with PBS, fixed for 30 minutes with 4% formaldehyde, washed again with PBS, stained for at least 2h with 4',6'-diamidino-2-phenylindole (DAPI 300nM) and finally washed with PBS. Up to 12 replicates were taken for each sample.

Images were acquired with an INCell Analyzer 2000 automated epi-fluorescent microscope (G.E. Healthcare). The excitation and emission filters used to detect DAPI were 350/50 nm and 460/40 nm respectively. Three image fields were acquired per well with a 20X objective. The proprietary INCell Developer Toolbox 1.7 software was used for image analysis. Segmentation parameters were set to identify host nuclei with an area between 7 and 20μm^2 and parasite kinetoplast with an average area of 1μm^2. False positive parasite detection in the nucleus was excluded from the calculation. Host cell nuclei and parasite kinetoplasts were counted and the ratio of parasites DNA to host nuclei was selected as the measurement output.

3.3. Results

3.3.1. Heat-killed *L. mexicana* induces transcriptional response in bone marrow-derived macrophages characterized by interferon-stimulated genes

The macrophage response to infection with *L. mexicana* is highly unique because it results in very few transcriptional changes in the host (6). In fact, transcriptional responses of *L. mexicana*-infected BMMs were almost indistinguishable from that of uninfected BMMs (**Figure 1A**). In order to determine if the lack of response in infected macrophages was due to an active suppression on the part of the parasite, we treated BMMs with heat-killed *L. mexicana* and evaluated the transcriptional response by microarray analysis. BMMs treated with heat-killed *L. mexicana* produced a much more robust transcriptional response than BMMs infected with live *L. mexicana* (**Figure 1B**). In fact, when arrays representing BMMs treated with heat-killed *L. mexicana* were clustered along with arrays representing BMMs infected with live *L. mexicana* and arrays representing BMMs stimulated with LPS, heat-killed *L. mexicana*-treated macrophages clustered more closely with LPS-stimulated macrophages than with live *L. mexicana*-infected macrophages (**Figure 1C**).

A total of 373 genes were significantly changed in BMMs treated with heat-killed *L. mexicana* compared to uninfected cells, whereas only 15 genes were significantly changed in BMMs infected with live *L. mexicana* compared to uninfected cells. Most of the significantly changed genes in BMMs stimulated with heat-killed *L. mexicana* were upregulated relative to uninfected cells. The most prominent group of genes within this upregulated set were the so-called Interferon-Stimulated Genes (ISG), which included interferon activated gene 205 (*ifi205*) and interferon-induced protein with

tetratricopeptide repeats 3 (*ifit3*) (**Table 1**). The upregulation of these ISGs were confirmed by quantitative PCR (**Figure 1D**). In order to determine if the upregulation of ISGs at the transcriptional level translated to increased production of inflammatory cytokines and chemokines in the cell supernatant, we performed cytometric bead assays to measure the level of IL-12, TNF, IFNG, IL-10, IL6, and MCP-1 in the supernant of macrophages that were either infected with live *L. mexicana* or treated with heat-killed *L. mexicana*. Although there was no different in the concentration of the cytokines in the supernatant (data not shown), BMMs treated with heat-killed *L. mexicana* produced greater amounts of MCP-1 (also known as CCL2) than BMMs infected with live *L. mexicana* throughout the 24 h timecourse (**Figure 1E**). This is consistent with the increased *ccl2* gene expression in heat-killed *L. mexicana*-treated BMMs seen in the microarray analysis (**Table 1**).

These data suggest that live *L. mexicana* suppresses host activation via a mechanism that is inactivated in the heat killing process of the parasite. The induction of ISGs by heat-killed *L. mexicana* suggests that a specific pathway leading to ISG induction is blocked by live *L. mexicana*. However, this pathway does not involve induction of interferons as IFNG and other pro-inflammatory cytokines are not present in higher levels in the supernatant of cells treated with heat-killed *L. mexicana*. Furthermore, neither IFNG nor the type I interferons IFNB and IFNA were shown to be upregulated by microarray analysis or quantitative PCR (data not shown). Therefore, the induction of ISGs by heat-killed *L. mexicana* occurs via an alternative pathway that does not involved the induction of interferons. The increased production of the chemokine MCP-1 by cells treated with heat-killed *L. mexicana* suggests that live *L. mexicana* may

also suppress a pathway leading to its induction. It cannot be ruled out that elements of the parasite that are disrupted and released during the process of heat killing are the cause of the increased activation in host macrophages. To address this question, we turned our focus to the macrophage response of specific *L. mexicana* mutants.

3.3.2. CPB-/- and CPB/CPA-/- *L. mexicana* induces transcriptional response in bone marrow-derived macrophages characterized by interferon-stimulated genes

The *L. mexicana* virulence factor cysteine protease B has been shown to be involved in the inhibition of IL-12 by host macrophages and subsequently the inhibition of a Th1-type immune response (5, 7). In order to determine if *L. mexicana* CPB and the related protease CPA are involved in the suppression of macrophage transcriptional responses, we infected BMMs with either CPB-/- *L. mexicana* or CPB/CPA-/- *L. mexicana* and compared the transcriptional profiles of these BMMs with that of BMMs infected with WT *L. mexicana*. When we compared the transcriptional response of BMMs infected with CPB-/- *L. mexicana* with that of uninfected BMMs via pairwise SAM analysis, we found that 48 genes were significantly different with all of these genes being upregulated in the infected BMMs (**Figure 2A**). When the same pairwise SAM analysis was used to compare BMMs infected with CPB/CPA-/- *L. mexicana* and uninfected BMMs, 287 genes were significantly different (**Figure 2B**). The more robust transcriptional response following infection with CPB/CPA-/- *L. mexicana* is consistent with the fact that CPA is predominantly expressed the promastigote form of the parasite, whereas CPB is predominantly expressed in the amastigote form with only 2 out of 19 genes in the expression array expressed in promastigotes (2). When we analyzed the genes that were upregulated by CPB-/- and CPB/CPA-/- *L. mexicana*, we found that

many of the same interferon-stimulated genes that were upregulated in BMMs treated with heat-killed *L. mexicana* were also upregulated in BMMs infected with the mutant *L. mexicana*. Genes upregulated by heat-killed, CPB-/-, and CPB/CPA-/- *L. mexicana* included *ifi205, ifit3,* and *ccl2* (**Table 2 and Table 3**). Quantitative PCR confirmation of *ifit3* expression showed that heat-killed, CPB/CPA-/-, and CPB-/- *L. mexicana* all induced the gene in BMMs by 24 h post-infection, with the level of induction highest in BMMs treated with heat-killed *L. mexicana*, followed by BMMs infected with CPB/CPA-/- *L. mexicana*, and finally BMMs infected with CPB-/- *L. mexicana* (**Figure 2C**). BMMs infected with WT *L. mexicana* and uninfected BMMs did not express *ifit3.*

These data suggested that *L. mexicana* CPB and CPA play a role in the suppression of host macrophage responses following infection. However, subsequent experiments yielded results inconsistent with the initial findings. For example, when the infection timecourse was repeated, we found ISG induction even in uninfected BMMs. This aberrant induction of ISGs was resolved by switching the infection media used from DMEM + 0.5% FBS to BMM media. However, under these experimental conditions the macrophages appeared to be less responsive to stimulation, failing to induce ISGs when infected by CPB/CPA-/- *L. mexicana* and even when treated with heat-killed or lysed *L. mexicana* (see Appendix Section A1.3). Even the response to the positive control LPS was significantly diminished as compared to previous experiments. These results suggested that mouse bone marrow-derived macrophages were not a reliable model to study host responses to *Leishmania* infection. Therefore, we turned our focus to another type of primary mouse macrophage, thioglycollate-elicited peritoneal macrophages.

3.3.3. WT *L. mexicana* induces host arginase in thioglycollate-elicted macrophages, but CPB/CPA-/- *L. mexicana* does not

Thioglycollate-elicited peritoneal macrophages (TM) and bone marrow-derived macrophages (BMM) taken from the same mouse and stimulated under the same conditions produce highly divergent transcriptional profiles (6). One possible explanation for this is that TMs exist in a more activated state as they have been recruited to the peritoneum in response to stimulation by thioglycollate, whereas macrophages derived from the bone marrow are resident monocytes that are then differentiated into macrophages in MCSF-containing culture. In order to compare the transcriptional response of TMs to infection with WT versus CPB/CPA-/- *L. mexicana*, we hybridized RNA from macrophages infected with WT *L. mexicana* directly against RNA from macrophages infected with CPB/CPA-/- *L. mexicana* on a single microarray. We found that the overall transcriptional response to WT and CPB/CPA-/- *L. mexicana* was very similar (**Figure 3A**). However, a single gene of interest, *arg1*, was identified as being more highly expressed in macrophage infected with WT *L. mexicana* than in macrophages infected with CPB/CPA-/- *L. mexicana*. When the same analysis was performed comparing macrophages infected with WT *L. mexicana* and macrophages treated with heat-killed *L. mexicana*, *arg1* was also identified as being more highly expressed in the macrophages infected with WT *L. mexicana* (**Figure 3B**). These microarray data were confirmed by quantitative PCR analysis of *arg1*, which showed that WT *L. mexicana* induced *arg1* more strongly than CPB/CPA-/- or heat-killed *L. mexicana* by 24 h post-infection (**Figure 3C**). Lysed *L. mexicana* also induced *arg1* by 24 h post-infection more strongly than CPB/CPA-/- and heat-killed *L. mexicana*. This

may be attributed to the release of cellular components by the parasite during lysis that led to *arg1* induction via engagement of pattern recognition receptors on the macrophage.

As arginase is known to inhibit Th1-type immunity in the host, its induction by WT *L. mexicana* suggests that *L. mexicana* is inducing *arg1* to promote its own survival within the macrophage. In the macrophage, arginase competes with iNOS for the same substrate, L-arginine. Whereas iNOS converts L-arginine into nitric oxide, important in pathogen killing, arginase converts L-arginine into L-ornithine and other polyamines, important for parasite growth (8). In order to determine if *L. mexicana* inhibited iNOS, we performed quantitative PCR on the iNOS transcript, *nos2*. We found that *nos2* was not induced by heat-killed or CPB/CPA-/- *L. mexicana* although it was induced robustly by LPS, as is expected (**Figure 3D**). The induction of *arg1* by WT *L. mexicana* appeared to occur specifically in TMs as *arg1* induction was not observed in BMMs by microarray and qPCR analysis (data not shown). The induction also appeared to be specific to TMs derived from C57BL/6 mice, as TMs derived from BALB/c mice did not express *arg1* over baseline following *L. mexicana* infection (data not shown). This may be due to BALB/c mice expressing much higher background levels of *arg1*, making the induction over baseline difficult to detect.

3.3.4. CPB-/- and CPB/CPA-/- *L. mexicana* are defective at establishing infection in thioglycollate-elicted macrophages

Our finding that *arg1* is induced in TMs by WT but not by CPB/CPA-/- *L. mexicana* suggests that WT *L. mexicana* are able to employ methods to promote its own growth in macrophages that *L. mexicana* lacking CPB and CPA are not. In order to

determine if CPB/CPA-/- and CPB-/- *L. mexicana* exhibited a growth defect in TMs, we utilized a high-throughput infectivity assay that allowed us to count intracellular amastigotes using the InCell Analyzer. When the assay was performed using TMs form BALB/c mice, we found that CPB-/- and CPB/CPA-/- *L. mexicana* exhibited a significant defect in establishment of infection and growth in macrophages (**Figure 4A**). Although WT *L. mexicana* diminished in numbers over time, the number of intracellular WT amastigotes at 2 h post-infection was approximately 5-fold greater than the number of intracellular CPB-/- or CPB/CPA-/- amastigotes at 2 h post-infection. The number of intracellular amastigotes in CPB-/- and CPB/CPA-/- *L. mexicana*-infected macrophages also diminished over time, suggesting that the TMs are ultimately able to destroy the amastigotes. In order to determine if *L. mexicana* CPB and CPA played a role in host cell survival, we compared the total number of host cell nuclei under the various infection conditions. We found that the number of host cell nuclei in the cultures infected with WT, CPB-/-, and CPB/CPA-/- *L. mexicana* were similar during the first 24 h of infection, but at 48 h post-infection, the number of host cell nuclei in cultures infected with WT *L. mexicana* decreased while host cell nuclei in cultures infected with CPB-/- and CPB/CPA-/- *L. mexicana* continued to increase (**Figure 4B**). This suggests that WT *L. mexicana* are killing TMs between 24 and 48 h post-infection, while CPB-/- and CPB/CPA-/- *L. mexicana* are not able to kill TMs.

Unexpectedly, the pattern observed in TMs taken from BALB/c mice was not seen in infections using TMs from C57BL/6 mice. CPB-/- and CPB/CPA-/- *L. mexicana* still exhibited a defect in establishing early infection, as evidenced by significantly higher numbers of intracellular amastigotes in WT *L. mexicana*-infected cells at 4 h post-

infection (**Figure 4C**). However, the number of intracellular CPB-/- and CPB/CPA-/- *L. mexicana* amastigotes per host cell increased by the later timepoints of infection while intracellular WT *L. mexicana* amastigotes per host cell decreased in number. By 48 h post-infection, the number of intracellular amastigotes in CPB-/- and CPB/CPA-/- *L. mexicana*-infected cells was significantly higher than the number of intracellular amastigotes in WT *L. mexicana*-infected cells. In order to determine if this was the result of macrophage cell death, we compared the number of host cell nuclei in cultures infected with WT, CPB-/-, and CPB/CPA-/- *L. mexicana.* We found that the number of host nuclei decreased significantly between 8 and 48 h post-infection in cultures infected with CPB-/- and CPB/CPA-/- *L. mexicana* (**Figure 4D**). However, in cultures infected with WT *L. mexicana,* the number of host nuclei increased between 8 and 48 h post-infection. This suggests that TMs in the cultures infected with CPB-/- and CPB/CPA-/- *L. mexicana* are dying during the later timepoints of infection, whereas TMs from cultures infected with WT *L. mexicana* continue to grow. Since the values in Figure 4C represent a ratio of intracellular parasites to host cells, the decrease in the number of host cells in the cultures infected with CPB-/- and CPB/CPA-/- *L. mexicana* could account for the increase in the ratio of parasites to host cells. These data suggest that CPB and CPA play a role in the successful establishment of infection in TMs taken from C57BL/6 mice. Unexpectedly, they may also play a role in the survival of host cells in *L. mexicana*-infected cultures.

3.3.5. IL-4 and nor-NOHA have minimal effects on *L. mexicana* growth in thioglycollate-elicited macrophages

In order to determine if host arginase plays a role in *L. mexicana* growth within TMs, we compared the growth of parasites in the presence and absence of the arginase inhibitor nor-NOHA as well as in the presence and absence of the arginase inducer IL-4. The inhibitor nor-NOHA had a minimal effect on parasite growth within TMs taken from BALB/c mice (**Figure 4A**). The number of intracellular WT *L. mexicana* was not significantly reduced in macrophages treated with nor-NOHA compared to untreated macrophages. The inhibitor also did not have a significant effect on the growth of intracellular parasites in TMs taken from C57BL/6 mice (**Figure 5A**). Since the activity of the inhibitor has not been confirmed, these negative results are difficult to interpret. One explanation may be that the induction of arginase at the transcriptional level did not translate into increased protein expression and activity. These results may suggest that the defect in intracellular growth exhibited by CPB-/- and CPB/CPA-/- *L. mexicana* is unrelated to their inability to induce arginase.

The addition of IL-4 did not significantly improve the growth of CPB-/- and CPB/CPA-/- *L. mexicana* in TMs taken from BALB/c mice (**Figure 4A**) or from C57BL/6 mice (data not shown). However, IL-4 did improve growth of WT *L. mexicana* in C57BL/6 TMs (**Figure 5B**). While the number of intracellular amastigotes diminished over time in untreated TMs, treatment with IL-4 rescued the growth of the parasites by 48 h post-infection. This increase in the number of intracellular parasites may be attributed to a decrease in the number of host cells in cultures infected with WT *L. mexicana* and then treated with IL-4 (**Figure 4D**). The negative effect on host cell survivial brought about by IL-4 is consistent with the fact that IL-4 inhibits the microbicidal activities of the macrophage through induction of arginase, which inhibits

the production of nitric oxide. These data suggest that the addition of IL-4 to TMs infected with WT *L. mexicana* results in increased parasite growth and host cell death, possibly through an arginase-dependent mechanism.

3.4. Discussion

In this study, we have described several important aspects of the interaction between the infective *Leishmania* promastigote and the host macrophage. These interactions account for the unique ability of *L. mexicana* to infect macrophages in a transcriptionally silent manner. We found that although infection of bone marrow-derived macrophages by live *L. mexicana* resulted in almost no transcriptional changes in the host, treatment of BMMs with heat-killed or lysed *L. mexicana* resulted in a host transcriptional signature characterized by the upregulation of a group of interferon-stimulated genes. Interestingly, infection of BMMs with *L. mexicana* lacking either CPB or both CPB and CPA also resulted in the upregulation of interferon-stimulated genes in the host. These data suggest that *L. mexicana* promastigotes actively suppress host macrophage transcription via a mechanism at least partially dependent upon CPB and CPA.

An unexpected outcome of our experiments in bone marrow-derived macrophages was the realization that these primary cells are extremely sensitive to specific culture conditions. This resulted in several aberrant transcriptional responses that made experiments done with these macrophages difficult to interpret. The first issue we encountered was an aberrant expression of interferon-stimulated genes in unstimulated cells. After ruling out culture contamination, improper cell differentiation, and cell death as causes of this phenomenon, we discovered that the aberrant expression could be remedied by keeping the macrophages in BMM media throughout the infection timecourse. Although these culture conditions remedied the issue of gene activation in unstimulated cells, under these conditions, the cells were less responsive to activation by

stimuli in general. They no longer responded to treatment with heat-killed or lysed *L. mexicana* and showed significantly reduced responses to potent macrophage stimulators such as LPS and IFNG. Although these many issues made our initial findings in BMMs difficult to reproduce, we believe those data are biologically meaningful and provide insight into the interaction between the *Leishmania* promastigote and the host macrophage.

In addition to the interactions between *L. mexicana* and bone marrow-derived macrophages, we also analyzed the transcriptional effects of *L. mexicana* infection on thioglycollate-elicited macrophage taken from the peritoneum. We found that WT *L. mexicana* induced arginase in host TMs, but CPB/CPA-/- *L. mexicana* did not. Arginase is known to be a mediator of disease in *Leishmania* infection. It has been shown to be induced in both susceptible (BALB/c) and resistant (C57BL/6) mice by *L. major* (9). Inhibition of arginase by nor-NOHA resulted in decreased parasite load and delayed disease outcome in BALB/c mice, whereas L-ornithine supplementation resulted in increased lesion size in C57BL/6 mice. In order to determine whether the inability to induce arginase accounted for the decreased virulence of CPB/CPA-/- *L. mexicana*, we analyzed the infectivity and growth of WT and mutant *L. mexicana* within TMs. We found that CPB-/- and CPB/CPA-/- *L. mexicana* were defective in their ability to establish infection in host macrophages taken from either BALB/c or C57BL/6 mice. However, this defect did not appear to be due to the parasite's inability to induce arginase as addition of IL-4 had little effect on the infectivity of CPB-/- and CPB/CPA-/- parasites. IL-4 did have an effect on TMs infected with WT *L. mexicana* as the number of intracellular parasites per host cell increased in cultures treated with IL-4 relative to

untreated cultures. This may be due to inhibition of NO and Th1-type cytokine production by IL-4 in these macrophages, leading to increased parasite survival. Addition of the arginase inhibitor nor-NOHA to WT *L. mexicana*-infected cells also did not significantly affect the infectivity and growth within TMs. These data suggest that arginase may play a role in the survival of WT *L. mexicana* amastigotes within macrophages at later timepoints of infection. However, the defect in the establishment of infection seen by CPB-/- and CPB/CPA-/- *L. mexicana* may not be related to their inability to induce host arginase but rather due to an as yet unknown mechanism.

An unexpected finding in these experiments was that CPB-/- and CPB/CPA-/- *L. mexicana* appeared to fare better than their WT counterparts in TMs derived from C57BL/6 mice. Although they were still defective in establishing infection in the macrophages, these mutant *leishmania* were able to increase in number relative to host cells whereas WT *L. mexicana* decreased in number relative to host cells. Further analysis revealed that in cultures infected with the mutant *leishmanias*, host cells significantly decreased in number over time, suggesting that infection by CPB-/- and CPB/CPA-/- *L. mexicana* was contributing to host cell death. This was unexpected given that all previous evidence points to a decrease in virulence for these CPB and CPA-deficient parasites. It is possible that *L. mexicana* interact with C57BL/6 TMs in a unique way and that CPB and CPA actually play a role in preventing cell death in this system. This unique interaction merits further investigation to both confirm and expand upon these findings.

3.5. Acknowledgements

I would like to thank my advisor Jim McKerrow for his mentorship throughout this project as well as P'ng Loke for his mentorship in the first part of this project. I would also like to thank my committee members Anita Sil and Tony Defranco for helpful discussions and advice. In addition, I am grateful to Jeremy Mottram for providing the CPB-/- and CPB/CPA-/- *L. mexicana* used in these studies, to Ryan Swenerton for help with BMM extraction, to KC Lim for help with mouse injections, to Charlotte Berkes for advice on macrophage infections, to Geraldine DeMuylder for help with the high-throughput intracellular amastigote assay, and to the entire McKerrow lab for scientific and moral support.

3.6. References for Chapter Three

1. Alexander J, Kaye PM. Immunoregulatory pathways in murine leishmaniasis: different regulatory control during Leishmania mexicana mexicana and Leishmania major infections. Clin Exp Immunol. 1985;61(3):674-82. PMCID: 1577261.
2. Mottram JC, Coombs GH, Alexander J. Cysteine peptidases as virulence factors of Leishmania. Curr Opin Microbiol. 2004;7(4):375-81.
3. Alexander J, Coombs GH, Mottram JC. Leishmania mexicana cysteine proteinase-deficient mutants have attenuated virulence for mice and potentiate a Th1 response. J Immunol. 1998;161(12):6794-801.
4. Denise H, McNeil K, Brooks DR, Alexander J, Coombs GH, Mottram JC. Expression of multiple CPB genes encoding cysteine proteases is required for Leishmania mexicana virulence in vivo. Infect Immun. 2003;71(6):3190-5. PMCID: 155739.
5. Buxbaum LU, Denise H, Coombs GH, Alexander J, Mottram JC, Scott P. Cysteine protease B of Leishmania mexicana inhibits host Th1 responses and protective immunity. J Immunol. 2003;171(7):3711-7.
6. Zhang S, Kim CC, Batra S, McKerrow JH, Loke P. Delineation of diverse macrophage activation programs in response to intracellular parasites and cytokines. PLoS Negl Trop Dis. 2010;4(3):e648. PMCID: 2846935.
7. Cameron P, McGachy A, Anderson M, Paul A, Coombs GH, Mottram JC, et al. Inhibition of lipopolysaccharide-induced macrophage IL-12 production by Leishmania mexicana amastigotes: the role of cysteine peptidases and the NF-kappaB signaling pathway. J Immunol. 2004;173(5):3297-304.
8. Das P, Lahiri A, Chakravortty D. Modulation of the arginase pathway in the context of microbial pathogenesis: a metabolic enzyme moonlighting as an immune modulator. PLoS Pathog. 2010;6(6):e1000899. PMCID: 2887468.
9. Iniesta V, Carcelen J, Molano I, Peixoto PM, Redondo E, Parra P, et al. Arginase I induction during Leishmania major infection mediates the development of disease. Infect Immun. 2005;73(9):6085-90. PMCID: 1231060.

3.7. Figure legends

Figure 1 - Heat-killed *L. mexicana* induces a transcriptional response in BMMs characterized by the upregulation of interferon stimulated genes.

Pairwise SAM analysis was performed to compare the transcriptional profiles of BMMs infected with *L. mexicana* and uninfected BMMs (A) and to compare the transcriptional profiles of BMMs treated with heat-killed *L. mexicana* and untreated BMMs (B). (C) Unsupervised two-dimensional cluster analysis was performed on genes exhibiting statistically significant variability between the three conditions, as determined by multiclass SAM analysis. (D) Quantitative real-time PCR analysis of *ifi205* and *ifit3* was performed on cDNA from uninfected, WT *L. mexicana*-infected, and heat-killed *L. mexicana*-treated BMMs. (E) Cytometric bead analysis was performed using the supernatants of cells infected with live *L. mexicana* and cells treated with heat-killed *L. mexicana*.

Figure 2 - CPB-/- and CPB/CPA-/- *L. mexicana* also induce interferon stimulated genes in BMMs.

Pairwise SAM analysis was performed to compare the transcriptional profiles of BMMs infected with CPB-/- *L. mexicana* and uninfected BMMs (A) and to compare the transcriptional profiles of BMMs infected with CPB/CPA-/- *L. mexicana* and uninfected BMMs (B). (C) Quantitative real-time PCR analysis of *ifit3* was performed on cDNA from uninfected, WT *L. mexicana*-infected, heat-killed *L. mexicana*-treated, CPB-/- *L. mexicana*-infected, and CPB/CPA-/- *L. mexicana*-infected BMMs.

Figure 3 - Arginase is induced by WT but not CPB/CPA-/- *L. mexicana* in TMs derived from C57BL/6 mice

RNA from TMs infected with WT or CPB/CPA-/- *L. mexicana* (A) or RNA from TMs treated with heat-killed or live *L. mexicana* (B) were hybridized on a single microarray, and the relative fluorescence intensities of the genes were plotted using SpotReader. Quantitative real-time PCR analysis of *arg1* (C) or *nos2* (D) was performed on cDNA from uninfected, WT *L. mexicana*-infected, CPB/CPA-/- *L. mexicana*-infected, heat-killed *L. mexicana*-treated, lysed *L. mexicana*-treated, and LPS-treated TMs. The four bars per condition represent the kinect timepoints 2h, 6h, 12h, and 24h.

Figure 4 - *L. mexicana* CPB and CPA affect parasite infectivity and growth in TMs derived from C57BL/6 and BALB/c mice.

Intracellular growth assay was performed to measure the number of intracellular amastigotes per host cell (A) and the number of total host cells (B) following infection with WT, CPB-/-, and CPB/CPA-/- *L. mexicana* and following treatment with the arginase inhibitor nor-NOHA and with the arginase inducer IL-4. TMs were derived from BALB/c mice. The infection occurred over a 48 h timecourse, and timepoints were taken at 2, 4, 8, 24, and 48h post-infection. The same assay and analysis was performed to determine intracellular amastigotes per host cell (C) and total number of host cells (D) for infections using TMs derived from C57BL/6 mice.

Figure 5 - The effect of nor-NOHA and IL-4 on *L. mexicana* infectivity and growth within TMs taken from C57BL/6 mice.

C57BL/6 TMs infected with *L. mexicana* were treated with either nor-NOHA (A) or IL-4 (B) to determine the effect on intracellular growth. In (A) the asterisk indicates a statistically significant difference between the WT+nor-NOHA (100mM) and WT conditions as determined by t-test with n=5 for WT+nor-NOHA (100mM) and n=8 for WT. In (B) the asterisk indicates a statistically significant difference between the two conditions as determined by t-test with n=3 for WT+IL-4 and n=4 for WT.

3.8. Figures

Figure 1 - Live *L. mexicana* do not activated BMMs during infection, but heat-killed *L. mexicana* do activate BMMs.

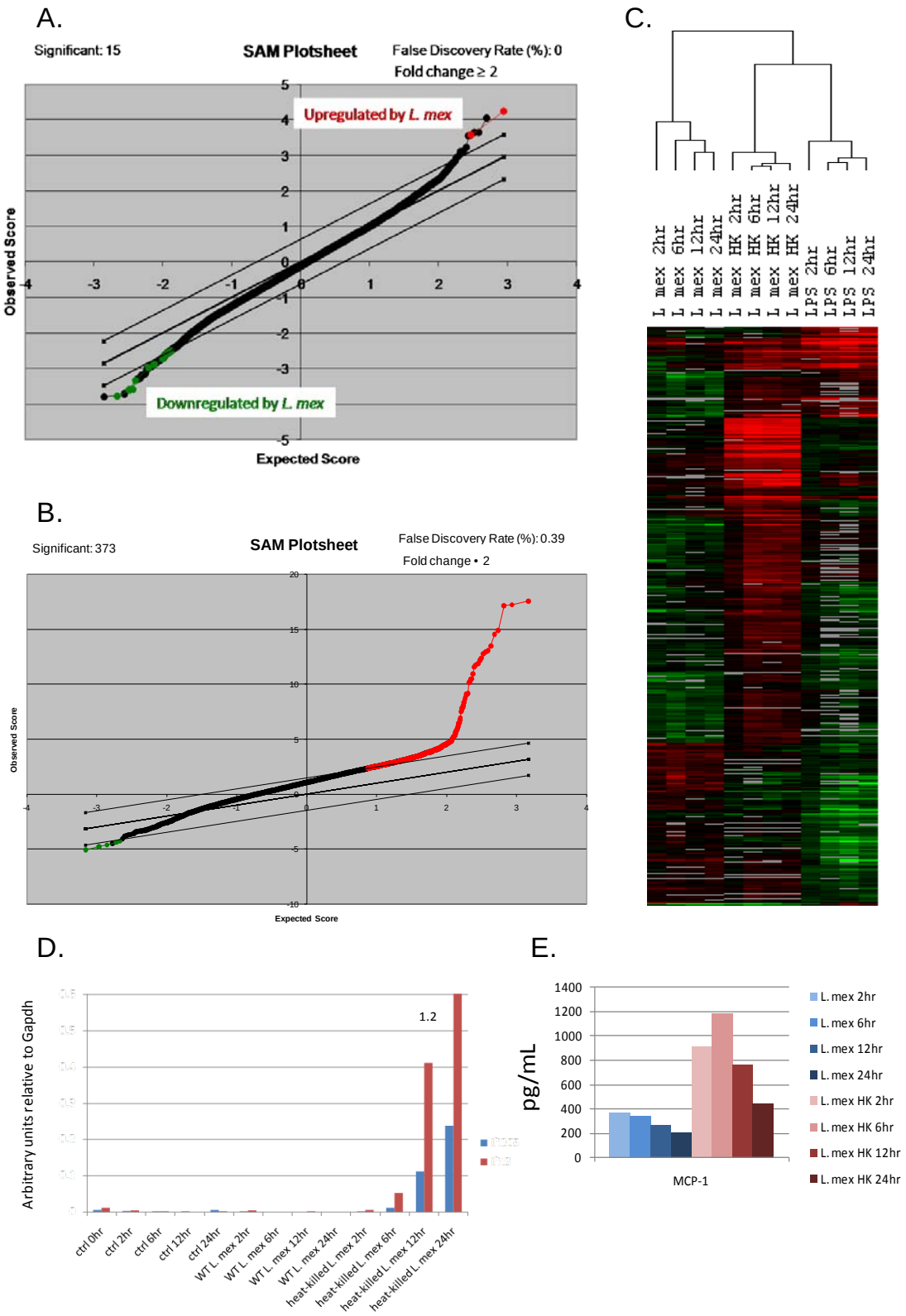

Figure 2 - CPB-/- and CPB/CPA-/- *L. mexicana* produce a transcriptional signature in BMMs characterized by induction of ISGs.

A.

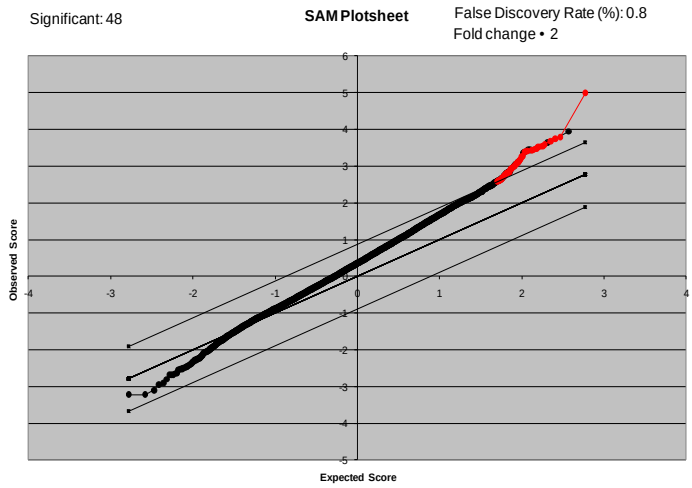

B.

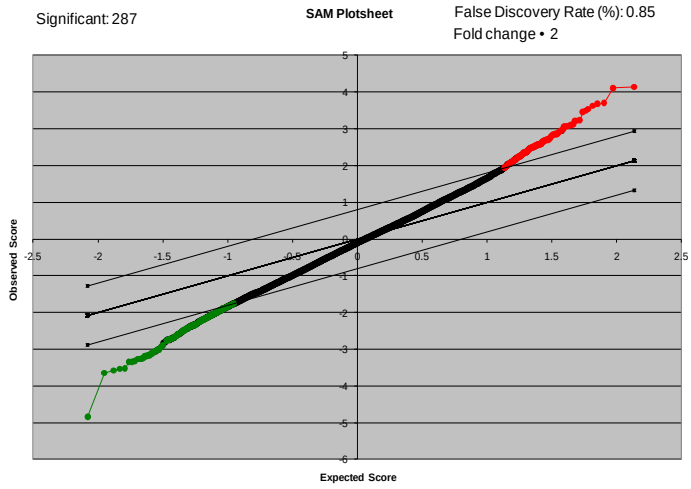

C.

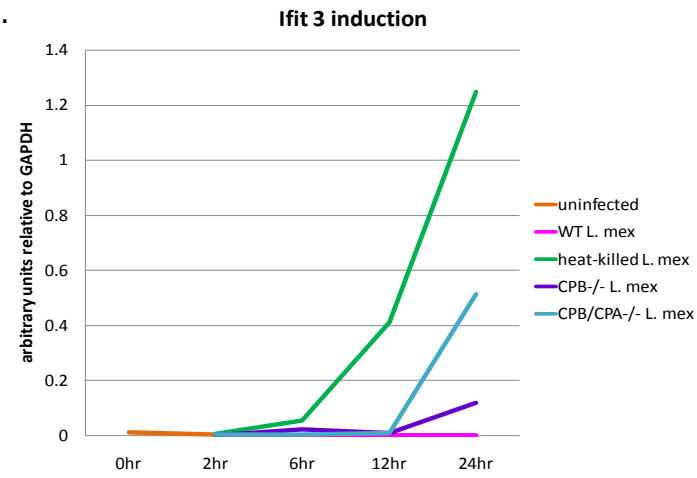

Figure 3 - WT *L. mexicana* induces arginase in TMs from C56BL/6 mice, but CPB/CPA-/- *L. mexicana* does not.

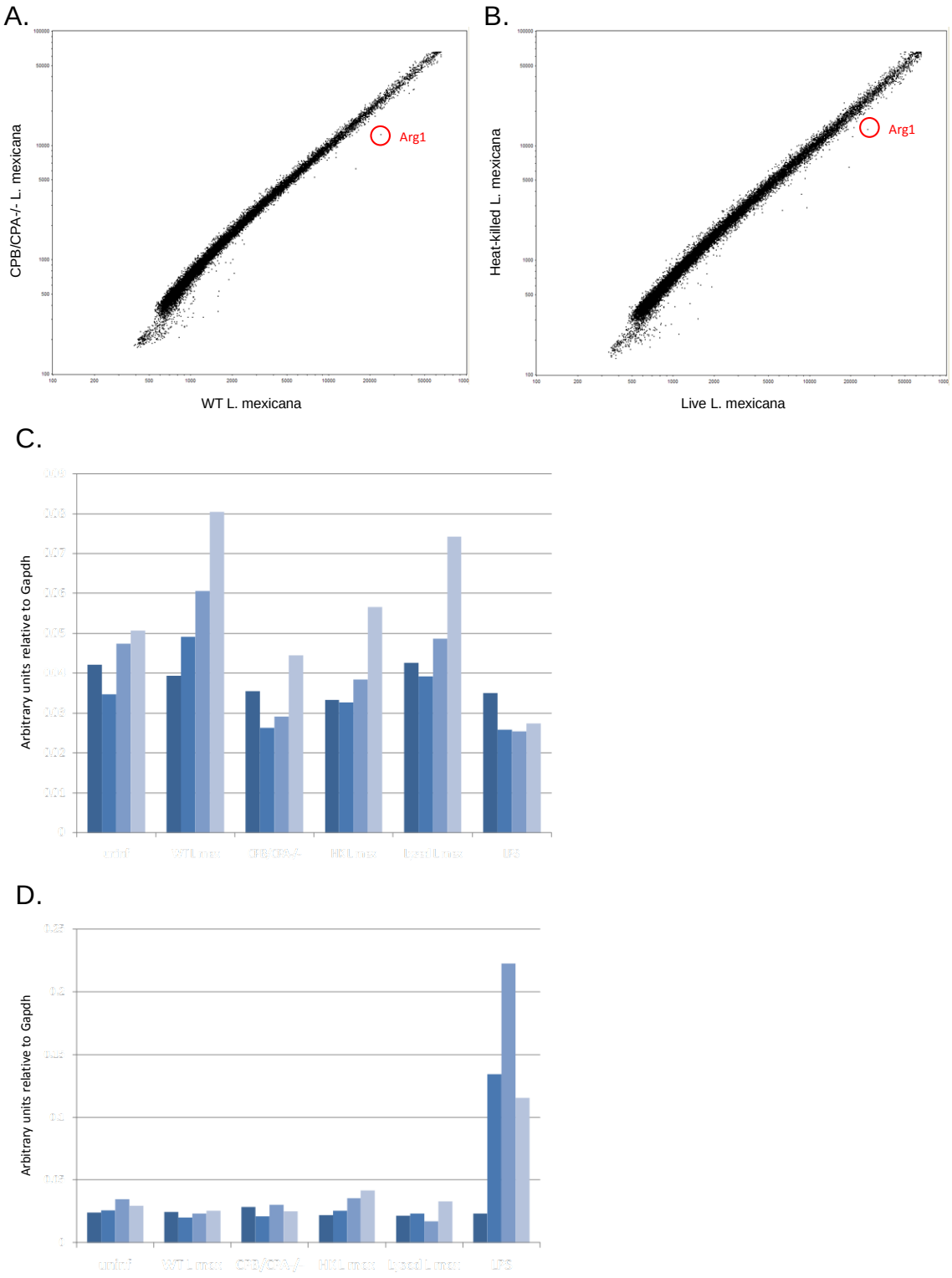

Figure 4 - Effect of CPB on growth of *L. mexicana* in TMs taken from BALB/c or C56BL/6 mice

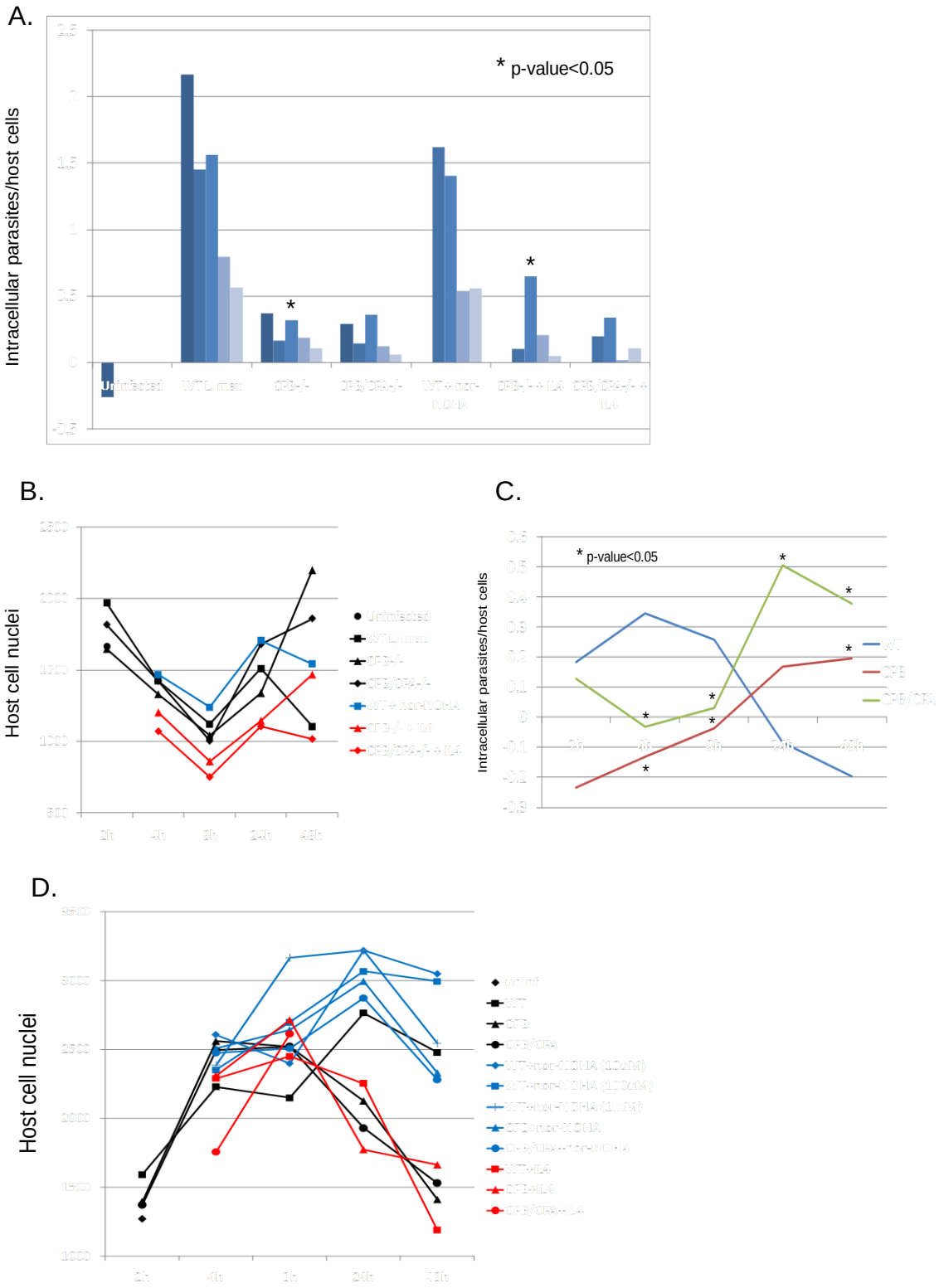

Figure 5 - Role of arginase on growth of *L. mexicana* in TMs taken from C57BL/6 mice

A.

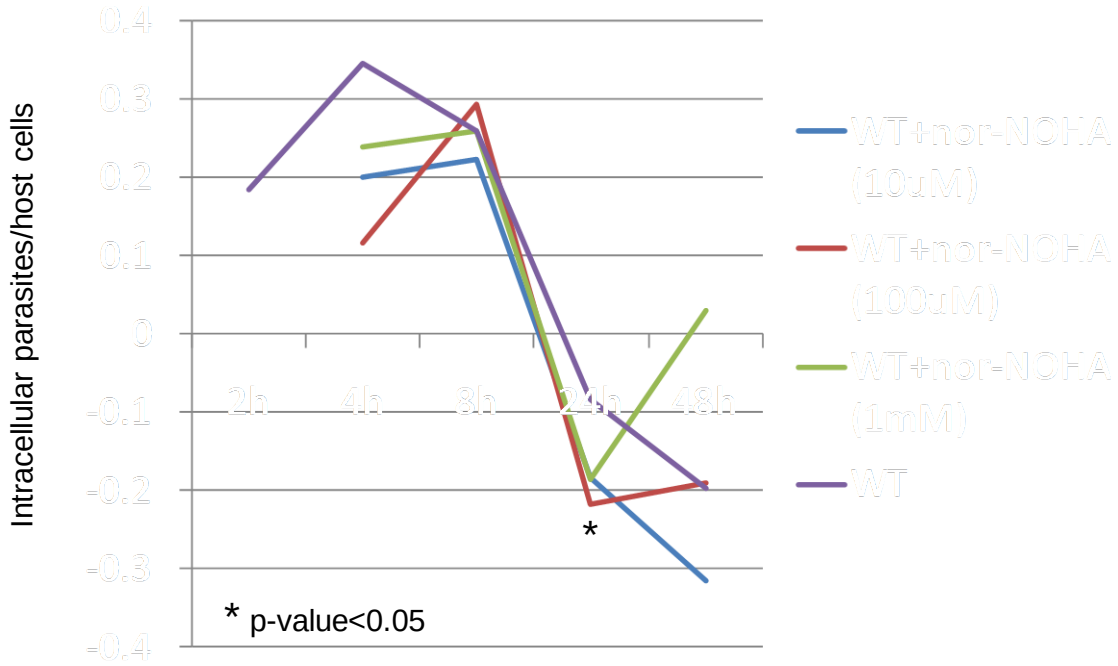

B.

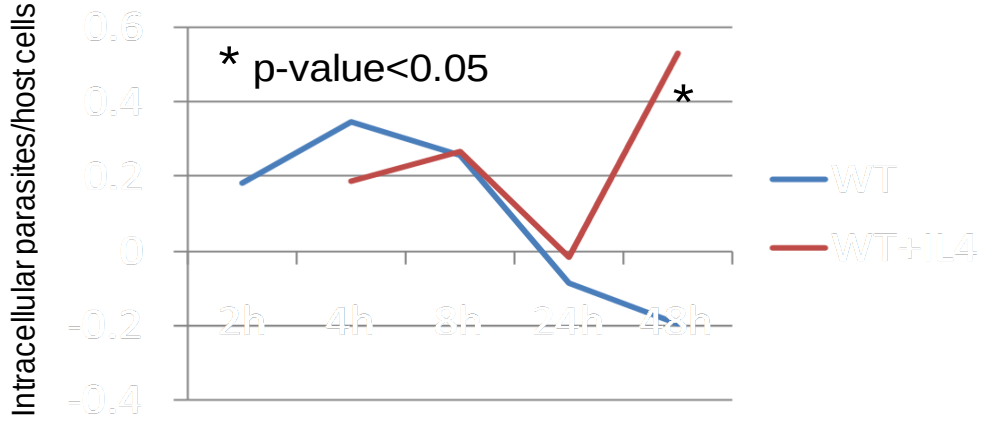

3.9. Tables

Table 1 – Genes upregulated in BMMs treated with heat-killed *L. mexicana*

Gene Name	Fold Change
interferon activated gene 205	10.6
chemokine (C-C motif) ligand 2	9.8
chemokine (C-C motif) ligand 12	9.6
Fc receptor, IgG, high affinity I	8.6
chemokine (C-C motif) ligand 7	8.6
Mus musculus interferon activated gene 205 (Ifi205), mRNA	8.4
interferon-induced protein with tetratricopeptide repeats 2	7.9
interferon gamma-inducible protein 16	7.3
interferon activated gene 203	5.7
interferon-induced protein with tetratricopeptide repeats 3	5.4
signal transducer and activator of transcription 1	5.0
2'-5' oligoadenylate synthetase 2	4.7
interferon activated gene 205	4.4
interferon induced with helicase C domain 1	4.4
interferon gamma induced GTPase	4.2
interferon gamma inducible protein 47	4.1
2'-5' oligoadenylate synthetase-like 2	4.1
Mus musculus signal transducer and activator of transcription	3.7
interferon-induced protein 35	2.8
interferon inducible protein 1	2.7
interferon-induced protein 75	2.0

Table 2 – Genes upregulated in BMMs infected with CPB-/- *L. mexicana*

Gene Name	Fold Change
chemokine (C-C motif) ligand 2	7.4
chemokine (C-C motif) ligand 7	6.7
chemokine (C-X-C motif) ligand 10	4.2
interferon activated gene 203	3.7
interferon activated gene 205	3.3
interferon induced with helicase C domain 1	3.2
2'-5' oligoadenylate synthetase-like 2	3.2
2'-5' oligoadenylate synthetase 2	2.6
Mus musculus signal transducer and activator of transcription	2.4

Table 3 – Genes upregulated in BMMs infected with CPB/CPA-/- *L. mexicana*

Gene Name	**Fold Change**
interferon-induced protein with tetratricopeptide repeats 3	11.8
interferon-induced protein with tetratricopeptide repeats 3	10.8
chemokine (C-C motif) ligand 2	7.3
chemokine (C-C motif) ligand 7	5.0
interferon, gamma-inducible protein 16	4.5
chemokine (C-X-C motif) ligand 10	4.4
interferon, alpha-inducible protein	4.0
Mus musculus signal transducer and activator of transcription	2.8
Mus musculus toll-like receptor 4 (Tlr4), mRNA.	2.8
2'-5' oligoadenylate synthetase 1G	2.2

Chapter Four:

Perspectives and Future Directions

4.1. Discussion

Macrophages were first described in the late 1800's by Russian immunologist Elie Metchnikoff as phagocytic cells that could engulf and digest microorganisms (1). This trait became the hallmark of macrophage activity. Macrophages serve as our first line of defense against invading pathogens, as they reside in a variety of tissues and are readily available to combat pathogens without requiring prior exposure. Once a macrophage encounters a pathogen, a dramatic change occurs at the transcriptional and protein level, transforming the resting cell into an "activated" macrophage. Due to this interaction, activated macrophages came to be defined as cells that secrete inflammatory cytokines and kill intracellular pathogens.

In more recent years, immunologists have come to realize that activated macrophages are far more heterogenous than originally described. The first evidence of this heterogeneity was the observation of a very different macrophage response following stimulation with the Th2-type cytokine IL-4. This "alternative macrophage activation" was characterized by the upregulation of mannose receptor, polyamines, and collagen but not by the induction of nitric oxide and reactive oxygen species. These macrophages were therefore ineffective at killing intracellular pathogens (2). Despite its name, alternative macrophage activation was not the only alternative way macrophages could be activated. For example, macrophages stimulated with a TLR ligand along with IgG immune complexes resulted in a very different type of response characterized by upregulation of IL-10 and inhibition of acute inflammatory responses (2).

We have shown in the study described in Chapter Two that the heterogeneity of macrophage activation is even broader than previously described. In our study, we

described the macrophage transcriptional response to the cytokines IFNG, IL-4, IL-10, TNF, IFNG, and IL17, and delineated the relationships between the various responses. Our dataset provides a valuable resource for the further study of macrophage activation. As new forms of macrophage activation are discovered, they can be compared to the activation patterns that we have described, allowing a more complete understanding of the heterogeneity of macrophage activation.

We have also shown through our study that the macrophage response to intracellular protozoan pathogens is highly disparate from the "classical" macrophage activation response, which is characteristic of infection by intracellular bacterial pathogens. When we compared our macrophage derived transcriptional profiling data to all publicly available expression profiling studies of the host response to *Leishmania* and *Trypanosoma* species, we found that the transcriptional responses observed in our study showed high commonality with the transcriptional responses observed in other studies, despite differences in the species of parasites and the types of mammalian cells characterized. Specifically, we found that all *Leishmania* species produced a transcriptional signature in host cells characterized by very small numbers of upregulated genes and a much larger number of downregulated genes. This observation suggests that infection by *Leishmania* species may have a suppressive effect on host transcription.

In our study described in Chapter Three, we showed that the *L. mexicana* virulence factors cysteine protease B (CPB) and cysteine protease A (CPA) may play a role in the suppression of macrophage transcriptional responses during initial infection. Further work is required to confirm our results in an alternative source of macrophages and also to elucidate the mechanism of the suppression. We showed that CPB/CPA-/- *L.*

mexicana induced interferon-stimulate genes (ISG) in infected macrophages, but that this ISG induction was not associated with the presence of interferons in the supernatant of the macrophages. This suggests that the induction of ISGs by the knock-out *L. mexicana* occurred via an interferon-independent pathway. Further investigation is needed to determine what pathway leads to the induction of the ISGs and how CPB and CPA are interfering with that pathway. It has been previously shown that CPB is able to directly degrade NF• B and I• B, leading to inhibition of IL-12 (3). However, the mechanism by which CPB is leaves the parisitophorous vacuole and enters the host nucleus to interact with these transcription factors is unknown. Further understanding of parasite protease trafficking within the host cell will be important in elucidating *L. mexicana* immune evasion mechanisms.

In our studies using mouse thioglycollate-elicited peritoneal macrophages (TM), we found that WT *L. mexicana* induced host arginase upon infection but CPB/CPA-/- *L. mexicana* did not. Arginase in macrophages competes with iNOS for the same substrate, L-arginine. It catalyzes the reaction that leads to the production of polyamines, which promote parasite growth, and at the same time inhibits the reaction that leads to the production of NO, which is important for parasite killing. Our data suggested that CPB and CPA play a role in the induction of host arginase, which then promotes parasite survival in the macrophage. Further work is required to determine the exact role of CPB and CPA in the induction of arginase and to determine if the induction also occurs at the protein and activity level.

In our parasite infectivity and growth studies, we found that CPB-/- and CPB/CPA-/- *L. mexicana* exhibited a significant defect in the establishment of infection

in TMs. This is in contrast to a previous study using peritoneal exudate cells from BALB/c mice that showed no difference in the establishment of infection between WT and CPB-/- promastigotes, but a defect in parasite survival for the knock-out *Leishmania* (4). This discrepancy may be due to our use of thioglycollate-elicited macrophages, which are cells that have been recruited to the peritoneum by thioglycollate injection and therefore in a more activated state than resident peritoneal macrophages. The role that CPB and CPA play in the establishment of infection in these cells requires further investigation.

Our infectivity experiments also showed that the addition of IL-4 to macrophages infected with WT *L. mexicana* significantly improved parasite survival at 48 h post-infection. As IL-4 is a potent inducer of arginase, this suggested that further induction of arginase prevents parasite killing by TMs by 48 h post-infection. However, addition of IL-4 had little effect on the growth of CPB-/- and CPB/CPA-/- *L. mexicana* within macrophages, suggesting that induction of arginase is not sufficient to rescue the infectivity defect of CPB-/- and CPB/CPA-/- *L. mexicana*. The arginase inhibitor nor-NOHA also had little effect on parasite survival within macrophages. However, further work is required to determine the activity of this inhibitor. Preliminarily, these findings suggest that the defect in the establishment of infection exhibited by CPB-/- and CPB/CPA-/- *L. mexicana* is not related to the inability to induce arginase.

Unexpectedly, we observed a significant difference in the pattern of parasite growth in macrophages taken from BALB/c vs. C57BL/6 mice. Whereas in BALB/c mice, CPB-/- and CPB/CPA-/- *L. mexicana* exhibited decreased growth and survival as compared to their wild-type counterparts over the entire 48 h timecourse, in C57BL/6

mice, CPB-/- and CPB/CPA-/- *L. mexicana* appeared to survive better than their wild-type counterparts in the later timepoints of infection. This was shown to be due to a significant decrease in host cell survival in cultures infected by CPB-/- or CPB/CPA-/- *L. mexicana*. Further investigation is needed to identify the differences between TMs taken from BALB/c vs. C57BL/6 mice that have caused the significant difference in parasite infectivity. Further work is also needed to confirm the unexpected finding that CPB-/- and CPB/CPA-/- *L. mexicana* contributes to increased cell death in infected TMs taken from C57BL/6 mice.

In the studies described here, we have broadened the definition of macrophage activation to include a type of intracellular pathogen that produces very few transcriptional changes in the host cell. The transcriptionally silent nature of this infection may be due in part to parasite proteases that interact with host cell proteins and also due in part to the upregulation of host factors that inhibit an inflammatory response. The ability of *Leishmania* to manipulate the host macrophage response serves as an important model of host-pathogen interactions, as other pathogens may employ similar techniques to evade host immunity. Therefore, further study of this system is important not just as a means to solve the global health issues created by *Leishmania spp*, but also to gain a better understanding of the relationship between intracellular pathogens and the host macrophage.

4.2. References

1. Janeway C. Immunobiology : the immune system in health and disease. 6th ed. New York: Garland Science; 2005.
2. Mosser DM. The many faces of macrophage activation. J Leukoc Biol. 2003;73(2):209-12.
3. Cameron P, McGachy A, Anderson M, Paul A, Coombs GH, Mottram JC, et al. Inhibition of lipopolysaccharide-induced macrophage IL-12 production by Leishmania mexicana amastigotes: the role of cysteine peptidases and the NF-kappaB signaling pathway. J Immunol. 2004;173(5):3297-304.
4. Frame MJ, Mottram JC, Coombs GH. Analysis of the roles of cysteine proteinases of Leishmania mexicana in the host-parasite interaction. Parasitology. 2000;121 (Pt 4):367-77.

Appendix:

Supplementary Data for Chapter Three

A1. Results

A1.1. *L. mexicana* does not suppress bone marrow-derived macrophage activation by LPS

Previous studies have implicated *L. major* promastigotes (1), the *L. major* surface protein LPG (1), and *L. mexicana* amastigotes (2) in the inhibition of IL-12 production by macrophages following LPS stimulation. Direct inhibition of IL-12 production by *L. mexicana* amastigotes has been shown to be mediated by *L. mexicana* cysteine protease B (CPB) (3). *L. mexicana* amastigotes that were CPB-deficient lacked the ability to suppress IL-12 production in infected macrophages. In our own study, we found that *L. mexicana* promastigotes were able to suppress the macrophage transcriptional response following infection. In order to determine whether *L. mexicana* promastigotes could also inhibit macrophage activation by LPS, we treated *L. mexicana*-infected macrophages with varying concentrations of LPS and assessed the production of the cytokines IL-12 and TNF by infected versus uninfected cells. We found that IL-12 and TNF production following LPS stimulation were the same in infected and uninfected macrophages (**Figure 1**). This suggests that *L. mexicana* promastigotes are unable to suppress macrophage activation by LPS. One reason for this may be that expression of CPB in *L. mexicana* promastigotes is insufficient for inhibition of IL-12 to take place.

A1.2. *L. mexicana, L. major,* and *L. donovani* produce similar transcriptional response in bone marrow-derived macrophages

The *Leishmania* species *mexicana*, *major*, and *donovani* produce very different disease outcomes in the host, ranging from mild, self-limiting skin lesions (in the case of *L. major*), to live-threatening systemic disease (in the case of *L. donovani*). We have found that the host response to *L. mexicana* infection is very silent with few changes in gene transcription (4). In order to determine the host response to other *Leishmania* species, we infected macrophages with *L. major* and *L. mexicana* and determined the host trancriptional response by microarray analysis. We found that both *L. major* (**Figure 2A**) and *L. donovani* (**Figure 2B**) produced few transcriptional changes in the host, similar to *L. mexicana*. When unsupervised two-dimensional clustering was performed on the transcriptional response of macrophages infected with *L. mexicana*, *L. major*, and *L. donovani*, as well as macrophages treated with heat-killed *L. mexicana*, we found that cells infected with the three species of *leishmania* produced a very similar response, while the response to heat-killed *L. mexicana* was signifcantly different (**Figure 2C**).

A1.3. Decreased responsiveness of bone marrow-derived macrophages to *L. mexicana* and to LPS

After our initial findings that heat-killed and CPB/CPA-/- *L. mexicana* elicited an interferon-stimulated gene (ISG) response in the bone marrow-derived macrophages (BMM), we experienced some variability in the responsiveness of these macrophages to various stimuli. For some time, we observed an aberrant induction of ISGs in unstimulated BMMs. After permuting many factors including culture medium, FBS concentration, glassware, MCSF-containing broth, mice, and the physical location of the experiment, we found that the aberrant induction could be abated by using MCSF-

containing BMM media throughout the course of the infection, including the wash steps. However, while this issue was resolved, we found that under these conditions, BMMs were less responsive to stimuli in general and were no longer inducing ISGs in response to heat-killed or lysed *L. mexicana* (**Figure 3**). Furthermore, we found that under the new media conditions, BMMs were not mounting as strong of a response to LPS or to IFNG, both of which had previously elicited a very robust transcriptional response in BMMs. This illustrates the sensitivity of primary BMMs to culture and laboratory conditions.

A2. References

1. Feng GJ, Goodridge HS, Harnett MM, Wei XQ, Nikolaev AV, Higson AP, et al. Extracellular signal-related kinase (ERK) and p38 mitogen-activated protein (MAP) kinases differentially regulate the lipopolysaccharide-mediated induction of inducible nitric oxide synthase and IL-12 in macrophages: Leishmania phosphoglycans subvert macrophage IL-12 production by targeting ERK MAP kinase. J Immunol. 1999;163(12):6403-12.
2. Weinheber N, Wolfram M, Harbecke D, Aebischer T. Phagocytosis of Leishmania mexicana amastigotes by macrophages leads to a sustained suppression of IL-12 production. Eur J Immunol. 1998;28(8):2467-77.
3. Cameron P, McGachy A, Anderson M, Paul A, Coombs GH, Mottram JC, et al. Inhibition of lipopolysaccharide-induced macrophage IL-12 production by Leishmania mexicana amastigotes: the role of cysteine peptidases and the NF-kappaB signaling pathway. J Immunol. 2004;173(5):3297-304.
4. Zhang S, Kim CC, Batra S, McKerrow JH, Loke P. Delineation of diverse macrophage activation programs in response to intracellular parasites and cytokines. PLoS Negl Trop Dis. 2010;4(3):e648. PMCID: 2846935.

A3. Figure Legends

Figure 1 - *L. mexicana* promastigotes do not suppress IL-12 and TNF production in LPS-stimulated macrophages.

BMMs were infected with CFSE-labelled *L. mexicana* and then stimulated 2 hours later with 10 pg/mL (A), 1 ng/mL (B), or 100 ng/mL (C) of LPS. Cells were harvested at 6 h post-infection and stained for intracellular IL-12 p40 and TNF. Flow cytometry was performed to determine the production of IL-12 p40 and TNF in infected and uninfected BMMs.

Figure 2 - *L. major* and *L. donovani* produce transcriptional response in macrophages similar to that of *L. mexicana*.

Pairwise SAM analysis was used to compare the transcriptional responses of *L. major*-infected vs. uninfected BMMs (A) and also to compare the transcriptional responses of *L. donovani*-infected vs. uninfected BMMs (B). Unsupervised two-dimensional clustering was performed to determine the relationships of the transcriptional responses to infection with *L. mexicana, L. major,* and *L. donovani* as well as to stimulation by heat-killed *L. mexicana* (C).

Figure 3 - BMMs under new culture conditions are less responsive to stimuli than BMMs under original culture conditions.

RNA extracted from BMMs from our original infection experiments was processed side by side along with RNA extracted from BMMs from new infection experiments, and quantitative PCR was performed to determine expression of a marker ISG, *ifi205*.

A4. Figures

Figure 1 - *L. mexicana* promastigotes do not suppress IL-12 and TNF production in LPS-stimulated macrophages.

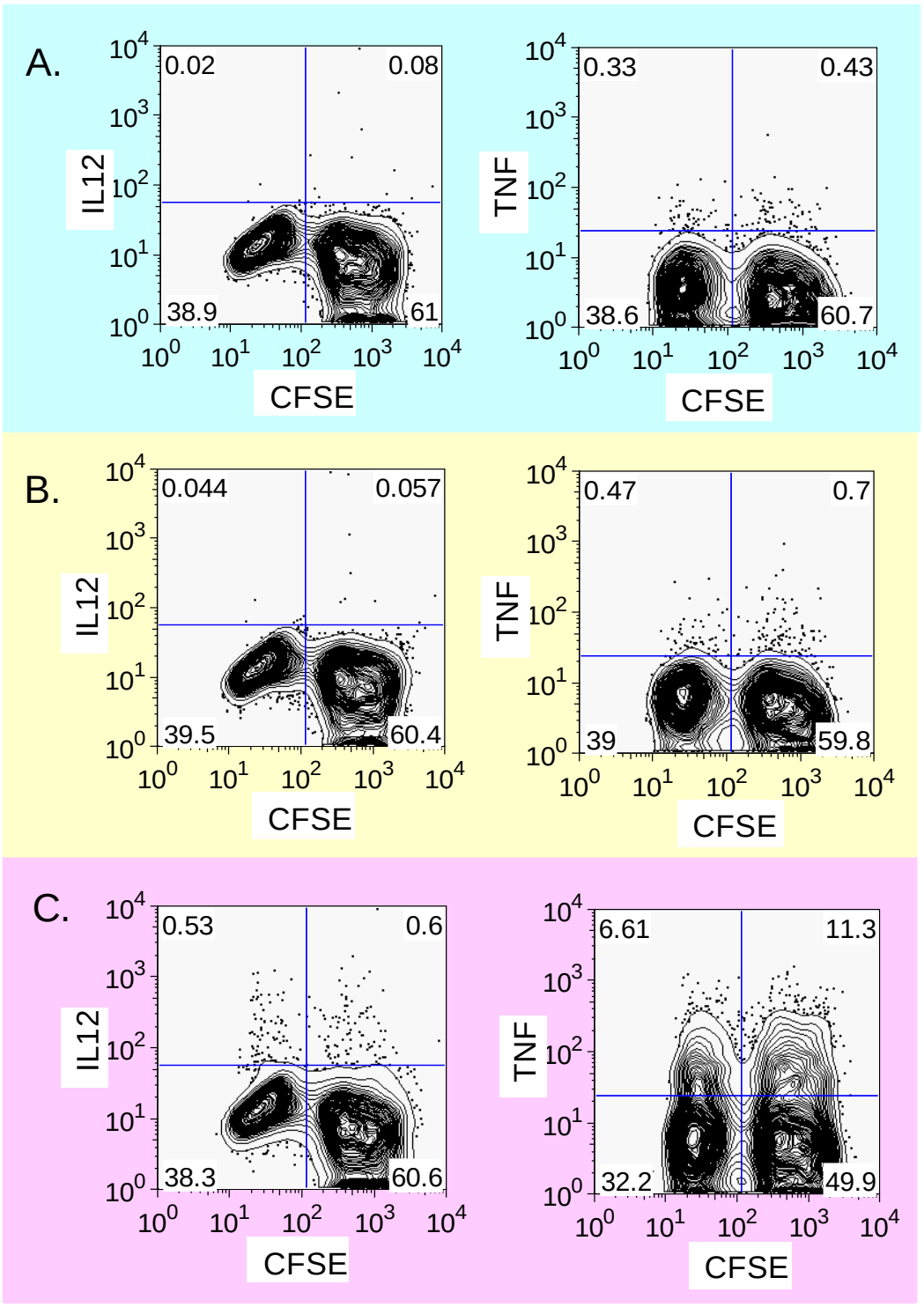

Figure 2 - *L. major* and *L. donovani* produce transcriptional response in macrophages similar to that of *L. mexicana*.

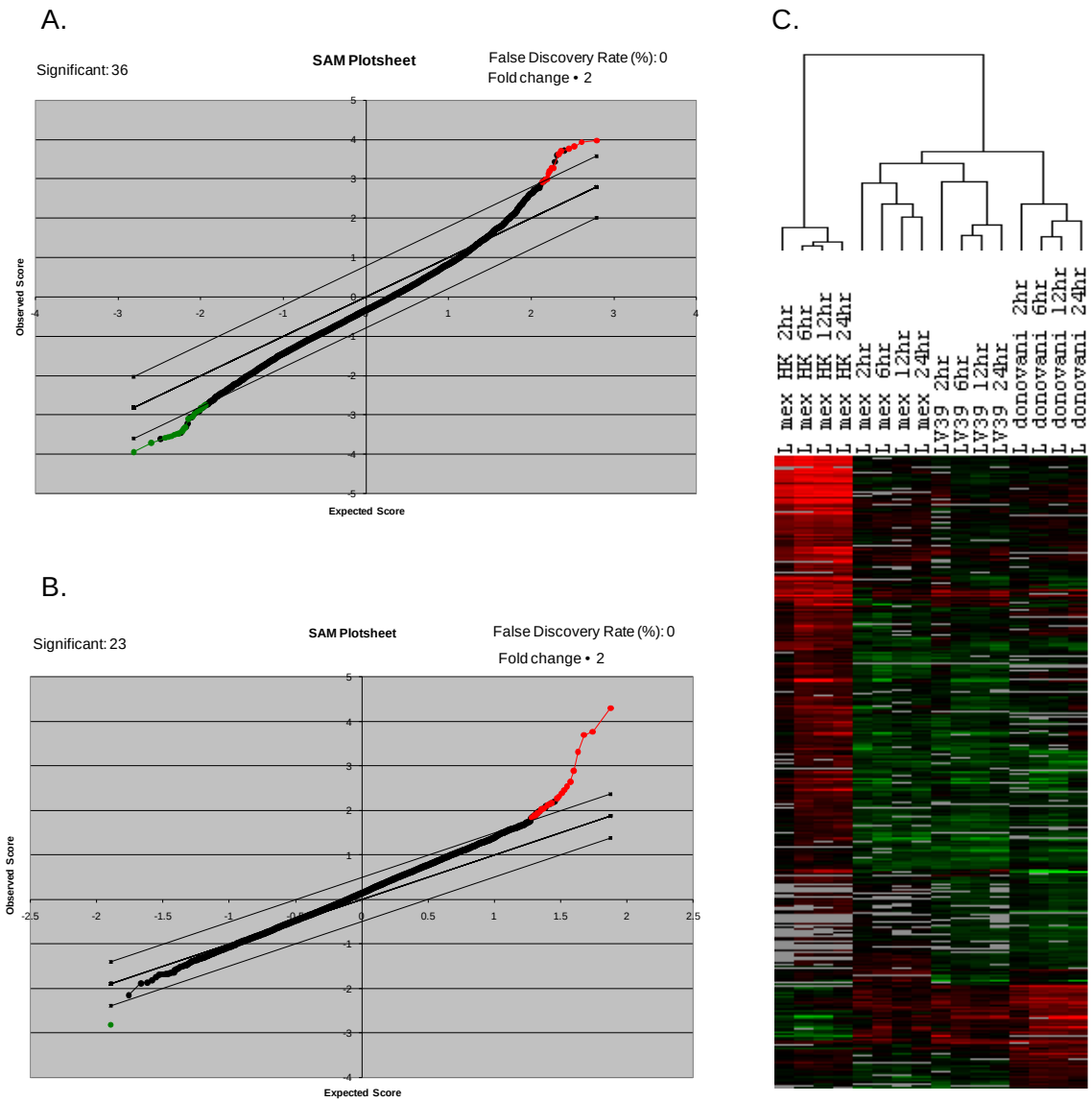

Figure 3 - BMMs under new culture conditions are less responsive to stimuli than BMMs under original culture conditions.

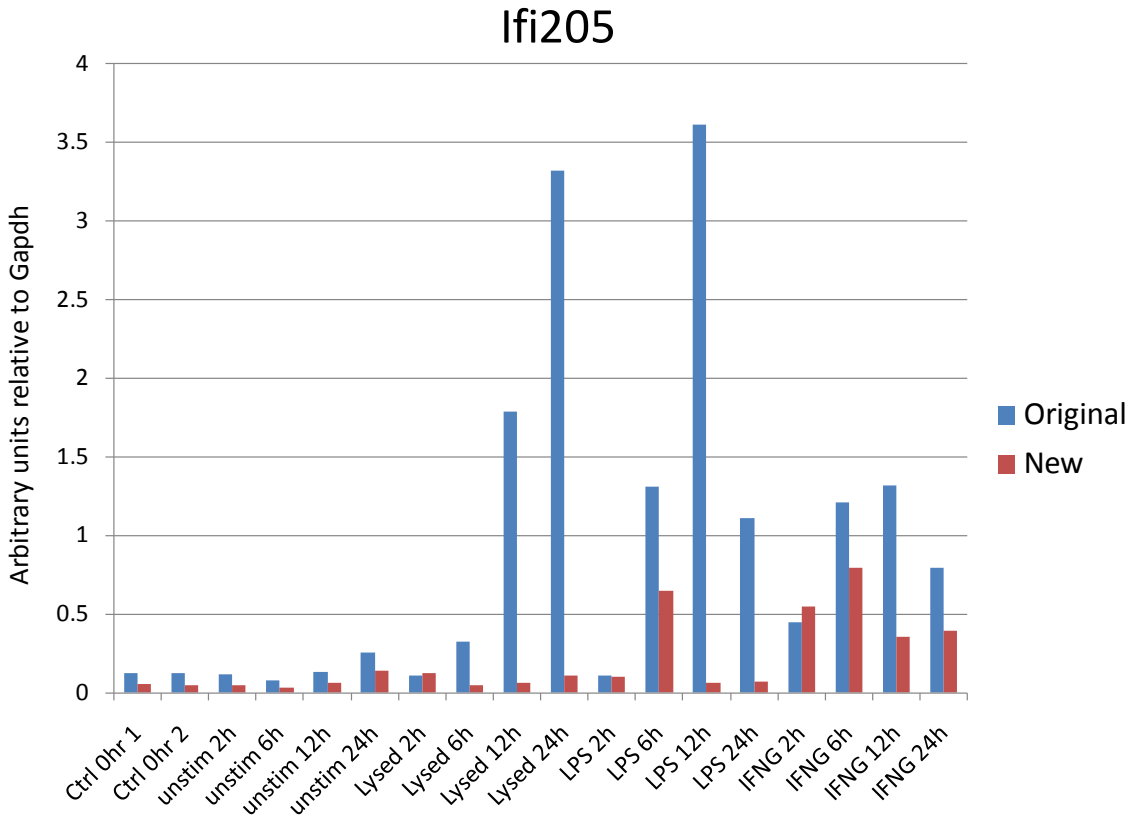

Publishing Agreement

It is the policy of the University to encourage the distribution of all theses, dissertations, and manuscripts. Copies of all UCSF theses, dissertations, and manuscripts will be routed to the library via the Graduate Division. The library will make all theses, dissertations, and manuscripts accessible to the public and will preserve these to the best of their abilities, in perpetuity.

Please sign the following statement:

I hereby grant permission to the Graduate Division of the University of California, San Francisco to release copies of my thesis, dissertation, or manuscript to the Campus Library to provide access and preservation, in whole or in part, in perpetuity.

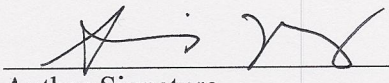

Author Signature

5/13/11

Date